Synaptopodin couples epithelial contractility to α-actinin-4–dependent junction maturation

Nivetha Kannan[1] and Vivian W. Tang[2]

[1]Program in Global Public Health and [2]Department of Cell and Developmental Biology, University of Illinois, Urbana-Champaign, Champaign, IL 61801

The epithelial junction experiences mechanical force exerted by endogenous actomyosin activities and from interactions with neighboring cells. We hypothesize that tension generated at cell–cell adhesive contacts contributes to the maturation and assembly of the junctional complex. To test our hypothesis, we used a hydraulic apparatus that can apply mechanical force to intercellular junction in a confluent monolayer of cells. We found that mechanical force induces α-actinin-4 and actin accumulation at the cell junction in a time- and tension-dependent manner during junction development. Intercellular tension also induces α-actinin-4–dependent recruitment of vinculin to the cell junction. In addition, we have identified a tension-sensitive upstream regulator of α-actinin-4 as synaptopodin. Synaptopodin forms a complex containing α-actinin-4 and β-catenin and interacts with myosin II, indicating that it can physically link adhesion molecules to the cellular contractile apparatus. Synaptopodin depletion prevents junctional accumulation of α-actinin-4, vinculin, and actin. Knockdown of synaptopodin and α-actinin-4 decreases the strength of cell–cell adhesion, reduces the monolayer permeability barrier, and compromises cellular contractility. Our findings underscore the complexity of junction development and implicate a control process via tension-induced sequential incorporation of junctional components.

Introduction

The epithelial junction experiences mechanical force from an array of cellular processes such as tugging force from cellular contractions (Ganz et al., 2006; Ladoux et al., 2010; Borghi et al., 2012), hydrostatic force from intracellular osmotic pressure (Papakonstanti et al., 2000; Di Ciano et al., 2002; Thirone et al., 2009; Stewart et al., 2011; Jiang and Sun, 2013), and shear stress from cytoplasmic streaming (Iwasaki and Wang, 2008; Keren et al., 2009). Cell–cell adhesion also experiences mechanical stress from extrinsic stimuli such as shear stress from extracellular fluid flow (Tzima et al., 2005; Duan et al., 2008) and hydrostatic pressure from the surrounding tissue (Lorentz et al., 1972; Knight et al., 2006). Fluctuation of intercellular tension can be created by changes of intracellular and extracellular osmotic pressures in disease states such as diabetes (Hsueh and Anderson, 1992; Goel et al., 2007). Moreover, inhibition or stimulation of the cellular contractile system can alter the tension applied to cell–cell adhesions (Smutny et al., 2010; Engl et al., 2014; Hoj et al., 2014). Thus, the levels of tension exerted on epithelial junction vary depending on the physiological states of the body.

The ability of epithelial junction to withstand mechanical stress depends on many factors, including the adhesiveness of cell–cell adhesion proteins (Harrison et al., 2012; Leckband and Sivasankar, 2012; Rikitake et al., 2012; Samanta et al., 2012; Sivasankar, 2013) and the stability of the junctional complex (Sato et al., 2006; Ishiyama et al., 2010; Tang and Brieher, 2013), which is intimately coupled to the attachment of the junctional complex to the actin cytoskeleton (Abe and Takeichi, 2008; Ting et al., 2012; Desai et al., 2013; Hong et al., 2013; Huveneers and de Rooij, 2013; Twiss and de Rooij, 2013; Buckley et al., 2014). In addition, the epithelial junction can respond to changes of mechanical stress and adjust its functions (Gomez et al., 2011; Maître and Heisenberg, 2011; Leerberg et al., 2014). For example, cell–cell adhesion has to become stronger when faced with increased mechanical stress such as elevated blood pressure in hypertension (Preston et al., 2002; Falqui et al., 2007) or during exercise (Goel et al., 2007). Dissecting the complex relationships between mechanical force and cell–cell adhesion is becoming essential for understanding epithelial physiology and the regulation of cell junction in health and disease.

The apical junctional complex in epithelial cells, originally described using EM, consists of morphologically distinct cell–cell contacts (Farquhar and Palade, 1963), including the tight junction, defined morphologically to contain intermittent kisses from the outer leaflets of apposing plasma membranes, and the adherens junction, defined morphologically to contain extracellular spacers of ∼15–40 nm formed between apposing cells (Hirokawa, 1980; Hirokawa and Heuser, 1981; Miyaguchi, 2000; Franke, 2009; Meng and Takeichi, 2009). The tight and adherens junctions are characterized by cytoplasmic membrane-associated electron densities of ∼150 nm and attachment to cytoskeletal structures (Farquhar and Palade, 1963; Hirokawa and Heuser, 1981; Hirokawa and Tilney, 1982; Hirokawa et al., 1982, 1983;

Correspondence to Vivian W. Tang: vtang@illinois.edu

Abbreviation used in this paper: dpc, day post-confluence.

The Rockefeller University Press $30.00
J. Cell Biol. Vol. 211 No. 2 407–434
www.jcb.org/cgi/doi/10.1083/jcb.201412003

Hirokawa, 1986; Madara et al., 1986). In differentiated epithelial cells, the tight and adherens junctions are positioned next to each other but can reorganize in dynamic cellular processes such as disassembly and reassembly of junctions during wound healing, intercellular neighbor exchanges during morphogenetic movement, and lateral mixing of junctional components in cell extrusion (Boyer et al., 1989; Madara, 1990; Collares-Buzato et al., 1998; Tamada et al., 2007; Ebnet, 2008; McGill et al., 2009; Collinet and Lecuit, 2013). The tight and adherens junctions in cells of epithelial lineage such as endothelial cells and kidney podocytes are positioned in close proximity and frequently intermingled (Schnabel et al., 1990; Wolburg et al., 1994; Adamson et al., 1998; Underwood et al., 1999; Reiser et al., 2000; Rüffer et al., 2004; Fukasawa et al., 2009; Tornavaca et al., 2015).

Junctional complexes found in epithelial cells are heterogeneous in composition and size (Hinck et al., 1994; Näthke et al., 1994; McGill et al., 2009; Wu et al., 2015). Proteomics studies have identified hundreds of proteins associating with the tight and adherens junctions (Catimel et al., 2005; Tang, 2006; Guo et al., 2014; Toret et al., 2014; Van Itallie et al., 2014), which can be categorized into functional modalities (Tang, 2006; Guo et al., 2014; Toret et al., 2014; Padmanabhan et al., 2015). Thus, the key to understanding epithelial junctions lies in dissecting the dynamical interactions and regulations of individual proteins within the junctional complexes and among the different functional modalities (Howarth and Stevenson, 1995; Müller et al., 2005; Choi et al., 2009; Garbett and Bretscher, 2014; Pokutta et al., 2014; Viswanatha et al., 2014).

Engagement of cadherin, a key intercellular adhesion molecule at the adherens junction (Sedar and Forte, 1964; Behrens et al., 1985; Vestweber and Kemler, 1985; Volk and Geiger, 1986a; Hirano et al., 1987), initiates biochemical events that lead to structural organization and actin attachment, resulting in strong cell–cell adhesion with a functional epithelial permeability barrier (Gumbiner and Simons, 1986; Madara et al., 1986; Gumbiner et al., 1988; Siliciano and Goodenough, 1988; Capaldo and Macara, 2007). Cadherin organizes the adherens junctional domain through self-association (Yap et al., 1997, 1998; Katz et al., 1998; Strale et al., 2015), as well as by interacting with other cell–cell adhesion complexes such as nectins (Takahashi et al., 1999; Miyahara et al., 2000; Yamada et al., 2004) and Epcam (Litvinov et al., 1997; Winter et al., 2003). Cadherin interacts directly with p120-catenin (Reynolds et al., 1994; Shibamoto et al., 1995), β-catenin (Ozawa et al., 1989), and plakoglobin (Knudsen and Wheelock, 1992), as well as indirectly with α-catenin via β-catenin (Ozawa et al., 1990; Ozawa and Kemler, 1992; Aberle et al., 1994) to form the core cadherin–catenin complex. The catenins interact with many junctional proteins including ZO-1 (Rajasekaran et al., 1996; Itoh et al., 1997; Maiers et al., 2013), afadin (Ikeda et al., 1999), α-actinin (Knudsen et al., 1995; Nieset et al., 1997; Hazan and Norton, 1998), vinculin (Hazan et al., 1997; Watabe-Uchida et al., 1998; Weiss et al., 1998), EPLIN (Abe and Takeichi, 2008; Taguchi et al., 2011), and MAGI (Dobrosotskaya and James, 2000; Nishimura et al., 2000; Stetak and Hajnal, 2011), which can interact with each other (Yamamoto et al., 1997; Ebnet et al., 2000; Ooshio et al., 2010), providing multiple and overlapping interfaces within the apical junctional complex (Takahashi et al., 1999; Tachibana et al., 2000; Yokoyama et al., 2001; Ooshio et al., 2004; Peng et al., 2010).

The cadherin–catenin complex plays an essential role in linking cell–cell adhesions to actin structures (Hirokawa and Heuser, 1981; Volk and Geiger, 1986b; Hirano et al., 1987; Nagafuchi and Takeichi, 1988; Jaffe et al., 1990; Matsuzaki et al., 1990; Balsamo et al., 1991; Miyaguchi, 2000; Zhang et al., 2005; Lambert et al., 2007). Several distinct actin structures are present at the apical junction in epithelial cells, including a centrally positioned actomyosin belt separating two additional actin networks positioned immediately at the level of the tight and adherens junctions (Tamada et al., 2007; Ebrahim et al., 2013). In addition, intercellular junctions between multiple cells form a specialized vertex structure, the tricellular junction (Walker et al., 1985), containing additional junctional proteins (Ikenouchi et al., 2005; Byri et al., 2015) and distinct actin arrangements (Yonemura, 2011), that plays an important role in junctional and epithelial dynamics (Oda et al., 2014). The apical junction also contains a population of stabilized actin associated with the latrunculin-resistant junctional complexes (Yamada et al., 2004; Abe and Takeichi, 2008; Cavey et al., 2008; Tang and Brieher, 2012). Distinct pools of actin are thought to associate with junctional complexes on the lateral membrane (Drenckhahn and Franz, 1986; Yonemura et al., 1995). During junction remodeling, actin reorganizes into bundled cables that can position perpendicular (Vasioukhin et al., 2000; Kishikawa et al., 2008; Taguchi et al., 2011) or parallel (Bement et al., 1993; Mandato and Bement, 2001; Tamada et al., 2007) to the plasma membrane at cell–cell adhesions. Junctional actin structures can be controlled by local and global actin regulation, including actin polymerization (Kobielak et al., 2004; Carramusa et al., 2007; Ryu et al., 2009; Bernadskaya et al., 2011; Verma et al., 2012; Grikscheit et al., 2015), actin depolymerization (Lin et al., 2010; Chu et al., 2012; Slee and Lowe-Krentz, 2013), and actin stabilization (Weber et al., 2007; Cox-Paulson et al., 2012; Tang and Brieher, 2013).

In addition to biochemical inputs, the cadherin–catenin complex provides a platform for biophysical inputs (Miyake et al., 2006; Ladoux et al., 2010; Liu et al., 2010) by integrating actin dynamics and actomyosin activities (Clark et al., 2009; Fernandez-Gonzalez et al., 2009; Saravanan et al., 2013). Ablation of myosin II or disruption of myosin II activities compromises cell–cell adhesion and the development of a mature junction (Conti et al., 2004; Shewan et al., 2005; Lambert et al., 2007; Kishikawa et al., 2008; Franke et al., 2010; Reyes et al., 2014). In turn, cadherin-mediated adhesions are essential for modulating the activities of the cellular actomyosin network and propagating mechanical force to neighboring cells, ultimately determining the overall contractile properties of the epithelial tissue (Harris et al., 2012, 2014; Kuipers et al., 2014). Thus, actin dynamics can directly influence the behavior of the cellular actomyosin network and indirectly through its effect on cell–cell adhesions to control the barrier function and mechanical properties of epithelial cells (Fischer et al., 2014). Therefore, the development of epithelial cell–cell junctions is controlled by both biochemical inputs via protein–protein interactions and assembly of junctional complexes as well as biophysical inputs via actomyosin behavior and actin dynamics.

Mechanistically, how biochemical and biophysical inputs regulate the assembly and maturation of epithelial junctional complexes is unclear but likely to depend on multiple and sequential molecular events. Cadherin has different binding affinity states that can be influenced by its interactions with the catenins (Yap et al., 1998; Imamura et al., 1999; Thoreson et al., 2000; Chu et al., 2004; Bajpai et al., 2009, 2013; Petrova et al., 2012; Shashikanth et al., 2015). Regulating the interaction between cadherin and the catenins provides one level of regulation (Qin et al., 2005). Reg-

ulating the interaction between actin filaments and the cadherin–catenin complex provides another level of regulation (Buckley et al., 2014). Regulating the interactions between the cadherin–catenin complex and other junctional actin-binding components such as α-actinin and vinculin provides additional control over complex cellular processes (Hazan and Norton, 1998).

Both α-actinin and vinculin bind to a central region of α-catenin (Knudsen et al., 1995; Nieset et al., 1997; Imamura et al., 1999) that is necessary for promoting force-induced strengthening of cadherin-mediated adhesion (le Duc et al., 2010; Huveneers and de Rooij, 2013; Thomas et al., 2013; Barry et al., 2014), stimulation of junction development (Watabe-Uchida et al., 1998; Twiss et al., 2012), and organization of junctional actin structures (Taguchi et al., 2011; Huveneers and de Rooij, 2013). The vinculin/α-actinin–binding domain (VAABD) of α-catenin is usually buried within the cadherin–catenin complex (Ishiyama et al., 2013) but can be exposed/opened by exogenous mechanical force (Yao et al., 2014; Kim et al., 2015) or endogenous actomyosin contractility (Yonemura et al., 2010). Unfolding of α-catenin can be triggered by a combination of actin filament and a fragment of vinculin, corresponding to a region that is usually buried in the full-length molecule (Rangarajan and Izard, 2012). Exposure of the buried α-catenin–binding site on vinculin requires unfolding of vinculin from an autoinhibited closed configuration (Johnson and Craig, 1995a,b; Bakolitsa et al., 2004), which can be stimulated by a combination of actin filaments and a fragment of α-catenin, corresponding to the central region of α-catenin that is usually buried (Choi et al., 2012; Peng et al., 2012). Thus, in addition to the requirement of actin filament for the activation of α-catenin and vinculin, either α-catenin or vinculin needs to be in a preactivated open configuration before they can activate the other. The complexity of junction regulation is further revealed by the findings that vinculin shows a delayed response to tension-induced conformational changes in α-catenin (Kim et al., 2015) and does not have an obligatory role in cell–cell adhesion and morphogenetic events (Ozawa, 1998; Maiden et al., 2013). Less is known about the role of α-actinin in cell–cell adhesion and junction regulation.α-Actinin colocalizes with the cadherin–catenin complex, vinculin, and actin at the apical junction and lateral membrane of epithelial cells (Drenckhahn and Franz, 1986; Tang and Brieher, 2013). Upon junction maturation, α-actinin preferentially colocalizes with the cadherin–catenin complex at the apical junction and becomes TX-100 insoluble (Tang and Brieher, 2013). Exogenous expression of a chimera E-cadherin–α-catenin protein in CHO cells results in accumulation of α-actinin to sites of cell–cell contacts, indicating that E-cadherin–α-catenin plays an instructive role in α-actinin recruitment (Tang and Brieher, 2012).

α-Actinin contains an actin-binding domain (Otey and Carpen, 2004; Sjöblom et al., 2008), a central spectrin repeat that can bind to α-catenin and vinculin (McGregor et al., 1994; Nieset et al., 1997), and a tail region with EF hands that confers calcium and phosphoinositide regulation (Rosenberg et al., 1981; Noegel et al., 1987; Witke et al., 1993; Tang et al., 2001; Corgan et al., 2004; Franzot et al., 2005). α-Actinin exists as an antiparallel dimer via high-affinity interactions between the spectrin repeats (Flood et al., 1997) and thus acts as an actin filament cross-linker. The mechanical and dynamical properties of actin filament gels is influenced by the affinity of α-actinin to actin (Wachsstock et al., 1993; Broedersz et al., 2010; Yao et al., 2011, 2013), which can be regulated by α-actinin phosphorylation (Zhang et al., 2005; Travers et al., 2013). The actin-binding domain of α-actinin is required for its actin assembly activity (Tang and Brieher, 2012). However, the central spectrin repeats of α-actinin alone are sufficient for junctional targeting (Hijikata et al., 1997), indicating that α-actinin is recruited to the membrane via junctional proteins other than actin filaments. α-Actinin can interact with vinculin (Belkin and Koteliansky, 1987; Wachsstock et al., 1987; McGregor et al., 1994; Kelly et al., 2006) and is capable of activating vinculin in the absence of actin filament (Bois et al., 2005, 2006). The vinculin-binding site of α-actinin is located within the spectrin repeat of α-actinin, which is usually buried in between the dimer interfaces of α-actinin (Bois et al., 2005, 2006). However, spectrin repeats are flexible and can form stable stretched intermediates under force to expose the vinculin-binding site (Rief et al., 1999; Lenne et al., 2000; Ylänne et al., 2001; Ortiz et al., 2005). Binding of α-actinin to vinculin can dramatically shift the energy landscape of vinculin to expose multiple protein-interacting regions, including a binding site for filamentous actin on vinculin (Bois et al., 2005, 2006). Consequently, binding of vinculin to the vinculin-binding site of α-actinin results in conformational changes throughout the rest of α-actinin (Shams et al., 2012), potentially contributing to tension sensing and altering the overall protein–protein interaction landscape at the junction (Altmann et al., 2002; Law et al., 2003; Hampton et al., 2007). Thus, α-actinin may be part of a mechanotransduction mechanism for vinculin recruitment to the cadherin–catenin complex. Besides binding to α-catenin and vinculin, α-actinin also interacts with other junctional proteins, including ADIP (Asada et al., 2003), LMO7 (Ooshio et al., 2004), LPP (Hansen and Beckerle, 2008), MAGI (Patrie et al., 2002), and β-catenin (Catimel et al., 2005; Gujral et al., 2013).

In this study, we provide evidence for a central role of α-actinin in the regulation of vinculin and actin accumulation at the junction. We have identified synaptopodin as an upstream regulator of α-actinin that modulates junction maturation through α-actinin–dependent strengthening of cell–cell adhesion and actin assembly.

Results

The epithelial junction is a large membrane-associated structure ∼150 nm in size that supports α-actinin-4–dependent actin assembly

Mature epithelial junction in polarized epithelial cells is a membrane specialization that associates with a cytoplasmic density of ∼150–200 nm (Fig. S1 A). Super-resolution microscopy shows that E-cadherin at the apical junction forms clusters of ∼200–250 nm (Wu et al., 2015). Our goal is to understand the assembly and regulation of this junctional complex. We have previously developed a biochemical protocol to study actin assembly using purified junctional membranes (Fig. S1, B and C). Correlating structural information using EM and biochemical information from ex vivo samples is fundamental to the discoveries of both the molecular composition and structure–function relationships in the junction field, including the adherens, tight, and gap junctions (Goodenough and Revel, 1970, 1971; Goodenough, 1975; Kensler and Goodenough, 1980; Colaco and Evans, 1981; Stevenson and Goodenough, 1984; Stevenson et al., 1986; Tsukita and Tsukita, 1989; Tsukita et al., 1989a,b; Itoh et al., 1991; Stauffer et al., 1991). EM approaches can generate information to fill the resolution gap between light microscopy and crystallography. In addition, EM has recently been used to determine structural organization of proteins within a large macromolecular complex (Huang et al., 2014; Schlager et al.,

2014; Shukla et al., 2014; Staals et al., 2014; Durand et al., 2015; Peisley and Skiniotis, 2015). Thus, we would like to get some basic understanding of the overall structural organization of the junctional complex to aid the design of our experiments. For example, whether the complexes are stable and how heterogeneous the complexes are will determine the approaches and the conclusions that we can draw. Using immunogold labeling of α-actinin-4, we found that α-actinin-4 is localized to discreet domains on the purified membranes (Fig. S1 A). Exogenous addition of actin monomers to the purified membranes results in actin polymerization and attachment (Fig. S1, E–G) at sites of α-actinin accumulation (Fig. S1 H), indicating that actin assembly is coupled to filament association with the junctional complex.

We have previously shown, using immunofluorescence microscopy, that E-cadherin, α-catenin, β-catenin, and α-actinin-4 colocalize to the junctional complex on TX-100–extracted membranes and in cells after detergent TX-100 extraction (Tang and Brieher, 2012, 2013). Here, we show that the apical junction retains a cytoplasmic density of ∼150 nm under the electron microscope after extraction with TX-100 (Fig. S1 I). Detergent-extracted junctional complexes that contain α-actinin-4 are heterogeneous in size, ∼100–200 nm (Fig. S2, A and B). Detergent-extracted junctional complexes can support actin assembly in the presence of exogenously added actin monomers and show multiple interactions with actin filaments (Fig. S2, C and D). In the absence of detergent, junction-enriched membranes can be found to consist of discreet globular densities aligned in a row where a single actin filament is being held (Fig. S2, E and F). Several actin-binding proteins are associated with cell junctions, including α-actinin, vinculin, α-catenin, eplin, and afadin. Dissecting the structural organization and assembly of the junctional complex is essential for understanding the molecular mechanisms governing actin assembly and epithelial junction development.

The formation of a membrane complex of this size cannot be trivial even for a cell, which can synthesize and fold all of the essential protein components. Multiple molecular and biochemical events are most likely to be required for individual components to come together in the right configurations within the context of the membrane and cell–cell interactions. Our goal is to understand how cells assemble the membrane junctional complex by first characterizing the overall temporal and spatial parameters for cell junction formation.

α-Actinin-4 is required for vinculin recruitment and junction maturation

During normal epithelial maturation, actin and α-actinin-4 accumulated at the cell junction over a period of several days (Fig. 1 A). By the second day post-confluence (2 dpc), most canonical junctional components, E-cadherin, α-catenin, and β-catenin, p120-catenin, and ZO-1, were already present (Fig. 1, A and B). However, vinculin has not been targeted at this early stage of junction development (Fig. 1 B). By 5 dpc, α-actinin-4 and vinculin became localized to the cell junction (Fig. 1 B). During this maturation period, the permeability barrier of the epithelial cell monolayer gradually formed (Fig. 1 C). Knockdown of α-actinin-4 prevented this maturation process and compromised the development of the barrier function (Fig. 1 C), indicating that α-actinin-4 recruitment is part of a normal maturation process during junction development. We have previously built a pressure chamber device that can deliver hydrostatic pressure to the intercellular junction to study the strength of cell–cell adhesion in an epithelial cell monolayer (Tang and Brieher, 2013). Using this setup, we show that intercellular stress induces α-actinin-4 knockdown cells to break away from each other (Fig. 1 D) and eventually detach from the monolayer (Fig. 1 E), suggesting that cell–cell adhesion has been compromised.

Knockdown of α-actinin-4 abolished junctional accumulation of vinculin (Fig. 1 F) without changing the cellular levels of vinculin (Fig. 1 G). Thus, α-actinin-4 is incorporated into the maturing junctional complex before vinculin targeting and behaves as an upstream regulator of vinculin at the cell junction during junction maturation.

We have previously built a pressure chamber device that can deliver hydrostatic pressure to the intercellular junction to study the strength of cell–cell adhesion in an epithelial cell monolayer (Tang and Brieher, 2013). Using this setup, we show that intercellular stress induces α-actinin-4 knockdown cells to break away from each other (Fig. 1 F) and eventually detach from the monolayer (Fig. 1 G), suggesting that cell–cell adhesion has been compromised.

MDCK cells exert forces on junctions through a myosin II–dependent mechanism

To further characterize the temporal and spatial regulation of α-actinin-4 during junction maturation, we imaged α-actinin live in MDCK cells (Fig. 2). We observed two main characteristics: (1) junction mobility along the length of the junction and (2) junctional deflection perpendicular to the junction. First, the length within the individual junction oscillated during junction maturation (Fig. 2, A, B, D, and E; and Videos 1, 2, and 3). But as the junction matured, these fluctuations subsided (Fig. 2, F and G). Application of blebbistatin abolished the length oscillations (Fig. 2 H), indicating that the behavior is caused by myosin II activities, which is in agreement with the presence of myosin II–dependent tension along the length of epithelial junction (Wu et al., 2014).

More intriguingly, we observed junctional deflection perpendicular to the plasma membrane (Fig. 2, I and J; and Videos 4, 5, and 6), which lead to a transient decrease or increase in the apical diameter of the cell (Fig. 2 K). Fluctuations in apical cell radius have also been described in dynamic cell rearrangements (Blanchard et al., 2010), and variations in apical cell diameters have been shown to correlate with cell shape changes during morphogenetic cell movements (Roh-Johnson et al., 2012; Razzell et al., 2014). In addition, these junctional deflections may be a mechanotransduction mechanism similar to the tugging deflections seen at cell substrate adhesions (Plotnikov et al., 2012; Plotnikov and Waterman, 2013). The force required to induce deflection of cell junction has been experimentally measured to be ∼100 pN, a force that can be supplied by a few tens of myosin II molecules (Bambardekar et al., 2015). Junctional tugging was especially prominent at stable α-actinin–enriched junctional puncta (Videos 7, 8, and 9). Tugging between neighboring cells led to positive and negative junctional deflections, resulting in fluctuations in the apical cell diameter (Fig. 2 L and Videos 7, 8, 9, and 10). The frequency of tugging increased as the epithelial monolayer matured (Fig. 2 M) and was dependent on endogenous myosin II activities (Fig. 2 N). On occasions, actin bundles emanating from epithelial junction could be found to directly connect to the cellular contractile apparatus (Fig. 2 O).

Design of a pressure chamber to apply hydraulic pressure to cell–cell adhesion in a cell monolayer

Endogenous contractions acting on cell junctions can create tension at cell–cell adhesions and may be a mechanism to

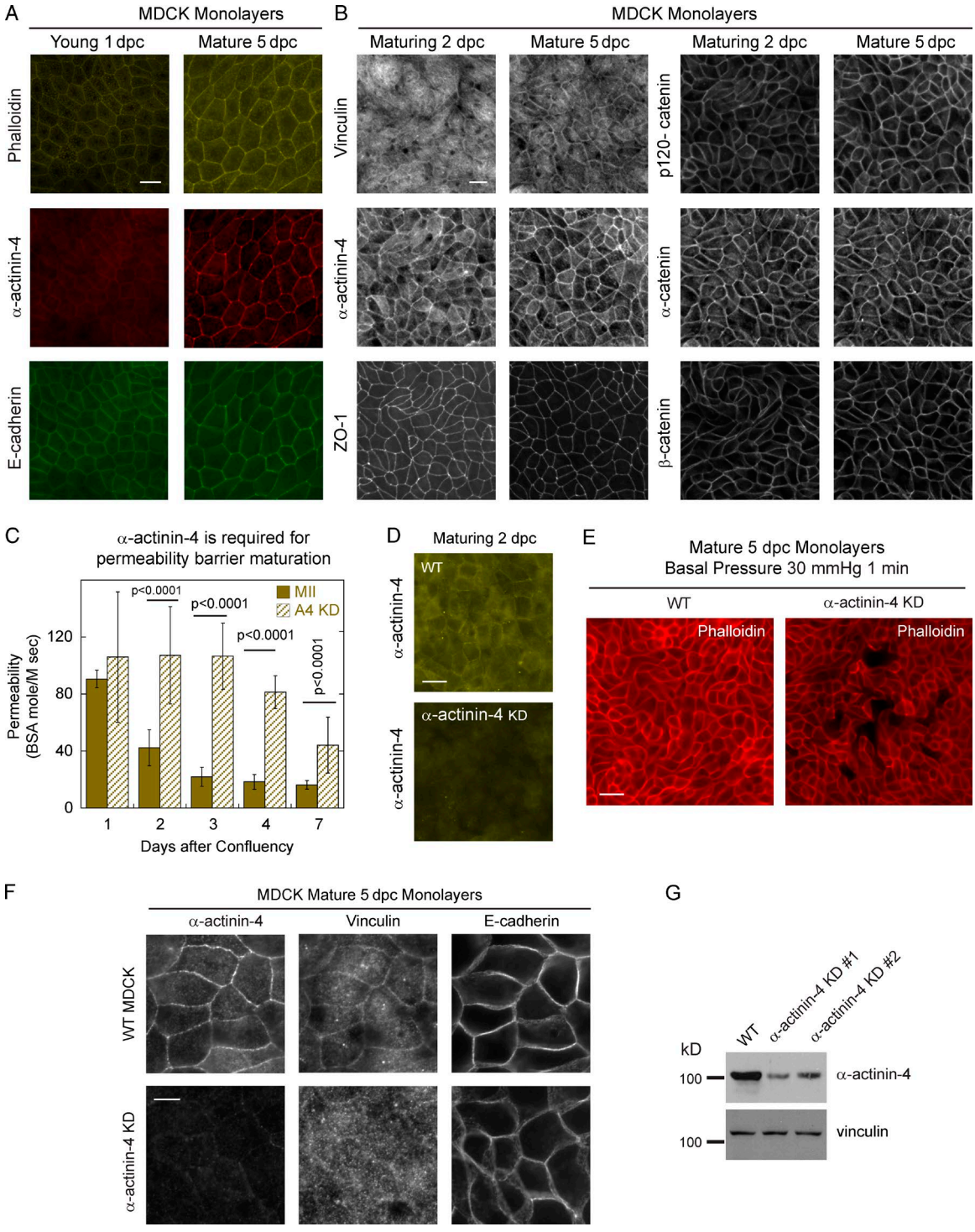

Figure 1. **α-Actinin-4 is required for vinculin recruitment, permeability barrier formation, and cell–cell adhesion strengthening during junction development.** (A) Wide-field immunofluorescence images showing accumulation of α-actinin-4 and actin at the cell junction from young 1 dpc to mature 5 dpc monolayers. (B) Wide-field immunofluorescence images showing α-actinin-4 accumulation preceding that of vinculin at the maturing junction in 2 dpc monolayers. (C) BSA flux assays showing maturation of barrier function over several days, which is compromised in α-actinin-4 knockdown cells. Error bars are standard errors. $n = 3$. (D) Wide-field immunofluorescence images showing lack of junctional vinculin in α-actinin-4 knockdown cells. (E) Wide-field fluorescence images showing holes in the α-actinin-4 knockdown cell monolayer after mechanical stress. (F) Wide-field immunofluorescence images showing mechanical stress to cell–cell adhesion results in disruption of α-actinin-4 knockdown in the 2 dpc cell monolayer. (G) Western blots showing normal levels of vinculin in α-actinin-4 knockdown cells. Bars, 10 μm.

control α-actinin-4 targeting and junction maturation. To further study the role of mechanical force in the assembly of junctional complexes, we induced junctional tension by applying hydraulic pressures to cell–cell adhesions (Fig. S3, B–D). We modified the pressure chamber apparatus to deliver cyclic or pulsatile mechanical force to cell junction in an epithelial

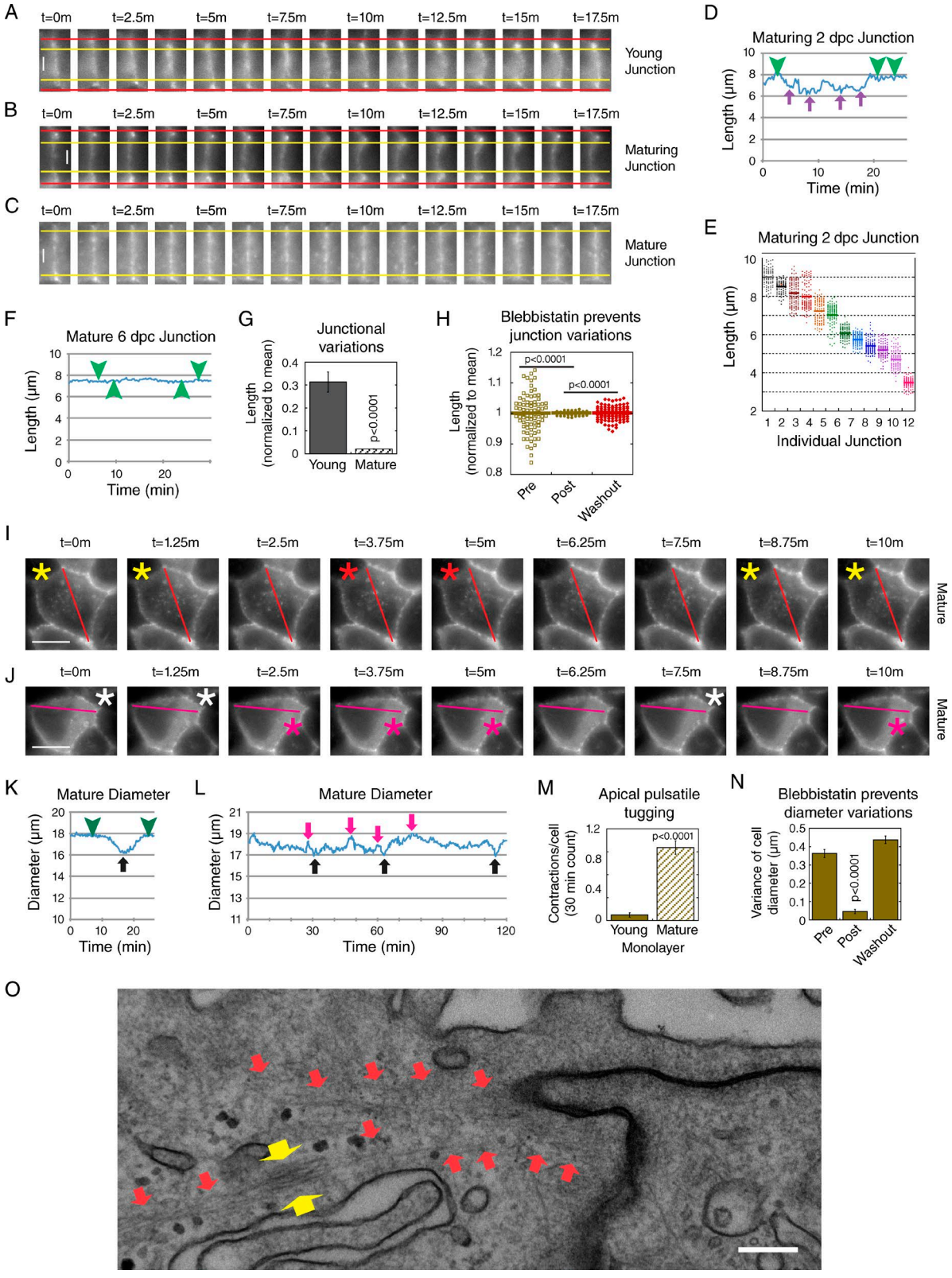

Figure 2. **MDCK cells exert forces on junction through myosin II–dependent contractility.** (A–C) Time-lapse frames showing oscillations in junctional lengths of young and maturing monolayers. (D) Measurements in maturing monolayer showing junctional length deviations (purple arrows) from steady state (green arrowheads). The trace shown is from a single representative experiment out of 12 traces. (E) Plotting of 12 individual junctional lengths shows variations independent of the absolute lengths. (F) Measurements of mature monolayer showing junctional length (green arrowheads) with a flat steady state baseline. The trace shown is from a single representative experiment out of six traces. (G) Variations of junctional length decrease with maturation of cell monolayer. $n = 6$. (H) Blebbistatin inhibits oscillations of junctional length. (E and H) Means are represented by horizontal lines. (I and J) Time-lapse frames of mature monolayer showing transient increases in cell diameter (red and pink asterisks) from original (yellow and white asterisks) diameter. Pink and red lines show the diameters of cells used for analysis. (K) Measurements of cell diameter in maturing monolayer showing decrease in diameter (black arrow) away

monolayer (Fig. S3 E). Using this pressure chamber, a cell monolayer can be subjected to cyclic, pulsatile, or sustained physiological (0–15 mmHg) or pathological (15–30 mmHg) pressures using a push-pull syringe pump.

The strength of the cell junction is a function of the adhesive bonds and the number of adhesions between cells

To guide our experiments, we used previously published measurements of cell–cell adhesive forces of ∼1–4 nN/μm^2 (Chu et al., 2004; du Roure et al., 2005; Martinez-Rico et al., 2005; Bajpai et al., 2009; Ladoux et al., 2010; Maruthamuthu et al., 2011; Ng et al., 2012; Tseng et al., 2012) to approximate the upper limit of hydraulic pressure that an epithelial cell monolayer could withstand (Fig. S4 A). The breakage force of a cell monolayer is estimated based on the surface area of the lateral cell membrane, thus the contact area and number of cell–cell contacts (Fig. S4 B). From these defined parameters, we calculated that young monolayers that are spread thinner with less cell–cell contact area have an upper limit of <5 mmHg, whereas mature cells that are taller with smaller diameters have an upper limit of >30 mmHg. From these calculations, we predicted that the tolerance level of an epithelial cell monolayer would increase over the course of monolayer maturation process simply because of geometry change. To eliminate the variations in temporal parameters, we synchronized the cell monolayers (Fig. S4 C; see Materials and methods) and showed that cyclic pressure of 10 mmHg would disrupt the barrier function of young monolayers, whereas the same amount of pressure would enhance the barrier function of maturing monolayers (Fig. S4 D). These observations indicate that the maturity of the cell junction determines the strength of cell–cell adhesion as well as the type of response to mechanical force. Thus, an epithelial monolayer can store biophysical information temporally, in addition to biochemical changes that occur during junction maturation.

Mechanical force induces α-actinin-4 recruitment to cell junctions and activates cellular contractility

To assess the effect of mechanical force on α-actinin-4 recruitment, we empirically tested cyclic, pulsatile, sustained pressure parameters, including the level of pressure, the duration of pressure application, the frequency of cyclic pressure, and the duration of pauses between cycles of pulsatile pressures (Fig. 3 A). We found two distinct responses: (1) increased accumulation of α-actinin-4 at the junction and (2) induction of cell extrusion (Fig. 3 A, red arrowheads). Tension-induced α-actinin-4 response depended on the intensity of applied pressure, the number of pressure cycles, and maturity of the cell junction, whereas tension-induced cell extrusion depended on the waveform of the applied pressure and the duration of the pressure experiment. In addition, young and mature monolayers exhibited different sensitivity and response. The induction of cell extrusion by cyclic pressure implicated activation of endogenous cellular contractility. Indeed, inhibition of endogenous myosin II activities with blebbistatin completely blocked tension-induced cell extrusion without affecting tension-induced α-actinin-4 recruitment (Fig. 3 B). Thus, tension-induced α-actinin-4 recruitment is myosin II independent, whereas tension-induced contractility requires myosin II activity. Tension-induced recruitment of α-actinin-4 was not isoform specific because exogenously expressed venus–α-actinin-1 also relocated in a tension-sensitive manner (Fig. 3 C). Tension-induced recruitment of α-actinin-4 was not caused by increased expression of cellular α-actinin-4, which was unchanged after 60 min of pressure treatment (Fig. 3 D). In general, application of sustained pressure had a less pronounced effect on α-actinin-4 recruitment than pulsatile and cyclic pressure cycles that had a comparable force-time product (amount of pressure × duration of pressure applied to the monolayer; Fig. 3 E).

Knockdown of α-actinin-4 abolishes tension-induced vinculin recruitment to the junction

Application of low cyclic pressure of ∼1 mmHg for 15 min induced redistribution of α-actinin-4 and vinculin from the cytoplasm to the junction in maturing 2 dpc monolayers (Fig. 4 A) without altering their total cellular levels (Fig. 4 B). This amount of mechanical force (∼10–30 nN force per cell depending on the size of spread area) was within the range that can be generated by MDCK cells, which has been measured to be ∼100 nN between a cell pair (Maruthamuthu et al., 2011). The redistribution of α-actinin-4 and vinculin was accompanied by a shift in TX-100 solubility of α-actinin-4 and vinculin from mostly TX-100 extractable in 1 dpc monolayers to mostly TX-100 insoluble in pressure-treated and mature monolayers (Fig. 4 B). Consistent with our earlier observation that junction localization of vinculin requires α-actinin-4 (Fig. 2 F), knockdown of α-actinin-4 completely abolished tension-induced vinculin recruitment to the junction and redistribution to the TX-100–insoluble fraction (Fig. 4, C and D), indicating that α-actinin-4 is an upstream regulator of vinculin targeting in MDCK cell monolayers. We have previously shown that α-actinin-4 plays an important role in actin assembly at epithelial junctions (Tang and Brieher, 2012). Here, we show that pretreatment of maturing monolayers with low cyclic pressure for 5 min was sufficient to induce actin accumulation and subsequently protect the cell monolayer from gross mechanical disruption by a high dose of pressure (Fig. 4 E).

Mechanical force induces actin accumulation at cell junction

Quantitation of deconvolved optical sections showed a sixfold increase in α-actinin-4 and a twofold increase in actin accumulation without dramatically changing the levels of canonical adherens junction proteins (Fig. 5, A and B). In mature cells where α-actinin-4 is already localized, a higher pressure was

from steady state (green arrowheads). The trace shown is from a single representative experiment out of seven traces. (L) Measurements of cell diameter in mature monolayer showing fluctuations with transient decrease (black arrows) and increases (pink arrows). The trace shown is from a single representative experiment out of six traces. (M) Centripetal apical junctional tugging persists in mature monolayers. n = 40. (N) Blebbistatin inhibits centripetal apical junctional tugging. n = 30. (G, M, and N) Error bars are standard errors. (O) Contractile apparatus is associated with cell–cell junction in T84 epithelial cells. Yellow arrows point to dense bodies, characteristic of myosin II–containing sarcomeric contractile unit, with associating actin filaments attached to the cell junction (red arrows). Bars: (A–C) 2 μm; (I and J) 10 μm; (O) 100 μm.

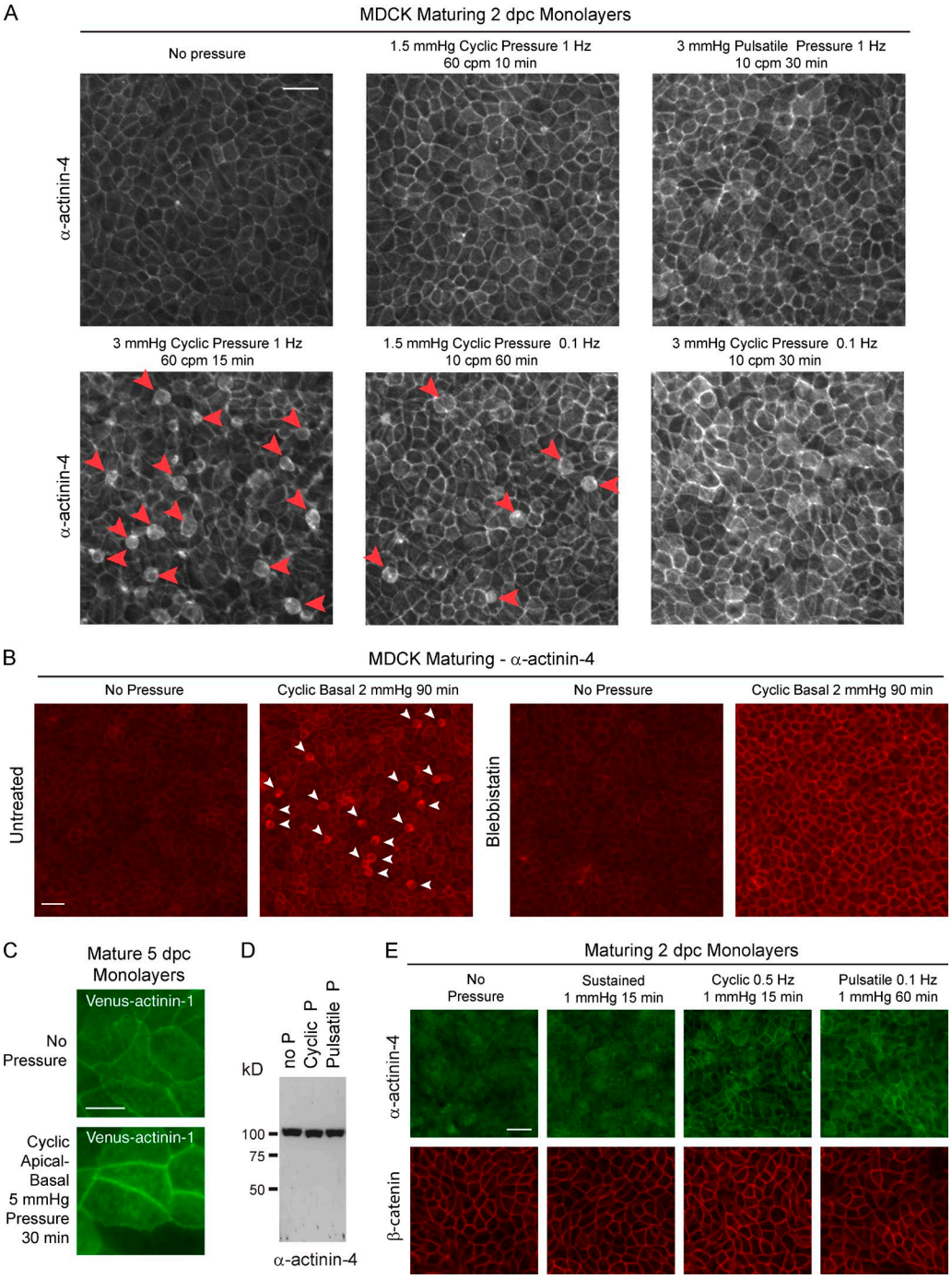

Figure 3. **Application of hydraulic pressure to cell monolayers induces α-actinin-4 recruitment to cell junction and activates cellular contractility.** (A) α-Actinin-4 recruitment can be induced by various durations and frequencies (Hz) of cyclic or pulsatile pressures in cycles per minute (cpm). Prolonged cyclic pressure induces α-actinin-4 recruitment and induces cell extrusion (red arrowheads). (B) Wide-field immunofluorescence images showing tension-induced cell extrusion (arrowheads) blocked by blebbistatin. (C) Wide-field images of venus–α-actinin-1 showing tension-induced localization at the cell junction. (D) Western blot showing unchanged levels of α-actinin-4 after pressure treatment. (E) Wide-field immunofluorescence images showing junction accumulation of α-actinin-4 after cyclic and pulsatile pressure. Bars, 20 µm.

required to trigger a mechanical-induced response (Fig. 5, C and D). These results show that the sensitivity of junctional complexes to mechanical stimuli depends on the maturity of the junction. Prolonged application of cyclic pressure in maturing junction resulted in reduction in junctional accumulation of β-catenin and p120 (Fig. 5, E and F). However, tension-stimulated α-actinin-4 recruitment remained intact (Fig. 5 G), suggesting that additional factors other than the known canonical junctional proteins are involved. Previously, we used chemical cross-linking to identify interacting proteins of α-actinin-4 in a membrane preparation (Tang and Brieher, 2013). Here, we show that one of the identified proteins, synaptopodin, is localized to cell junction with β-catenin (Fig. 5 H). Synaptopodin levels were unchanged after prolonged mechanical stimulation (Fig. 5, H–J) despite reduction in β-catenin, suggesting that it might play a role in tension-induced α-actinin-4 recruitment.

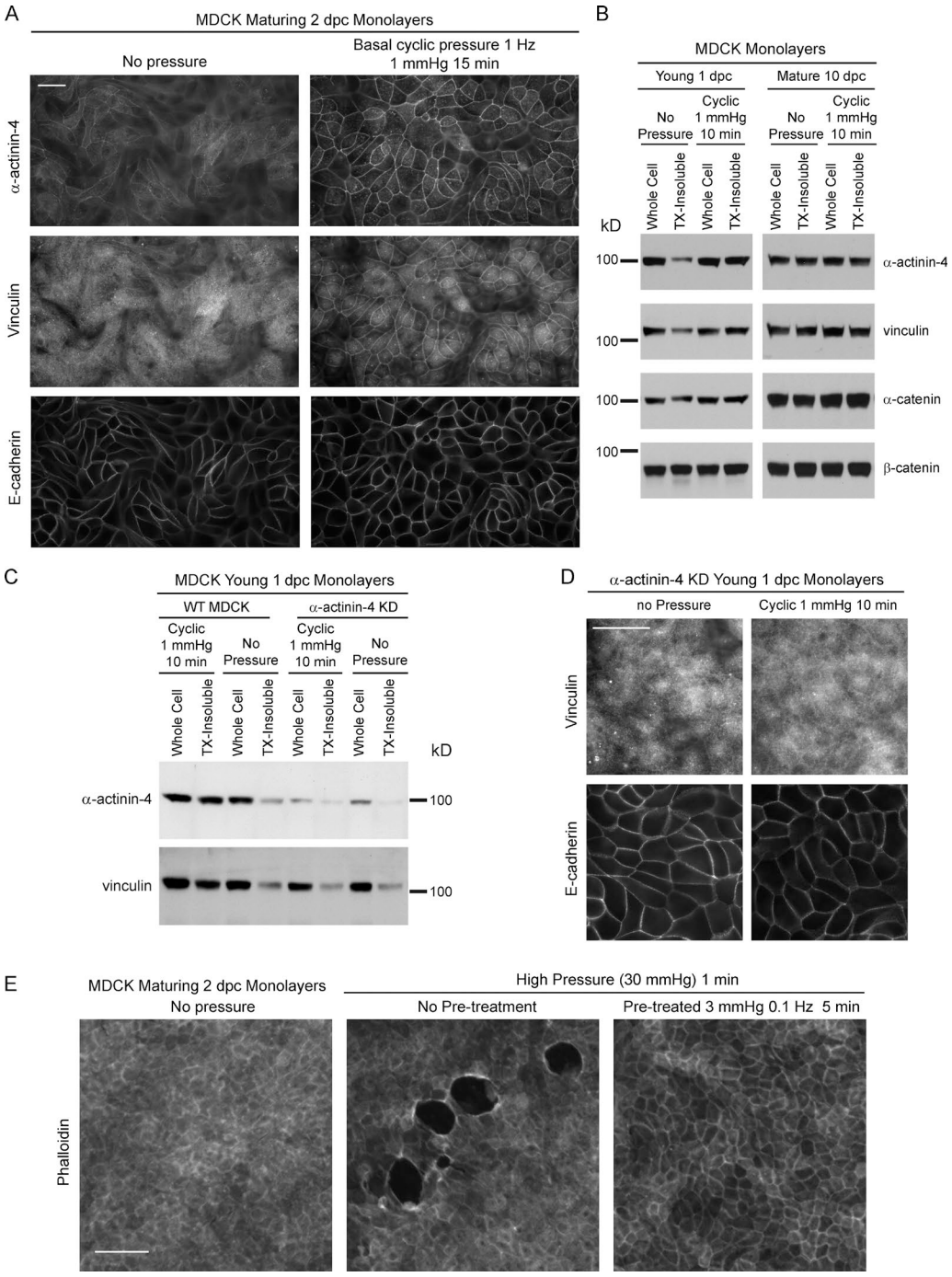

Figure 4. **Mechanical force induces α-actinin-4–dependent vinculin redistribution from the cytoplasm to the cell junction.** (A) Wide-field immunofluorescence images showing tension-induced α-actinin-4 and vinculin accumulation at the cell junction. (B) Western blots showing tension-induced redistribution of α-actinin-4 and vinculin into the TX-100–insoluble pool. (C) Knockdown of α-actinin-4 prevents tension-induced vinculin incorporation into the TX-100–insoluble pool. (D) Knockdown of α-actinin-4 prevents tension-induced vinculin targeting to the cell junction. (E) Wide-field immunofluorescence images showing pretreatment of young monolayer with low cyclic pressure for 5 min strengthened cell–cell adhesions and prevented subsequent disruption by mechanical insult. Bars, 2 µm.

Identification of synaptopodin as a mechanosensitive junctional protein

Synaptopodin is expressed in vertebrates and shares no homology with other proteins (Fig. 6 A). Synaptopodin has been shown to interact with actin and α-actinin-4 in brain (Kremerskothen et al., 2005) and was thought to regulate α-actinin-4 function in kidney podocytes (Asanuma et al., 2005). Synaptopodin colocalizes with CD2AP at cell–cell contacts in podocytes upon formation of cell–cell interactions (Schiwek et al., 2004). In MDCK cells, synaptopodin colocalized with β-catenin on the lateral membrane and was concentrated at the apical junction with α-actinin-4, β-catenin, and E-cadherin (Fig. 6 B).

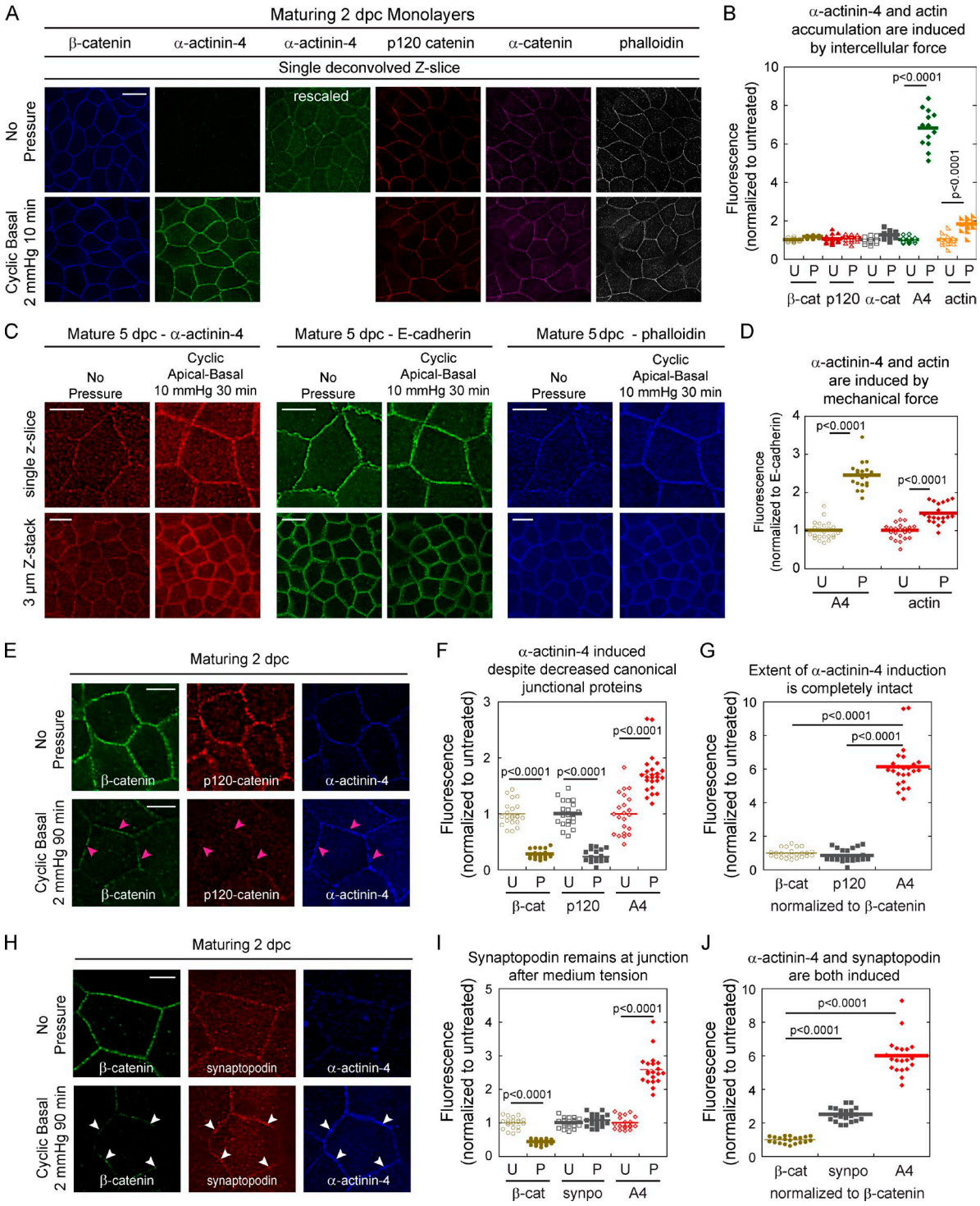

Figure 5. **Mechanical force induces α-actinin-4 and actin accumulation at the cell junction.** (A) Deconvolved optical section at the apical junction showing tension-induced α-actinin-4 and actin accumulation in maturing monolayers. (B) Quantitation of junctional stainings in A before (U) and after (P) cyclic pressure showing sixfold induction of α-actinin-4 and twofold induction of actin accumulation. (C) Deconvolved optical section and z-composites at the apical junction showing tension-induced α-actinin-4 and actin accumulation in mature monolayers. (D) Quantitation of junctional stainings in C before (U) and after (P) cyclic pressure showing a modest increase in α-actinin-4 and actin accumulation. (E) Deconvolved optical section at the apical junction showing tension-induced α-actinin-4 accumulation by prolonged cyclic basal 2 mmHg pressure despite decrease in β-catenin and p120 (pink arrowheads). (F) Quantitation of junctional stainings in E before (U) and after (P) cyclic pressure. (G) Normalization of junctional staining in E showing sixfold induction of α-actinin-4. (H) Deconvolved optical section at the apical junction showing unchanged levels of synaptopodin after prolonged cyclic pressure. White arrowheads show colocalization of synaptopodin, α-actinin-4, and β-catenin. (I) Quantitation of junctional stainings in H before (U) and after (P) cyclic pressure. (J) Normalization of junctional staining in H showing sixfold induction of α-actinin-4. (B, D, F, G, I, and J) Means are represented by horizontal lines. Bars, 5 μm.

Synaptopodin was localized to apical latrunculin-resistant actin puncta (Fig. 6 C), which are sites of α-actinin-4–dependent actin assembly (Tang and Brieher, 2012). At an early stage of junction development, synaptopodin and α-actinin-4 were poorly localized despite the presence of β-catenin at the junction (Fig. 6 D). Application of cyclic pressure induced accumulation of both synaptopodin and α-actinin-4 (Fig. 6, D and E), indicating that synaptopodin targeting is also tension sensitive. Quantitation of junctional staining showed a strong correlation between α-actinin-4, E-cadherin (Fig. 6 F), and synaptopodin (Fig. 6 G) before and after cyclic pressure. Importantly, both synaptopodin and α-actinin-4 correlated with actin levels before and after cyclic pressure (Fig. 6, H and I), suggesting that they function together in actin assembly at the junction. Upon junction maturation, low cyclic pressure no longer had any effect on synaptopodin and α-actinin-4 recruitment (Fig. 7, A and B), suggesting that the mature junction had reached a homeostatic state. Concomitant to synaptopodin targeting, cyclic pressure also induced an upward shift of synaptopodin in SDS-PAGE (Fig. 7 C), indicating that synaptopodin is modified in a tension-sensitive manner. Thus, tension-induced protein modifications may be one of the mechanisms to regulate the assembly of the junctional complex.

Synaptopodin is required for α-actinin-4 targeting to the cell junction

Knockdown of synaptopodin in MDCK cells caused a dramatic decrease in the accumulation of α-actinin-4 and actin at the junction (Fig. 7, D and E) without altering the total cellular level of α-actinin-4 (Fig. 7 F). Synaptopodin knockdown resulted in relocalization of venus–α-actinin from the cell junction to the cytoplasm in mature monolayer (Fig. 7 G), indicating that the absence of α-actinin-4 staining at the junction is not caused by a loss of antibody epitopes. Knockdown of synaptopodin slowed the development of a permeability barrier (Fig. 7 H), and the cells would physically detach from each other when faced with high mechanical stress (Fig. 7 I). In contrast, knockdown of α-actinin-4 had no significant effect on the cellular levels and junctional localization of synaptopodin (Fig. 7, J and K), indicating that synaptopodin targeting does not require α-actinin-4. Both synaptopodin and α-actinin-4 were required for tension-induced barrier enhancement (Fig. 7 L). Moreover, both synaptopodin and α-actinin-4 cells were required for adhesion strengthening (Fig. 7 M). Knockdown of synaptopodin and α-actinin-4 compromised the strength of cell junction (Fig. 7 M), although the levels of E-cadherin, occludin, β-catenin, and p120-catenin were unchanged (Fig. 7 N). Thus, synaptopodin is incorporated into the maturing junctional complex before α-actinin-4 targeting and behaves as an upstream regulator of α-actinin-4 at the cell junction during junction maturation.

Synaptopodin is required for mechanotransduction at the cell junction

Exogenous application of intercellular tension failed to rescue α-actinin-4 recruitment in synaptopodin knockdown monolayers (Fig. 8, A and B). Despite the diminished tension response, the levels of junctional α-actinin-4 remained tightly correlated with junctional synaptopodin (Fig. 8 C), indicating that tension-sensing is intact in synaptopodin knockdown cells. Thus, the defect in α-actinin-4 recruitment is likely to be caused by a downstream mechanism such as mechanotransduction or mechanoresponse rather than mechanosensation by itself.

Vinculin recruitment to cell junctions is compromised in synaptopodin knockdown monolayers

Vinculin accumulation during normal junction maturation and tension-induced targeting was absent in synaptopodin knockdown cell monolayers (Fig. 8 D). Knockdown of synaptopodin also prevented tension-induced redistribution of α-actinin-4 and vinculin to the TX-100–insoluble fraction (Fig. 8 E), consistent with the role of synaptopodin as an upstream regulator of α-actinin-4.

Synaptopodin links adhesion to contractility

We have described earlier that application of intercellular tension causes cell extrusion (Fig. 3 A). We are interested in understanding the roles of synaptopodin and α-actinin-4 in tension-induced contractility. Unfortunately, the level of tension that is required to activate endogenous cellular contractility also breaks the cells apart in synaptopodin and α-actinin-4 knockdown monolayers. Therefore, we have to find another way to assess the contribution of synaptopodin and α-acitnin-4 in junction-dependent contractility. In a cell-spreading assay that reports on the balance of forces between cell–cell and cell–substrate tension (Mertz et al., 2013), MDCK cells would form clusters on soft polyacrylamide gel, whereas synaptopodin knockdown cells would spread readily into a monolayer (Fig. 8 F), consistent with a reduction in cell–cell tension in the knockdown cells. However, cell spreading is not a direct readout of junction contractility. Therefore, we investigated wound-induced contraction that requires actomyosin activities coupled to engagement of cell–cell adhesion (Martin et al., 2010; Abreu-Blanco et al., 2011). Wounding MDCK monolayers triggered a contraction response that results in a diameter three times the original wound diameter (Fig. 8, G–I), which is comparable with observations of in vivo wounding measurements (Martin et al., 2010; Abreu-Blanco et al., 2011). In contrast, wound expansion was absent in synaptopodin and α-actinin-4 knockdown monolayers (Fig. 8, G–I), indicating a defect in tissue level contractility. Our results are consistent with other studies showing that the formation of adherens junctions leads to an increase in cell–cell adhesive strength and generation of tissue level tension (Harris et al., 2012, 2014).

Synaptopodin links adhesion to mechanotransduction

To understand the contribution of synaptopodin in the mechanotransduction pathway, we performed phospho-kinase array experiments before and after cyclic pressure (Fig. 9 A). 5 of 43 site-specific phosphorylation sites in the kinase array are activated by mechanical force. Of the 5 tension-induced phosphorylation sites, only Akt S473 was compromised in synaptopodin knockdown monolayers (Fig. 9 B). Another phosphorylation site on Akt, T308 (Fig. 9 A, gray boxes), was not induced by tension or affected by synaptopodin knockdown, indicating that the mechanoresponse is very specific. Application of cyclic pressure to cell monolayers resulted in the accumulation of phosphorylated Akt S473 at cell–cell adhesions (Fig. 9, C and D), suggesting that force-induced mechanotransduction is coupled to reorganization and assembly of epithelial junction.

Previous studies have shown that engagement of cell–cell adhesion activates PI3K signaling and Akt phosphorylation (Laprise et al., 2002, 2004; Brouxhon et al., 2013), which is

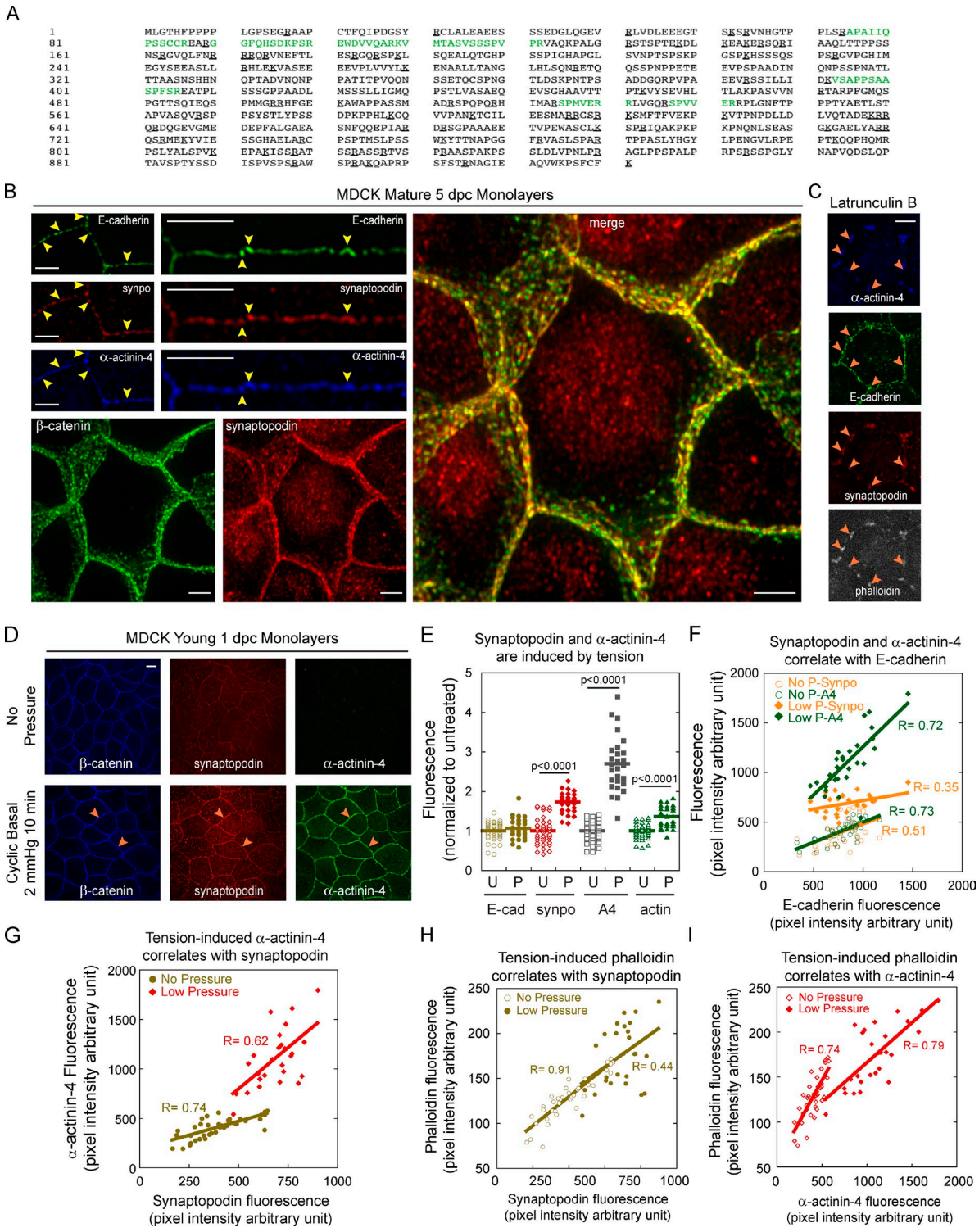

Figure 6. **Identification of synaptopodin as a mechanosensitive junctional protein.** (A) Peptides (green font) from α-actinin-4 cross-linking experiment matching synaptopodin sequence. Basic residues lysine (K) and arginine (R) are underlined. (B) Deconvolved optical section at the apical junction showing colocalization of synaptopodin, α-actinin-4, E-cadherin, and β-catenin in mature monolayer. Yellow arrowheads show colocalization of synaptopodin, α-actinin-4, and E-cadherin. (C) Deconvolved optical section at the apical junction showing colocalization of synaptopodin, α-actinin-4, E-cadherin, and actin (phalloidin) at latrunculin-resistant junctional puncta (orange arrowheads). (D) Deconvolved optical section at the apical junction showing tension-induced junctional accumulation of synaptopodin and α-actinin-4 (orange arrowheads). (E) Quantitation of junctional synaptopodin, α-actinin-4, and actin before (U) and after (P) cyclic basal 2 mmHg pressure in young monolayers. Means are represented by horizontal lines. (F) Correlation of junctional α-actinin-4 and E-cadherin before (No P) and after (Low P) cyclic basal 2 mmHg pressure in young monolayers. (G) Correlation of synaptopodin and α-actinin-4 junctional levels before (No Pressure) and after (Low Pressure) cyclic basal 2 mmHg pressure in young monolayers. (H) Correlation of synaptopodin and actin junctional levels before (No Pressure) and after (Low Pressure) cyclic basal 2 mmHg pressure in young monolayers. (I) Correlation of α-actinin-4 and actin junctional levels before (No Pressure) and after (Low Pressure) cyclic basal 2 mmHg pressure in young monolayers. (D–I) The images and quantitation shown are from a single representative experiment out of six experiments. Bars, 2 µm.

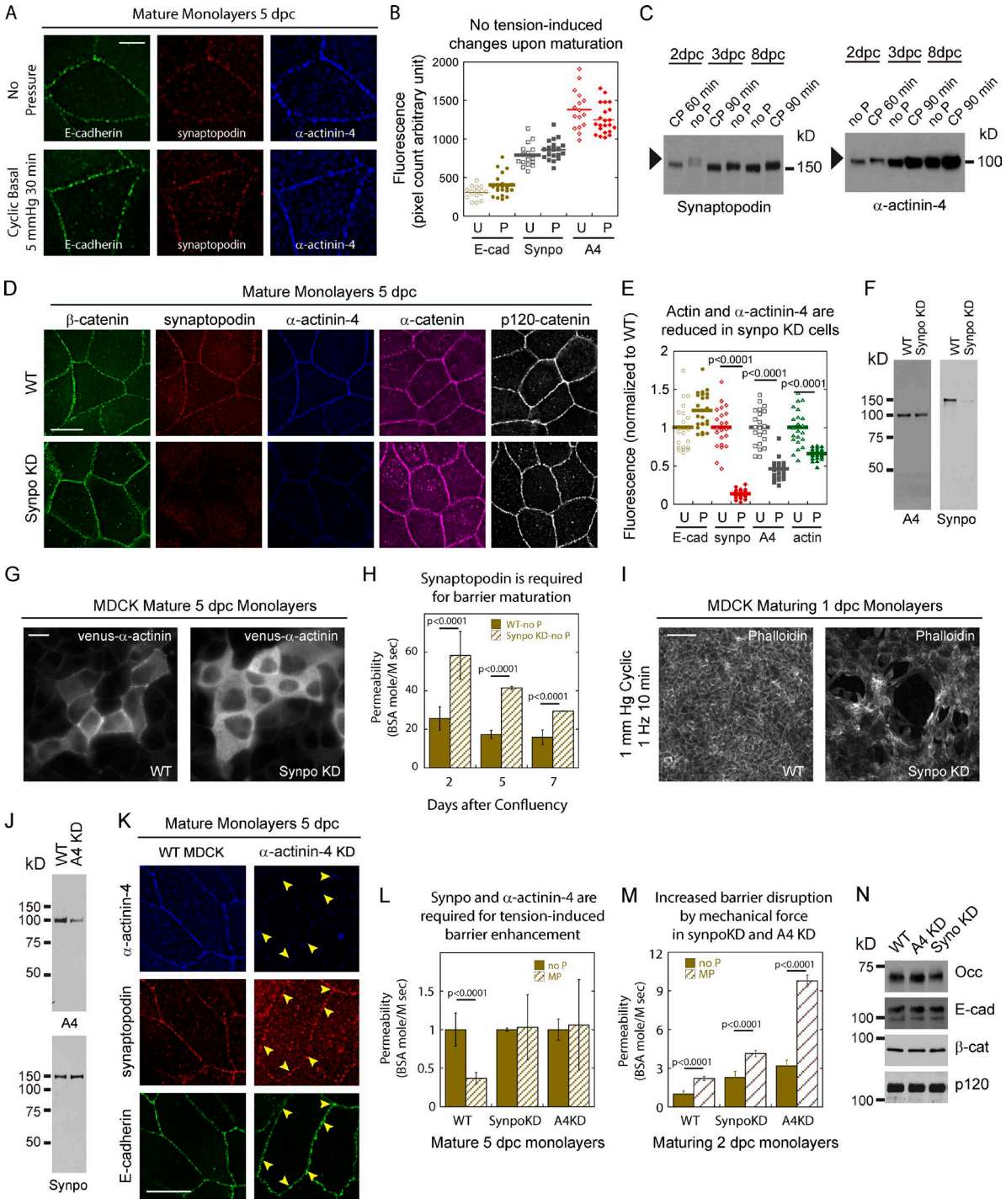

Figure 7. **Synaptopodin is required for α-actinin-4 recruitment to the cell junction.** (A) Deconvolved optical section at the apical junction showing unchanged levels of E-cadherin, synaptopodin, and α-actinin-4 after prolonged cyclic pressure in mature cell monolayer. (B) Quantitation of junctional stainings in A before (U) and after (P) cyclic pressure. (C) Western blots showing upward shift of synaptopodin (black arrowheads) in a tension-sensitive manner. (D) Deconvolved optical section at the apical junction showing decreased α-actinin-4 and actin accumulation at the cell junction in synaptopodin knockdown cells. (E) Quantification of D before (U) and after (P) cyclic pressure. (B and E) Means are represented by horizontal lines. (F) Western blots showing α-actinin-4 level unchanged by knockdown of synaptopodin. (G) Wide-field images of venus-actinin showing cytoplasmic localization in synaptopodin knockdown cells. (H) BSA flux assays showing decreased barrier formation in synaptopodin knockdown monolayers. (I) Wide-field images showing synaptopodin knockdown cells detaching from monolayer upon mechanical insult. (J) Western blots showing synaptopodin level unchanged by knockdown of α-actinin-4. (K) Deconvolved optical section showing normal synaptopodin colocalization with E-cadherin in α-actinin-4 knockdown cells (yellow arrowheads). (L) BSA flux assays showing that tension-induced barrier enhancement is absent in α-actinin-4 and synaptopodin knockdown monolayers. (M) BSA flux assays showing decreased ability to withstand mechanical insult in α-actinin-4 and synaptopodin knockdown monolayers. (H, L, and M) Error bars are standard errors. $n = 3$. (N) Western blots showing E-cadherin, occludin, β-catenin, and p120-catenin levels unchanged in synaptopodin and α-actinin-4 knockdown cells. Bars: (A, D, G, I, and K) 10 μm.

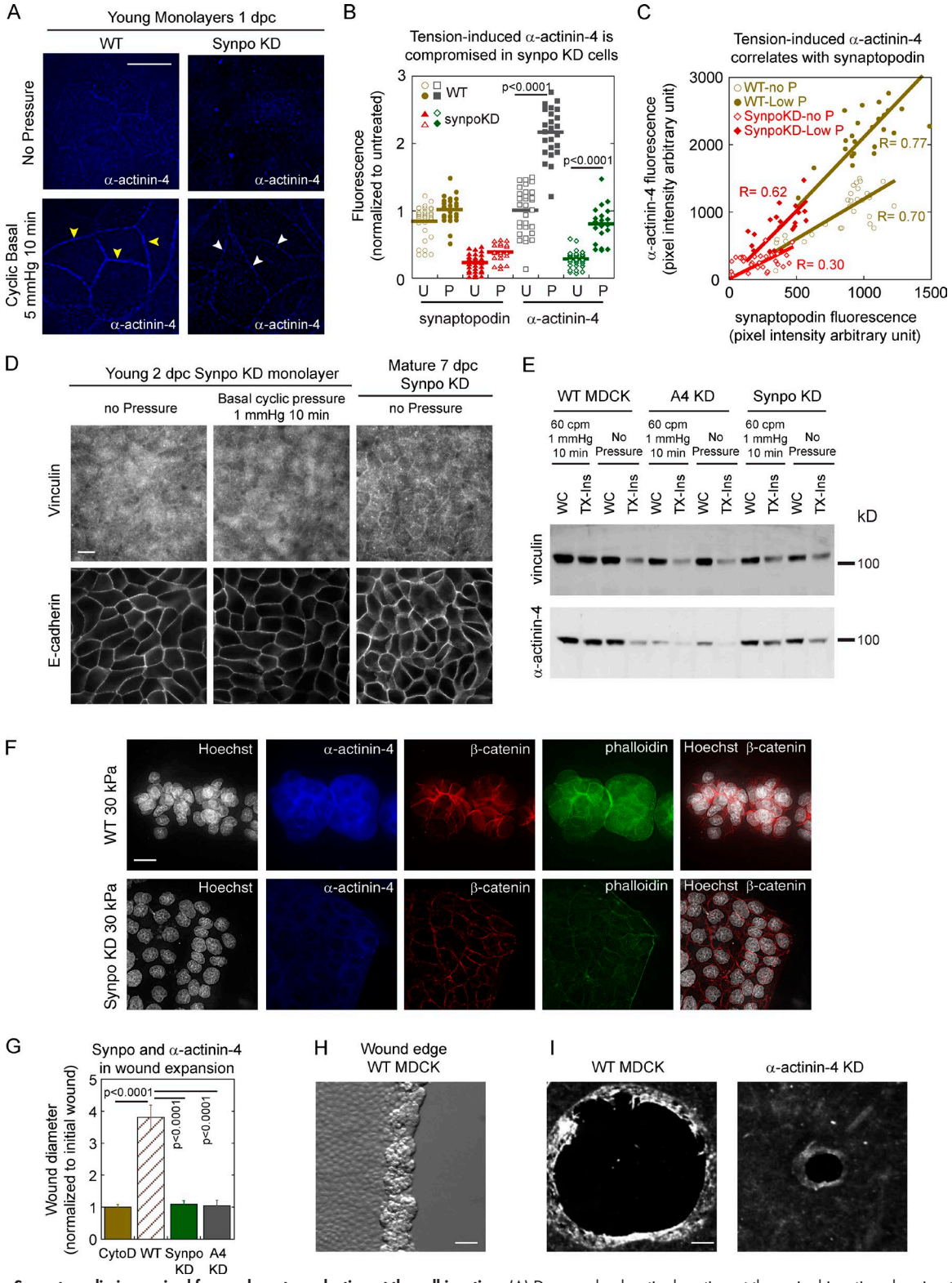

Figure 8. **Synaptopodin is required for mechanotransduction at the cell junction.** (A) Deconvolved optical section at the apical junction showing tension-induced α-actinin-4 recruitment (yellow arrowheads) is reduced in synaptopodin knockdown monolayers (white arrowheads). (B) Quantitation of junctional synaptopodin and α-actinin-4 in A before (U) and after (P) cyclic pressure. Means are represented by horizontal lines. (C) Plotting junctional levels of synaptopodin and α-actinin-4 before (no P) and after (Low P) cyclic pressure shows similar slope in tension-induced response in parental and synaptopodin knockdown cells. (A–C) The images and quantitation shown are from a single representative experiment out of three experiments. (D) Wide-field immunofluorescence images showing cytoplasmic localization of vinculin in maturing synaptopodin knockdown cells before and after cyclic pressure. Junctional localization of vinculin in mature synaptopodin knockdown monolayers is also compromised. (E) Western blots showing that redistribution of vinculin and α-actinin-4 to the TX-100–insoluble fraction induced by intercellular tension is compromised in maturing synaptopodin knockdown cells. (F) Deconvolved z-composites showing spreading of synaptopodin knockdown cells on collagen-coated polyacrylamide gel. (G) Measurements of wound diameters show-

required for the propagation and assembly of E-cadherin adhesions (Gavard et al., 2004). Our findings concur with the regulation of junctions via PI3K signaling pathways and extend the mechanism to Akt S473 phosphorylation via a synaptopodin-dependent mechanism at the cell junctions. These results show that synaptopodin is central to mechanotransduction at cell–cell adhesion and may play additional roles in tension-induced cellular processes.

Synaptopodin consists of three functional domains

To understand the function and regulation of synaptopodin, we performed a series of experiments using synaptopodin truncation mutants. We cut synaptopodin into three pieces, aa 1–600, 245–600, and 600–929. We found that synaptopodin aa 1–600 and aa 245–600 coimmunoprecipitated with endogenous α-actinin-4, β-catenin, and synaptopodin (Fig. 10 A), whereas expression of the C-terminal aa 600–929 disrupted the complex (Fig. 10 A). Interestingly, both aa 1–600 and aa 600–929 were targeted to the junction (Fig. 10, B and C), indicating that different regions of synaptopodin can interact with multiple junctional components. Previous studies have shown that substrate stiffness can regulate tension at cell–cell adhesion (Brevier et al., 2008; Ladoux et al., 2010; Liu et al., 2010; Saez et al., 2010; Maruthamuthu et al., 2011). Therefore, we tested the ability of mutant-expressing cells to respond to substrate stiffness. We found that aa 1–600 would redistribute to the cytoplasm when the cells were grown on soft silicone substrate (Fig. 10 B), suggesting that aa 1–600 contains the tension-responsive region. Consistent with these observations, application of cyclic pressure to maturing cell monolayers induced redistribution of synaptopodin aa 1–600 from the cytoplasm to cell junction (Fig. 10 C). Intriguingly, cyclic pressure wound induced cell rounding in cells expressing aa 600–929 (Fig. 10 C), suggesting that the C-terminal region of synaptopodin might link the cell–cell adhesion complex to the cellular contractile system. To identify the binding partner of synaptopodin aa 600–929, we used affinity chromatography to isolate synaptopodin aa 600–929 tagged with a streptavidin-binding domain. We pulled down one major protein and identified the protein as myosin II by mass spectroscopy analysis (Fig. 10 D). Hence, synaptopodin, through its three functional domains (Fig. 10 E), can (1) respond to mechanical force to accumulate at the cell junction, (2) form a complex with adhesion- and actin-regulating molecules, and (3) interac with myosin II. Thus, synaptopodin can physically link adhesion to the contractile machine, providing a mechanism to regulate cellular contractility by the epithelial junction. These findings provide a plausible molecular basis for the cell–cell adhesion complex to act as both a force-bearing mechanotransducing structure and a force-generating mechanoresponsive structure.

Discussion

The molecular mechanisms of sensing, transducing, and adapting to mechanical signals are not fully understood, partly because of a lack of cell culture model and methods to mechanically manipulate tension at cell–cell contacts in an epithelial sheet. Here, we have fabricated a pressure chamber that can deliver hydraulic forces to cell–cell adhesions in a monolayer of cells. In this study, we use this new setup to study how mechanical force plays an essential role in junction assembly and maturation. During a maturation process over several days, epithelial cell junctions experience both normal stress from centripetal contractions and shear stress from lateral movements. These mechanical inputs can be transmitted across cell–cell adhesions to induce junctional tension. Indeed, MDCK cells can produce substantial contractile force (Maruthamuthu et al., 2011), indicating that they can use mechanical-driven mechanisms to regulate molecular events. Coupling between cellular contractility and cell–cell adhesion is well established but not well understood at the molecular level (Conti et al., 2004; Ladoux et al., 2010; Wu et al., 2014). We observed that α-actinin-4, a protein that is required for actin assembly at junctional complex (Tang and Brieher, 2012), accumulates at the adherens junction during epithelial maturation. The accumulation of α-actinin-4 coincides with the onset of myosin II–dependent contractile activities, suggesting that mechanical forces may have a role in the maturation process. Exogenous application of intercellular force induces α-actinin-4 targeting in a time- and tension-dependent manner, with concomitant increase in actin and vinculin accumulation, adhesive strength, and permeability barrier function. Thus, endogenous cellular contractility could drive junction maturation via tension-induced recruitment of α-actinin-4. Our results show that α-actinin-4 is an upstream regulator of vinculin. However, it is unclear whether α-actinin directly recruits vinculin or indirectly recruits through an α-catenin–dependent interaction. Future experiments using more sophisticated methods to study the junction as a macromolecular assembly are necessary to dissect the molecular mechanism during tension-induced incorporation of α-actinin and vinculin.

We have identified an essential factor for α-actinin-4 accumulation at the adherens junction as synaptopodin. Synaptopodin and α-actinin-4 have been shown to bind MAGI-1 (Patrie et al., 2002), an adherens junctional protein that also binds β-catenin (Dobrosotskaya and James, 2000; Nishimura et al., 2000). MAGI-1 has also been shown to be necessary for robust cell–cell adhesion (Stetak and Hajnal, 2011) and permeability barrier function through its interaction with β-catenin (Gujral et al., 2013). Therefore, our results are consistent with earlier works and suggest that synaptopodin, MAGI-1, β-catenin, and α-actinin-4 may have functional relationships at the cell junction. Moreover, we found that synaptopodin can interact with myosin II (Fig. 10 D), providing a physical link between the adhesive contacts and the cellular contractile system. Recently, synaptopodin has been shown to play a role in shear stress–induced wound healing (Mun et al., 2014). Consistent with their observations, we show that synaptopodin is mechanoresponsive and would target to the cell junction in a tension-dependent manner. In addition, we found that synaptopodin is required for vinculin recruitment, adhesion strengthening, and epithelial barrier formation. Our results demonstrate a role for synaptopodin at cell–cell adhesion, which could help explain why disruption of synaptopodin function in kidney podocytes results in barrier

ing wound-induced contractility is absent in synaptopodin and α-actinin-4 monolayers. Error bars are standard errors. $n = 3$. (H) Phase-contrast image of wound edge of MDCK cells after 30 min of wound expansion. (I) Dark-field images of wound showing expanded wound in WT but not in α-actinin-4 knockdown cells. Bars: (A, D, and F) 10 µm; (H) 50 µm; (I) 500 µm.

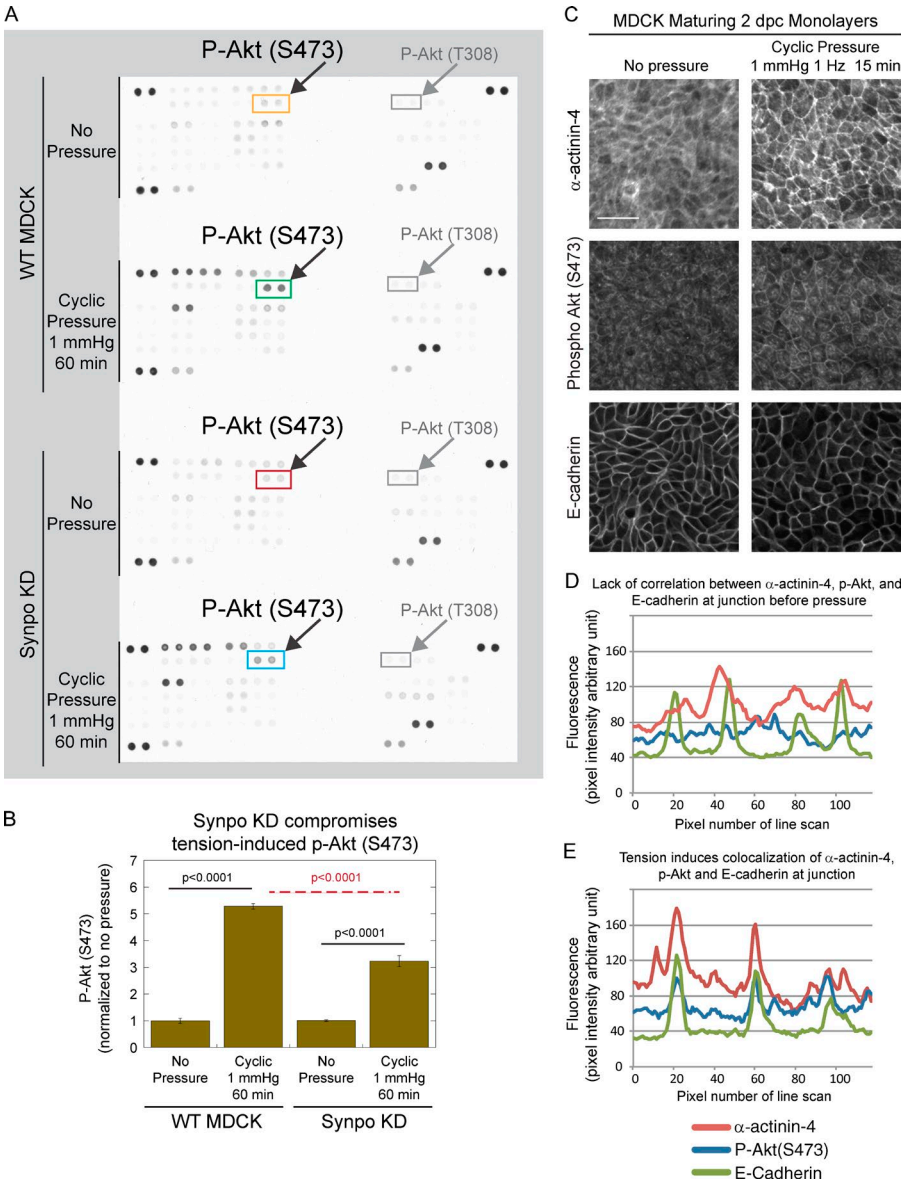

Figure 9. **Mechanical force induces Akt S473 phosphorylation that is compromised in synaptopodin knockdown monolayers.** (A) Site-specific phospho-kinase arrays (see Materials and methods for details) showing induction of Akt S473 phosphorylation by cyclic pressure that is compromised in synaptopodin knockdown cells. (B) Quantitation of A showing fivefold increase of Akt S473 phosphorylation in WT MDCK but only threefold increase in synaptopodin knockdown cells. Error bars are standard errors. $n = 2$. (C) Wide-field immunofluorescence images showing tension-induction accumulation of phospho-Akt S473 at cell junction. Bar, 50 µm. (D and E) Line scans of C showing redistribution and colocalization of E-cadherin, α-actinin-4, and p-Akt S473 after cyclic pressure. (C–E) The images and quantitation shown are from a single representative experiment out of four experiments.

disruption and proteinuria (Dai et al., 2010; Yaddanapudi et al., 2011; Kimura et al., 2013).

To summarize, this study narrowly describes cell junction development in three stages: (1) synaptopodin- and α-actinin-4–negative junction that contains E-cadherin, α-catenin, β-catenin, and p120-catenin; (2) synaptopodin-positive and α-actinin-4–negative junction; and (3) synaptopodin- and α-actinin-4–positive junction that would support vinculin targeting, actin assembly, and adhesion strengthening (Fig. S5 A). We showed that synaptopodin is incorporated into the maturing junctional complex before α-actinin-4 targeting and behaves as an upstream regulator of α-actinin-4 at the cell junction during junction maturation (Fig. 6 D). Knockdown of synaptopodin prevents α-actinin-4 targeting to the junction (Fig. 7 D). In turn, α-actinin-4 is incorporated into the maturing junctional complex before vinculin targeting and behaves as an upstream regulator of vinculin at the cell junction during junction maturation (Fig. 1 B). Knockdown of α-actinin-4 prevents vinculin targeting to the junction (Fig. 1 D). Thus, we conclude that mechanical force ushers the development of cell junction through these three stages by sequentially stimulating incorporation of tension-responsive components into maturing junctional complexes, resulting in the assembly of the final junctional structure.

Our findings uncover a new function for synaptopodin and a novel molecular mechanism explaining how epithelial contractility plays an important role in adhesion maturation and the integrity of epithelial tissue (Conti et al., 2004; Shewan et al., 2005; Miyake et al., 2006; Vasquez et al., 2014). Our results reveal a mechanism that allows cellular contractility to temporally and spatially control the recruitment of junctional components that are required for adhesion strengthening. By coupling mechanical stimuli to α-actinin-4 recruitment, synaptopodin provides a tunable molecular mechanism that can dictate the outcome of cellular contractility. In the presence of synaptopodin, cellular contractions result in adhesion strengthening, whereas in the absence of synaptopodin, contractions can disengage cell–cell adhesion, resulting in dissolution of the cell junction. Indeed, myosin II–dependent contractile forces have been shown to strengthen as well as weaken cell–cell adhesion. During cell division, myosin II activities are localized at specific membrane domains, which

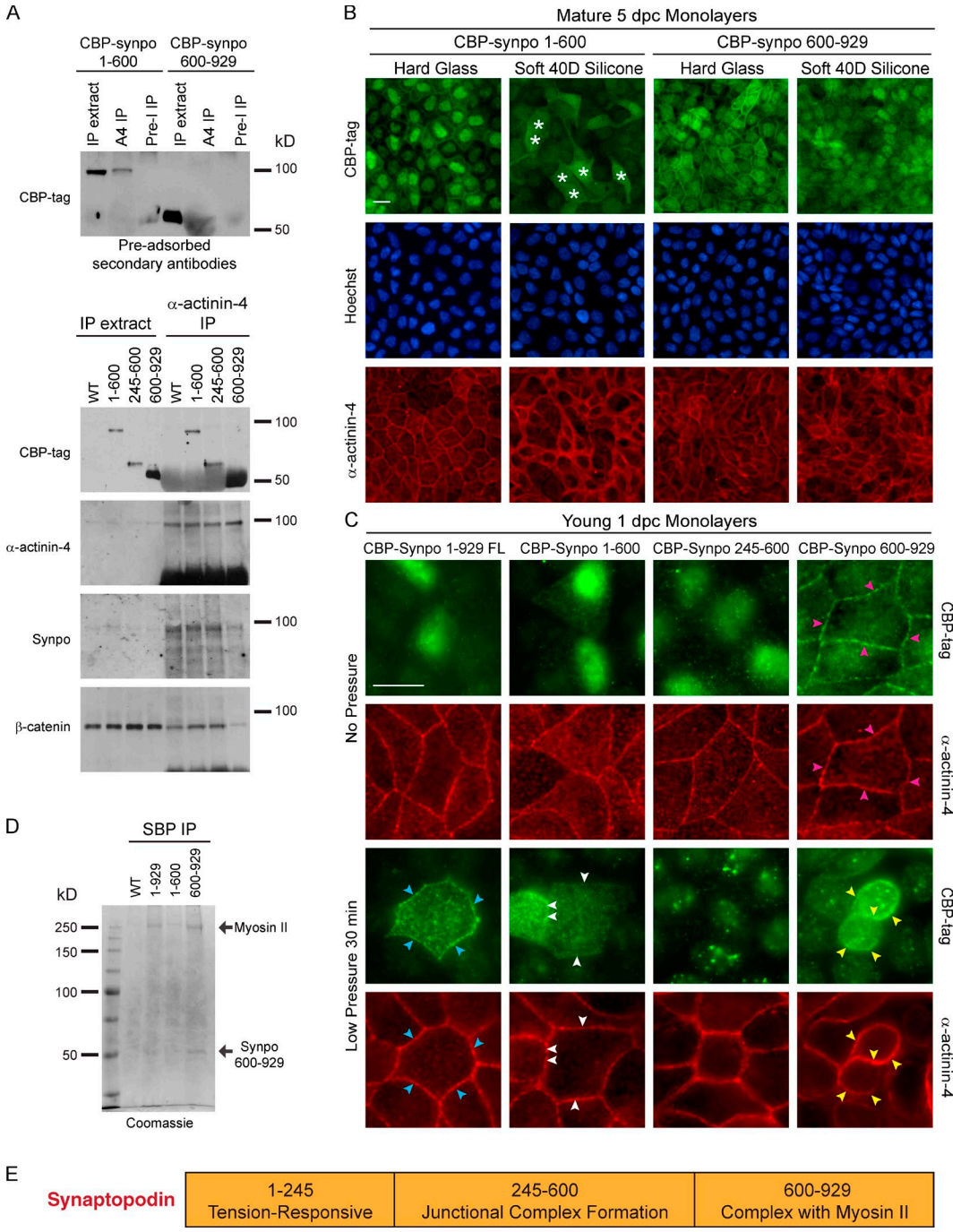

Figure 10. **Synaptopodin consists of three functional domains.** (A) Western blot showing coimmunoprecipitation of synaptopodin internal aa 245–600 with endogenous synaptopodin, β-catenin, and α-actinin-4, whereas synaptopodin C-terminal aa 600–929 disrupted interactions of endogenous synaptopodin, β-catenin, and α-actinin-4. (B) Wide-field immunofluorescence images showing junctional localization of synaptopodin N-terminal aa 1–600 and C-terminal aa 600–929 in mature monolayers. However, only aa 1–600 redistributed from cell junction to cytoplasm when cells were grown on soft silicone substrates (white asterisks). (C) Wide-field immunofluorescence images showing synaptopodin FL aa 1–929 (blue arrowheads) and N-terminal aa 1–600 (white arrowheads) targeting to the cell junction in response to cyclic pressure. Expression of synaptopodin C-terminal aa 600–929, which colocalizes with α-actinin-4 (pink arrowheads), caused cells to round up when mechanical force was applied to the junction (yellow arrowheads). (D) Coomassie blue staining showing a major band copurifies with the synaptopodin C-terminal aa 600–929 fragment from MDCK cells. Mass spectroscopy identifies the band as myosin II. (E) The three domains of synaptopodin. Bars, 10 µm.

pull on the membranes to create tension and trigger detachment of cell–cell contacts (Founounou et al., 2013; Guillot and Lecuit, 2013; Herszterg et al., 2013). During embryogenesis, myosin II activities are planar polarized to discrete domains of cell–cell interactions (Kasza et al., 2014; Shindo and Wallingford, 2014). These junctional domains are subsequently absorbed, leading to shrinking of selective myosin II–decorated junctions and expansion of nondecorated junctions. Conversely, contractile pulses and tension applied to cell–cell junction have been shown to enhance epithelial barrier function and support tissue integrity (Okano and Yoshida, 1993; Vasquez et al., 2014). Increasing tension at cell–cell adhesion induces accumulation of junctional components

and stabilization of E-cadherin (Yoshida et al., 1994; Shewan et al., 2005; Liu et al., 2010), whereas ablation of myosin II function decreases cell–cell adhesion (Conti et al., 2004). However, there remains no molecular explanation to reconcile the duality of myosin II–dependent contractility. Here, we provide a plausible mechanistic explanation to how a cell junction might switch between disengagement and strengthening via synaptopodin.

Depending on whether myosin II activities or α-actinin-4 functions are used for other cellular functions, epithelial cells can choose between using a biophysical input such as mechanical force generated by myosin II–dependent contractions or a biochemical input by regulating synaptopodin levels/activities to control α-actinin-4 recruitment. Thus, a cell can be expressing high levels of synaptopodin and α-actinin-4, but in the absence of tension generated by myosin II, synaptopodin and α-actinin-4 will not incorporate into the junctional complex and strong cell–cell adhesion will not happen. Conversely, a cell can have high contractility, but in the absence of synaptopodin, cell junction will not accumulate α-actinin-4 and strong cell–cell adhesion will not happen. Our findings reveal that mechanical tension through a series of force-dependent biochemical events induces sequential accumulation of junctional proteins, including synaptopodin (Mundel et al., 1997; Patrie et al., 2002; Asanuma et al., 2005), α-actinin-4 (Knudsen et al., 1995; Nieset et al., 1997), vinculin (Hazan et al., 1997; Watabe-Uchida et al., 1998; Imamura et al., 1999), and actin, ultimately leading to an enhancement of epithelial contractility and barrier function. Thus, this study reveals a temporal and spatial bipartite system at the intercellular junction, which is capable of integrating biophysical inputs and biochemical events to control cell–cell interactions.

In this study, we show that mechanical force can induce different biochemical events at the cell junction depending on the composition, i.e., maturity, of the junctional complex. This is manifested as an age dependency of the cell monolayers in their responses to mechanical force. Local, cell-nonautonomous feedback regulation of myosin dynamics has been shown to control the amplitude and spatial propagation of pulsed constrictions through regulation of tension and geometry during epithelial morphogenesis (Saravanan et al., 2013). Therefore, we propose that junction assembly in a monolayer of epithelial cell is the product of a positive feedback loop that requires iterations of multiple rounds of biophysical and biochemical events such as protein modifications, activation of signaling cascades, and contractility until a mature junction is formed (Fig. S5 B).

We discovered that cell–cell contacts have the ability to sense different levels and frequencies of tension. Whereas cyclic and pulsatile pressures could lead to α-actinin-4 accumulation, sustained pressure cannot. Furthermore, prolonged cyclic pressure would induce cell extrusion, whereas prolonged pulsatile pressure would not. These observations implicate the presence of a timer that can distinguish cyclic and pulsatile pressure. Thus, mechanotransduction at the cell junction is not simply an integration of stress over time. The future goal is to understand how cell–cell interactions achieve tension sensing at the molecular level, how mechanical signals are amplified and propagated to trigger junction assembly, and how adhesion receptors are coupled to the regulation of junction-dependent tissue contractility. Dissecting the coupling between actin dynamics, junctional complex formation, and actomyosin activities would require molecular mechanisms of how each protein works when they are simultaneously interacting with multiple partners at the junction. This is further complicated by the difficulties in obtaining biophysical measurement, such as the magnitude and frequency of endogenous forces, which has not been characterized yet. Thus, both biochemical and biophysical inputs have spatial and temporal requirements that would play differential roles in the regulation of junction assembly.

Materials and methods

Antibodies and reagents

Rabbit polyclonal antibodies to α-actinin-4 were raised in house against a synthetic N-terminal peptide, NQSYQYGPSSAGNGAGC, coupled to KLH. Mouse monoclonal antibodies to E-cadherin RR1 were made from hybridoma and a gift from W.M. Brieher (Department of Cell and Developmental Biology, University of Illinois, Urbana-Champaign). Antibodies to α-actinin-4 (catalog no. 49333, goat), β-catenin (catalog no. 7963, mouse; and 7199, rabbit), synaptopodin (catalog no. 50459, rabbit), α-catenin (catalog no. 1495, goat; and 9988, mouse), p120 (catalog no. 13957, rabbit), and CBP tag (catalog no. 33000, goat) were purchased from Santa Cruz Biotechnology, Inc. Secondary antibodies were purchased from Bio-Rad Laboratories (HRP goat anti–rabbit) and Invitrogen (FITC and Cy3 goat anti–mouse, FITC and Cy3 goat anti–rabbit, Alexa Fluor 488 donkey anti–mouse, Alexa Fluor 568 donkey anti–rabbit, and Alexa Fluor 647 donkey anti–goat). Alexa Fluor 350–phalloidin, Alexa Fluor 647–phalloidin, and *N*-hydroxysuccinimide–activated rhodamine were purchased from Invitrogen. Leupeptin, Pefabloc, E-64, antipain, aprotinin, bestatin, and calpain inhibitors I and II were purchased from AG Scientific, Inc. Latrunculin B, 3-aminopropyl-trimethoxysilane, hydrazine hydrate, blebbistatin, and BSA were purchased from Sigma-Aldrich. Sephadex S-200 was purchased from GE Healthcare. Protein A agarose and dithiothreitol were purchased form Gold Biotechnology, Inc. Biotin-agarose beads were obtained from Thermo Fisher Scientific. Medical-grade silicone sheeting (catalog no. SH-20002-005) was purchased from BioPlexus. Medical grade visco-gel silicone sheets (catalog no. 3081-S) were purchased from PediFix. Collagen I was purchased from BD.

DNA constructs

The coding sequence of human synaptopodin cDNAs (OriGene catalog no. RC228616) corresponding to aa 1–929, aa 1–600, aa 245–600, and aa 600–929 were subcloned into Sal1 and Xho1 sites of the G418-selectable mammalian expression vector pNTAPB (Agilent Technologies) with CBP and SBP tags at the N terminus for expression in MDCK cells. shRNAs for canine α-actinin-4 (5′-AGGTCCTGTTCCT CTGACTCGGTATCTAT-3′) and canine synaptopodin (5′-GAG GTGAGATCCAGCACACTTCTGATTGA-3′) were synthesized and subcloned into blasticidin-selectable pGFP-B-RS and puromycin-selectable pRS vectors, respectively (OriGene). Venus–α-actinin-1 cDNA was provided by F. Meng and F. Sachs (Physiology and Biophysics Department, SUNY at Buffalo, Buffalo, NY).

Purification and immunostaining of junction-enriched membrane

Purification of junction-enriched membranes was prepared as described previously (Tang and Brieher, 2012). In brief, frozen rat livers (Pel-Freez) were thawed in 2 vol of 10 mM Hepes, pH 8.5, and 10 mM DTT. Protease inhibitors (10 µg/ml Leupeptin, 1 mg/ml Pefabloc, 10 µg/ml E-64, 2 µg/ml antipain, 2 µg/ml aprotinin, 50 µg/ml bestatin, 20 µg/ml calpain inhibitor I, and 10 µg/ml calpain inhibitor II) were added and the livers were briefly blended in a Waring blender (5 × 15 s). The liver slush was filtered through four layers of cheesecloth to obtain the total liver homogenate. Total liver homogenate was centrifuged at 1,000 *g* for 30 min. The pellet was homogenized in 10 mM Hepes, pH 8.5, and 10 mM DTT in a Dounce homogenizer and centrifuged at 100 *g* for 30 min. The

supernatant was collected and centrifuged at 1,000 *g* for 30 min. The membrane pellet contains the majority of actin assembly activity and is frozen at −80°C before further purification immediately before use. The day of the experiment, membranes were thawed on ice, diluted 1:1 with 10 mM Hepes, pH 8.5, supplemented with 10 mM DTT, and homogenized through a 25G needle. The homogenates were spun through a 20% sucrose pad for 10 min at 16,000 *g*. The supernatant was discarded and the pellets were resuspended with 10 mM Hepes, pH 8.5, supplemented with 10 mM DTT. The homogenate was spun through a 20% sucrose pad for 15 min at 1,000 *g*. The pellet was discarded and the supernatant was spun through a 20% sucrose pad for 15 min at 16,000 *g*. The tiny membrane pellet contained junction-enriched plasma membrane vesicles.

Membrane actin assembly

Actin assembly reactions were performed in actin assembly buffer (50 mM KCl, 2 mM EGTA, 2 mM $MgCl_2$, and 100 mM Hepes, pH 7.8) supplemented with 2 mM buffered ATP, pH 8.0. In brief, a 20-µl reaction consisting of ∼15 µg of total proteins from the membrane fraction and 0.5 µM fluorescently labeled monomeric actin was allowed to carry out at room temperature for 30 min before incubation with primary antibodies in the presence of 0.1% TX-100. The membranes were spun through a 20% sucrose cushion and resuspended in 0.1% TX-100 in assay buffer. The membranes were incubated with secondary antibodies for 2 h, spun through a 20% sucrose cushion, and resuspended in 0.1% TX-100 in assay buffer. Stained membranes were imaged using an Axio Imager with the Colibri illumination system (both Carl Zeiss) using a 63× objective (NA 1.4) attached to a 1K × 1K ORCA-ER CCD camera (Hamamatsu Photonics).

Negative stain EM and immunogold labeling

For visualizing actin assembly, membrane reactions were performed as described in the previous section before processing for EM. For immunogold labeling of junction-enriched membrane, membranes were treated with 0.2% TX-100 in actin assembly buffer on ice for 1 h and spun through a 20% sucrose cushion before incubation with anti–α-actinin-4 antibodies for 2 h on ice. Unbound antibodies were removed by spinning membranes through a 20% sucrose cushion before incubation with 6-nm colloidal gold anti–rabbit antibodies for 2 h. Unbound gold antibodies were removed by spinning membranes through a 20% sucrose cushion before processing for EM. Membrane reactions were put onto glow-discharged carbon-coated grids for 10 min, washed three times with assembly buffer, and stained with 2% uranyl acetate. Images were collected with a microscope (2100EX; JEOL) at 120 kV using a 2K × 2K charge-coupled device camera (UltraScan; Gatan, Inc.). For figure generation, images were cropped, contrasted, and scaled using Photoshop software (Adobe) before importing into Illustrator (Adobe).

Kinase array

Human phosphor-Kinase Array (catalog no. ARY003B; R&D Systems) was performed according to the manufacturer's instructions using MDCK cells that had been grown on 24-mm Transwells for days with or without cyclic pressure treatment.

Cell culture and transfection

MDCK cells were maintained in MEM/Earle's balanced salt solution supplemented with 25 mM Hepes and 10% FBS. For transfection, cells were incubated in Opti-MEM (Invitrogen) with a 1:1 mixture of DNA/polyethylenimine and selected for 10 d using G418, puromycin, or blasticidin. For latrunculin treatment, cells grown on Transwells for 7 d were treated with 10 µM latrunculin in normal growth media for 2 h and then processed for immunofluorescence.

For soft substrate studies, glass coverslips or medical-grade silicone sheeting (40 Durometer, thickness 0.005 in) were soaked in 100% ethanol for 30 min and sterilized under UV for 60 min. Sterilized coverslips or silicone sheets were coated with 20 µg/ml collagen I in phosphate-buffered saline for 60 min and used immediately for plating of cells. Cells grown on collagen-coated glass coverslips (upside down) or collagen-coated silicone substrates (right-side up) were processed for immunofluorescence staining.

Live cell imaging

Glass coverslips were soaked in 100% ethanol for 30 min and sterilized under UV for 60 min. Sterilized coverslips were coated with 20 µg/ml collagen I in phosphate-buffered saline for 60 min and used immediately for plating of cells. Cells grown on collagen-coated glass coverslips (upside down) were mounted to the glass slide chamber. Cells were imaged using in-house fabricated glass slide chambers. The chamber was assembled by attaching a 1.5 × 1.5–cm medical-grade silicone gel (PediFix) onto a sterilized glass slide. The center of the silicone gel was removed and used as a sink for culture media during imaging. For blebbistatin perfusion and washout studies, 25 µM blebbistatin (from 5 mM stock solubilized in DMSO) was added to regular growth media and perfused into the sink of the glass slide chamber. For washout, regular media was perfused into the sink from an inlet while blebbistatin-containing media was removed from an outlet of the sink.

EM of cells

Cells grown on Transwell-Clear (Corning) were processed for EM as described previously (Tang, 2006). In brief, MDCK and T84 epithelial cells grown on Transwells were chilled at 4°C for 6 h before fixation with 3.75% glutaraldehyde, 150 mM NaCl, and 20 mM Hepes, pH 7.5, at 4°C for 18 h. The fixation reaction was quenched with 50 mM glycine and 150 mM Hepes, pH 7.5, on ice for 1 h. Cells/Transwells were rinsed in ice-cold distilled water three times, secondarily fixed with 1% osmium tetroxide/1.5% potassium ferrocyanide for 2 h on ice, rinsed four times in ice-cold distilled water, en bloc stained with freshly prepared and filtered 2% uranyl acetate in distilled water on ice for 2 h, and rinsed four times in ice-cold distilled water. Cells/Transwells were dehydrated with sequential 5-min incubations in 50%, 75%, 95%, 100%, 100%, and 100% ethanol at room temperature. epon-Araldite (EMbed 812) was added to Transwells and allowed to polymerize at 60°C for 48 h. Ultrathin sections were cut using an Ultracut-S microtome (Reichert), layered onto carbon-coated copper grids, and stained with freshly made/filtered 2% lead citrate. Grids were examined with Tecnai G2 Spirit BioTwin (FEI) equipped with an AMT 2K CCD camera. Digital images acquired were imported into Photoshop for figure preparation.

Hydraulic pressure application

Cells grown on Transwell-Clear were used in pressure experiments. Pressure chambers and adaptors were designed by V.W. Tang and fabricated from medical-grade stainless steel by the mechanical engineering machine shop at the University of Illinois, Urbana-Champaign. Transwell filter cups were mounted onto a pressure chamber, held in place to a lid by a screw and a top. Hydraulic pressure was applied to the basal compartment via a syringe hooked up to a syringe pump into the basal chamber that was filled with cell culture media and sealed with an O-ring between the pressure chamber and the Transwell cup. Pressure was monitored through an outlet from the basal pressure chamber to a pressure gauge. An apical adaptor is mounted onto the apical chamber of the Transwell cup that is filled with cell culture media and sealed with an O-ring. An outlet from the apical adaptor is either exposed to ambient pressure or connected via a bifurcation to a pressure gauge and a syringe hooked up to a syringe pump. The pressure chamber was

preheated to 37°C and kept at this temperature on a warm plate for the duration of the experiment. Cyclic, pulsatile, or sustained pressures were applied to cell monolayers by programmable infuse/withdrawal syringe pumps (Lagato SPLG270). Cyclic pressure was applied at 30 cycles per min or otherwise specified. Pulsatile pressure was applied at six cycles per minute or otherwise specified.

Cell extraction and immunoprecipitation

Total cell lysates were obtained by solubilization of cells directly in SDS-PAGE sample buffer containing 25 mM dithiothreitol, 2% SDS, 50 mM Tris-Cl, 5% glycerol, pH 8.8, and protease inhibitors (see section Purification and immunostaining of junction-enriched membrane). For immunoprecipitation, cells were grown to 100% confluency and maintained at confluency for 5 d. Then the cells were split 1:2 onto new dishes the night before use. The next day, the cells were rinsed and swelled with 10 mM Hepes, pH 8.5, for 3 h at 4°C. Cells were extracted with immunoprecipitation buffer (100 mM NaCl, 10 mM Hepes, pH 7.8, 2 mM EDTA, 0.01% TX-100, and 0.02% azide) containing protease inhibitors and homogenized with a 22G needle. Homogenate was centrifuged for 5 min at 5,000 *g*. The supernatant was collected and incubated with anti–α-actinin-4 antibodies overnight in the cold room. The next day, the supernatant was centrifuged for 10 min at 5,000 *g*. The supernatant was added to protein A–agarose beads and incubated overnight with agitation. The next day, the immunoprecipitation mixture was added to an Econo column (Bio-Rad Laboratories), and the beads were washed five times with immunoprecipitation buffer and three times with 10 mM Hepes, pH 8.5. Bound fraction was eluted with boiling 2× sample buffer (4% SDS, 100 mM Tris-Cl, and 10% glycerol, pH 8.8) and stored at −20°C until use. A final concentration of 100 mM dithiothreitol was added to the eluate, and the samples were boiled for 10 min before SDS-PAGE.

For streptavidin-binding protein affinity purification, the cells were split 1:2 onto new dishes the night before use. The next day, the cells were rinsed and swelled with 10 mM Hepes, pH 8.5, for 3 h at 4°C. Cells were extracted with immunoprecipitation buffer (100 mM NaCl, 10 mM Hepes, pH 7.8, 2 mM EDTA, 0.01% TX-100, and 0.02% azide) containing protease inhibitors and homogenized with a 22G needle on ice. Homogenate was centrifuged for 5 min at 5,000 *g*. The supernatant was collected and incubated with biotin-agarose beads and incubated overnight with agitation at 4°C. The next day, the bead–cell lysate mixture was added to an Econo column, and the beads were washed three times with immunoprecipitation buffer and two times with 10 mM Hepes, pH 8.5. Bound fraction was eluted with boiling 2× sample buffer (4% SDS, 100 mM Tris-Cl, and 10% glycerol, pH 8.8) and stored at −20°C until used. A final concentration of 100 mM dithiothreitol was added to the eluate, and the samples were boiled for 10 min before SDS-PAGE.

For cell TX-100 solubility assays, cells were grown on 24-mm Transwells for 1–8 d. Transwells were used in the pressure experiment before TX-100 extraction. In brief, cells were rinsed three times with ice-cold 10 mM Hepes, pH 8.5, and incubated on ice in 0.01% TX-100, 100 mM NaCl, 10 mM Hepes, pH 7.8, 2 mM EDTA, and 0.02% azide on Transwells for 2 h. Cells were then rinsed twice with ice-cold 10 mM Hepes, pH 8.5, while still attached on Transwells and solubilized immediately in boiling SDS-PAGE sample buffer (2% SDS, 50 mM Tris-Cl, and 5% glycerol, pH 8.8). Samples were stored at −20°C until use. A final concentration of 100 mM dithiothreitol was added to the eluate, and the samples were boiled for 10 min before SDS-PAGE.

Immunofluorescence of cells

Cells were rinsed twice in 150 mM NaCl, 2 mM $CaCl_2$, 2 mM $MgCl_2$, and 20 mM Hepes, pH 7.8, and fixed in 1% formaldehyde, 150 mM NaCl, 2 mM $CaCl_2$, 2 mM $MgCl_2$, and 20 mM Hepes, pH 7.8, at 4°C for 2 h. The reaction was quenched with 50 mM Tris in staining buffer (0.1% Triton X-100, 100 mM NaCl, and 20 mM Hepes, pH 7.8) for 1 h. After rinsing in staining buffer, the cells were incubated with primary antibodies in staining buffer overnight. After rinsing in staining buffer three times, the cells were incubated in secondary antibodies for 90 min. The cells were rinsed again three times and post-stain fixed with 1% formaldehyde in staining buffer. Finally, the cells were incubated with fluorescently labeled phalloidin or Hoechst for 60 min. Transwell filters were excised and mounted on glass slides using ProLong Gold antifade (Invitrogen).

Live cell and fixed cell image acquisition

Live cell and fixed cell fluorescence wide-field images were collected with an Axio Imager using AxioVision Release 4.7 with the Colibri illumination system (Carl Zeiss) using an oil 60× objective (NA 1.40) attached to a 1K × 1K charge-coupled device camera (ORCA-ER; Hamamatsu Photonics). For live cells, cells were imaged in normal growth media, and the images were acquired every 15 s for 120 min at 30°C. Individual cell diameter and junction for each image were measured using ImageJ (National Institutes of Health). Individual images of cropped cells were imported into QuickTime to generate video files. For deconvolution microscopy, optical z slices in 200-nm steps were collected using a 60× objective (NA 1.42) with a 1.6× auxiliary magnification with an inverted microscope (1X71; Olympus) attached to a 1K × 1K charge-coupled device camera (CoolSNAP HQ; Applied Precision). For deconvolution microscopy, fixed cell fluorescence images were obtained at room temperature using SoftWoRx DMS software (Applied Precision) and deconvolved by Enhanced Ratio Deconvolution using 10 iteration cycles (Applied Precision). Z stack projections were generated from deconvolved slices using the maximum intensity criteria. Composite images were generated using ImageJ software. For figure generation, images were cropped, contrasted, and scaled using Photoshop software (Adobe) before importing into Illustrator (Adobe).

Quantitation of junctional staining

Quantitation of immunofluorescence intensity was performed in ImageJ using unprocessed original single optical z slice images taken at the level of adherens junction. A defined junctional area was used to compare the fluorescence intensity of actin (phalloidin), E-cadherin (immunofluorescence using monoclonal RR1 antibodies), α-actinin-4 (immunofluorescence using antibodies against N-terminal peptide), α-catenin (immunofluorescence using antibodies against C-terminal peptide), β-catenin (immunofluorescence using monoclonal antibodies against aa 680–781), p120 (immunofluorescence using antibodies against aa 41–130), and synaptopodin (immunofluorescence using antibodies against aa 781–920). The measured intensities were subtracted from background (cytoplasm) before being used for calculating the intensity ratios. For figure generation, images were cropped, contrasted, and scaled using Photoshop software before importing into Illustrator. Calculation of correlation coefficient R and paired Student's *t* tests were performed using KaleidaGraph software (Synergy Software). All curves were fitted using original data points into an exponential function by KaleidaGraph software.

Permeability measurement

BSA was labeled on lysine residues using *N*-hydroxysuccinimide–activated rhodamine, purified by gel filtration using Sephadex S-200, and kept frozen until use. Thawed tracers were purified away from residual-free dye using Sephadex 25G spin columns immediately before use. Permeability assays were performed as described in detail previously (Tang and Goodenough, 2003). In brief, 12-mm Transwells were rinsed

with 50 ml of prewarmed flux buffer (145 mM NaCl, 2 mM $CaCl_2$, 2 mM $MgCl_2$, and 10 mM Hepes, pH 7.4). The apical well was filled with 0.5 ml of flux buffer, and the Transwells were placed in a 12-well plate with 1 ml of flux media containing 3 µM labeled extracellular tracers. Flux was performed at 37°C for 2 h. At the end of the flux experiment, the apical solutions were collected, and fluorescence was measured using a fluorimeter. Permeability is the amount of tracer in the apical bathing solution (µmol) per unit driving force (basal molar concentration of tracer), per unit time (hours), per area of the monolayer (square centimeters).

Wound expansion assay

Cells grown on collagen-coated glass coverslips were allowed to mature for 5 d after confluency. A puncture wound was introduced in the middle of the monolayer using a beveled 25G needle (machine shop, School of Molecular and Cell Biology, University of Illinois, Urbana-Champaign) attached to a vacuum line. The needle was lowered onto the monolayer, and cell debris at the punctured area was removed simultaneously during wounding through the vacuum line. Cells were returned back to the culture incubator for 30 min until fixed. Wounds were captured using the PentaView LCD digital microscope (Celestron) with an attached digital camera. Wound diameters were measured using ImageJ. For figure generation, images were cropped using Photoshop software before importing into Illustrator.

Polyacrylamide gel cell spreading assay

Polyacrylamide substrates were prepared using a modified protocol established by X. Tang and S. Taher in the Mechanical Engineering Department, University of Illinois, Urbana-Champaign, based on published procedures (Damljanović et al., 2005). In brief, glass coverslips were activated with 95% 3-aminopropyl-trimethoxysliane solution and washed with water, followed by treatment with 0.5% glutaraldehyde. Polyacrylamide gel mixtures were allowed to polymerize on the activated coverslips sandwiched with a nonderivatized coverslip. Polyacrylamide gel surface was activated with hydrazine and coated with collagen I before plating of cells. Polyacrylamide gel of different stiffness was prepared according to calibration using atomic force microscopy by X. Tang and S. Taher. Cells were trypsinized from confluent monolayers and plated the night before being fixed for immunofluorescence staining.

Online supplemental material

Figs. S1 and S2 show the epithelial junction is a large membrane-associated structure ∼150 nm in size that can support α-actinin-4–dependent actin assembly Fig. S3 shows the design of the pressure chamber to apply hydraulic pressure to cell–cell adhesion in a cell monolayer. Fig. S4 shows the strength of epithelial junction is a function of cell geometry and adhesive bonds. Fig. S5 shows that the junctional complex links adhesion molecules to cytoskeletal and contractile elements. Videos 1–3 show MDCK cells expressing venus–α-actinin at 2 dpc, showing mobility of junctions. Videos 4–6 show MDCK cells expressing venus–α-actinin at 2 dpc, showing contractions of cells. Videos 7–9 show MDCK cells expressing venus–α-actinin at 2 dpc, showing tugging of junctions. Video 10 shows MDCK cells expressing venus–α-actinin at 6 dpc, showing lack of mobility of junctions and very fast contraction pulses. Online supplemental material is available at http://www.jcb.org/cgi/content/full/jcb.201412003/DC1.

Acknowledgments

We apologize for not being able to credit all publications that contributed to the foundation of this work. We thank Xin Tang and Saif Taher for the help with polyacrylamide gel preparation. We thank Rahul Kantharia (Bioengineering Department, University of Illinois, Urbana-Champaign) for making the polyacrylamide gel substrates and culturing synaptopodin knockdown cells for cell-spreading assays. We thank Robert Dam (School of Molecular and Cell Biology, University of Illinois, Urbana-Champaign) and Cameron Shahnaz (Chemistry Department, University of Illinois, Urbana-Champaign) for making synaptopodin cDNA constructs. We thank the team at the Mechanical Engineering Shop, University of Illinois, Urbana-Champaign, for fabrication of all parts for the pressure chambers. EM was carried out in part in the University of Illinois Frederick Seitz Materials Research Laboratory central facilities.

Funding was provided by National Institute of Diabetes and Digestive and Kidney Diseases, National Institutes of Health (R01 DK098398) to V.W. Tang.

The authors declare no competing financial interests.

Submitted: 1 December 2014
Accepted: 17 September 2015

References

Abe, K., and M. Takeichi. 2008. EPLIN mediates linkage of the cadherin catenin complex to F-actin and stabilizes the circumferential actin belt. *Proc. Natl. Acad. Sci. USA.* 105:13–19. http://dx.doi.org/10.1073/pnas.0710504105

Aberle, H., S. Butz, J. Stappert, H. Weissig, R. Kemler, and H. Hoschuetzky. 1994. Assembly of the cadherin-catenin complex in vitro with recombinant proteins. *J. Cell Sci.* 107:3655–3663.

Abreu-Blanco, M.T., J.M. Verboon, and S.M. Parkhurst. 2011. Cell wound repair in *Drosophila* occurs through three distinct phases of membrane and cytoskeletal remodeling. *J. Cell Biol.* 193:455–464. http://dx.doi.org/10.1083/jcb.201011018

Adamson, R.H., B. Liu, G.N. Fry, L.L. Rubin, and F.E. Curry. 1998. Microvascular permeability and number of tight junctions are modulated by cAMP. *Am. J. Physiol.* 274:H1885–H1894.

Altmann, S.M., R.G. Grünberg, P.F. Lenne, J. Ylänne, A. Raae, K. Herbert, M. Saraste, M. Nilges, and J.K. Hörber. 2002. Pathways and intermediates in forced unfolding of spectrin repeats. *Structure.* 10:1085–1096. http://dx.doi.org/10.1016/S0969-2126(02)00808-0

Asada, M., K. Irie, K. Morimoto, A. Yamada, W. Ikeda, M. Takeuchi, and Y. Takai. 2003. ADIP, a novel Afadin- and α-actinin-binding protein localized at cell-cell adherens junctions. *J. Biol. Chem.* 278:4103–4111. http://dx.doi.org/10.1074/jbc.M209832200

Asanuma, K., K. Kim, J. Oh, L. Giardino, S. Chabanis, C. Faul, J. Reiser, and P. Mundel. 2005. Synaptopodin regulates the actin-bundling activity of α-actinin in an isoform-specific manner. *J. Clin. Invest.* 115:1188–1198. http://dx.doi.org/10.1172/JCI200523371

Bajpai, S., Y. Feng, R. Krishnamurthy, G.D. Longmore, and D. Wirtz. 2009. Loss of α-catenin decreases the strength of single E-cadherin bonds between human cancer cells. *J. Biol. Chem.* 284:18252–18259. http://dx.doi.org/10.1074/jbc.M109.000661

Bajpai, S., Y. Feng, D. Wirtz, and G.D. Longmore. 2013. β-Catenin serves as a clutch between low and high intercellular E-cadherin bond strengths. *Biophys. J.* 105:2289–2300. http://dx.doi.org/10.1016/j.bpj.2013.09.044

Bakolitsa, C., D.M. Cohen, L.A. Bankston, A.A. Bobkov, G.W. Cadwell, L. Jennings, D.R. Critchley, S.W. Craig, and R.C. Liddington. 2004. Structural basis for vinculin activation at sites of cell adhesion. *Nature.* 430:583–586. http://dx.doi.org/10.1038/nature02610

Balsamo, J., R. Thiboldeaux, N. Swaminathan, and J. Lilien. 1991. Antibodies to the retina N-acetylgalactosaminylphosphotransferase modulate N-cadherin-mediated adhesion and uncouple the N-cadherin transferase complex from the actin-containing cytoskeleton. *J. Cell Biol.* 113:429–436. http://dx.doi.org/10.1083/jcb.113.2.429

Bambardekar, K., R. Clément, O. Blanc, C. Chardès, and P.F. Lenne. 2015. Direct laser manipulation reveals the mechanics of cell contacts in vivo. *Proc. Natl. Acad. Sci. USA.* 112:1416–1421. http://dx.doi.org/10.1073/pnas.1418732112

Barry, A.K., H. Tabdili, I. Muhamed, J. Wu, N. Shashikanth, G.A. Gomez, A.S. Yap, C.J. Gottardi, J. de Rooij, N. Wang, and D.E. Leckband. 2014. α-catenin cytomechanics--role in cadherin-dependent adhesion and mechanotransduction. *J. Cell Sci.* 127:1779–1791. http://dx.doi.org/10.1242/jcs.139014

Behrens, J., W. Birchmeier, S.L. Goodman, and B.A. Imhof. 1985. Dissociation of Madin-Darby canine kidney epithelial cells by the monoclonal antibody anti-arc-1: mechanistic aspects and identification of the antigen as a component related to uvomorulin. *J. Cell Biol.* 101:1307–1315. http://dx.doi.org/10.1083/jcb.101.4.1307

Belkin, A.M., and V.E. Koteliansky. 1987. Interaction of iodinated vinculin, metavinculin and α-actinin with cytoskeletal proteins. *FEBS Lett.* 220:291–294. http://dx.doi.org/10.1016/0014-5793(87)80832-3

Bement, W.M., P. Forscher, and M.S. Mooseker. 1993. A novel cytoskeletal structure involved in purse string wound closure and cell polarity maintenance. *J. Cell Biol.* 121:565–578. http://dx.doi.org/10.1083/jcb.121.3.565

Bernadskaya, Y.Y., F.B. Patel, H.T. Hsu, and M.C. Soto. 2011. Arp2/3 promotes junction formation and maintenance in the *Caenorhabditis elegans* intestine by regulating membrane association of apical proteins. *Mol. Biol. Cell.* 22:2886–2899. http://dx.doi.org/10.1091/mbc.E10-10-0862

Blanchard, G.B., S. Murugesu, R.J. Adams, A. Martinez-Arias, and N. Gorfinkiel. 2010. Cytoskeletal dynamics and supracellular organisation of cell shape fluctuations during dorsal closure. *Development.* 137:2743–2752. http://dx.doi.org/10.1242/dev.045872

Bois, P.R., R.A. Borgon, C. Vonrhein, and T. Izard. 2005. Structural dynamics of α-actinin-vinculin interactions. *Mol. Cell. Biol.* 25:6112–6122. http://dx.doi.org/10.1128/MCB.25.14.6112-6122.2005

Bois, P.R., B.P. O'Hara, D. Nietlispach, J. Kirkpatrick, and T. Izard. 2006. The vinculin binding sites of talin and α-actinin are sufficient to activate vinculin. *J. Biol. Chem.* 281:7228–7236. http://dx.doi.org/10.1074/jbc.M510397200

Borghi, N., M. Sorokina, O.G. Shcherbakova, W.I. Weis, B.L. Pruitt, W.J. Nelson, and A.R. Dunn. 2012. E-cadherin is under constitutive actomyosin-generated tension that is increased at cell–cell contacts upon externally applied stretch. *Proc. Natl. Acad. Sci. USA.* 109:12568–12573. (published erratum appears in *Proc. Natl. Acad. Sci. USA.* 2012. 109:19034) http://dx.doi.org/10.1073/pnas.1204390109

Boyer, B., G.C. Tucker, A.M. Vallés, W.W. Franke, and J.P. Thiery. 1989. Rearrangements of desmosomal and cytoskeletal proteins during the transition from epithelial to fibroblastoid organization in cultured rat bladder carcinoma cells. *J. Cell Biol.* 109:1495–1509. http://dx.doi.org/10.1083/jcb.109.4.1495

Brevier, J., D. Montero, T. Svitkina, and D. Riveline. 2008. The asymmetric self-assembly mechanism of adherens junctions: a cellular push-pull unit. *Phys. Biol.* 5:016005. http://dx.doi.org/10.1088/1478-3975/5/1/016005

Broedersz, C.P., M. Depken, N.Y. Yao, M.R. Pollak, D.A. Weitz, and F.C. MacKintosh. 2010. Cross-link-governed dynamics of biopolymer networks. *Phys. Rev. Lett.* 105:238101. http://dx.doi.org/10.1103/PhysRevLett.105.238101

Brouxhon, S.M., S. Kyrkanides, X. Teng, V. Raja, M.K. O'Banion, R. Clarke, S. Byers, A. Silberfeld, C. Tornos, and L. Ma. 2013. Monoclonal antibody against the ectodomain of E-cadherin (DECMA-1) suppresses breast carcinogenesis: involvement of the HER/PI3K/Akt/mTOR and IAP pathways. *Clin. Cancer Res.* 19:3234–3246. http://dx.doi.org/10.1158/1078-0432.CCR-12-2747

Buckley, C.D., J. Tan, K.L. Anderson, D. Hanein, N. Volkmann, W.I. Weis, W.J. Nelson, and A.R. Dunn. 2014. The minimal cadherin-catenin complex binds to actin filaments under force. *Science.* 346:1254211. http://dx.doi.org/10.1126/science.1254211

Byri, S., T. Misra, Z.A. Syed, T. Bätz, J. Shah, L. Boril, J. Glashauser, T. Aegerter-Wilmsen, T. Matzat, B. Moussian, et al. 2015. The triple-repeat protein Anakonda controls epithelial tricellular junction formation in *Drosophila*. *Dev. Cell.* 33:535–548. http://dx.doi.org/10.1016/j.devcel.2015.03.023

Capaldo, C.T., and I.G. Macara. 2007. Depletion of E-cadherin disrupts establishment but not maintenance of cell junctions in Madin-Darby canine kidney epithelial cells. *Mol. Biol. Cell.* 18:189–200. http://dx.doi.org/10.1091/mbc.E06-05-0471

Carramusa, L., C. Ballestrem, Y. Zilberman, and A.D. Bershadsky. 2007. Mammalian diaphanous-related formin Dia1 controls the organization of E-cadherin-mediated cell-cell junctions. *J. Cell Sci.* 120:3870–3882. http://dx.doi.org/10.1242/jcs.014365

Catimel, B., J. Rothacker, J. Catimel, M. Faux, J. Ross, L. Connolly, A. Clippingdale, A.W. Burgess, and E. Nice. 2005. Biosensor-based micro-affinity purification for the proteomic analysis of protein complexes. *J. Proteome Res.* 4:1646–1656. http://dx.doi.org/10.1021/pr050132x

Cavey, M., M. Rauzi, P.F. Lenne, and T. Lecuit. 2008. A two-tiered mechanism for stabilization and immobilization of E-cadherin. *Nature.* 453:751–756. http://dx.doi.org/10.1038/nature06953

Choi, H.J., J.C. Gross, S. Pokutta, and W.I. Weis. 2009. Interactions of plakoglobin and β-catenin with desmosomal cadherins: basis of selective exclusion of α- and β-catenin from desmosomes. *J. Biol. Chem.* 284:31776–31788. http://dx.doi.org/10.1074/jbc.M109.047928

Choi, H.J., S. Pokutta, G.W. Cadwell, A.A. Bobkov, L.A. Bankston, R.C. Liddington, and W.I. Weis. 2012. αE-catenin is an autoinhibited molecule that coactivates vinculin. *Proc. Natl. Acad. Sci. USA.* 109:8576–8581. http://dx.doi.org/10.1073/pnas.1203906109

Chu, D., H. Pan, P. Wan, J. Wu, J. Luo, H. Zhu, and J. Chen. 2012. AIP1 acts with cofilin to control actin dynamics during epithelial morphogenesis. *Development.* 139:3561–3571. http://dx.doi.org/10.1242/dev.079491

Chu, Y.S., W.A. Thomas, O. Eder, F. Pincet, E. Perez, J.P. Thiery, and S. Dufour. 2004. Force measurements in E-cadherin–mediated cell doublets reveal rapid adhesion strengthened by actin cytoskeleton remodeling through Rac and Cdc42. *J. Cell Biol.* 167:1183–1194. http://dx.doi.org/10.1083/jcb.200403043

Clark, A.G., A.L. Miller, E. Vaughan, H.Y. Yu, R. Penkert, and W.M. Bement. 2009. Integration of single and multicellular wound responses. *Curr. Biol.* 19:1389–1395. http://dx.doi.org/10.1016/j.cub.2009.06.044

Colaco, C.A., and W.H. Evans. 1981. A biochemical dissection of the cardiac intercalated disk: isolation of subcellular fractions containing fascia adherentes and gap junctions. *J. Cell Sci.* 52:313–325.

Collares-Buzato, C.B., M.A. Jepson, G.T. McEwan, B.H. Hirst, and N.L. Simmons. 1998. Co-culture of two MDCK strains with distinct junctional protein expression: a model for intercellular junction rearrangement and cell sorting. *Cell Tissue Res.* 291:267–276. http://dx.doi.org/10.1007/s004410050996

Collinet, C., and T. Lecuit. 2013. Stability and dynamics of cell–cell junctions. *Prog. Mol. Biol. Transl. Sci.* 116:25–47. http://dx.doi.org/10.1016/B978-0-12-394311-8.00002-9

Conti, M.A., S. Even-Ram, C. Liu, K.M. Yamada, and R.S. Adelstein. 2004. Defects in cell adhesion and the visceral endoderm following ablation of nonmuscle myosin heavy chain II-A in mice. *J. Biol. Chem.* 279:41263–41266. http://dx.doi.org/10.1074/jbc.C400352200

Corgan, A.M., C. Singleton, C.B. Santoso, and J.A. Greenwood. 2004. Phosphoinositides differentially regulate alpha-actinin flexibility and function. *Biochem. J.* 378:1067–1072. http://dx.doi.org/10.1042/bj20031124

Cox-Paulson, E.A., E. Walck-Shannon, A.M. Lynch, S. Yamashiro, R. Zaidel-Bar, C.C. Eno, S. Ono, and J. Hardin. 2012. Tropomodulin protects α-catenin-dependent junctional-actin networks under stress during epithelial morphogenesis. *Curr. Biol.* 22:1500–1505. http://dx.doi.org/10.1016/j.cub.2012.06.025

Dai, S., Z. Wang, X. Pan, W. Wang, X. Chen, H. Ren, C. Hao, B. Han, and N. Chen. 2010. Functional analysis of promoter mutations in the ACTN4 and SYNPO genes in focal segmental glomerulosclerosis. *Nephrol. Dial. Transplant.* 25:824–835. http://dx.doi.org/10.1093/ndt/gfp394

Damljanović, V., B.C. Lagerholm, and K. Jacobson. 2005. Bulk and micropatterned conjugation of extracellular matrix proteins to characterized polyacrylamide substrates for cell mechanotransduction assays. *Biotechniques.* 39:847–851. http://dx.doi.org/10.2144/000112026

Desai, R., R. Sarpal, N. Ishiyama, M. Pellikka, M. Ikura, and U. Tepass. 2013. Monomeric α-catenin links cadherin to the actin cytoskeleton. *Nat. Cell Biol.* 15:261–273. http://dx.doi.org/10.1038/ncb2685

Di Ciano, C., Z. Nie, K. Szászi, A. Lewis, T. Uruno, X. Zhan, O.D. Rotstein, A. Mak, and A. Kapus. 2002. Osmotic stress-induced remodeling of the cortical cytoskeleton. *Am. J. Physiol. Cell Physiol.* 283:C850–C865. http://dx.doi.org/10.1152/ajpcell.00018.2002

Dobrosotskaya, I.Y., and G.L. James. 2000. MAGI-1 interacts with β-catenin and is associated with cell–cell adhesion structures. *Biochem. Biophys. Res. Commun.* 270:903–909. http://dx.doi.org/10.1006/bbrc.2000.2471

Drenckhahn, D., and H. Franz. 1986. Identification of actin-, alpha-actinin-, and vinculin-containing plaques at the lateral membrane of epithelial cells. *J. Cell Biol.* 102:1843–1852. http://dx.doi.org/10.1083/jcb.102.5.1843

Duan, Y., N. Gotoh, Q. Yan, Z. Du, A.M. Weinstein, T. Wang, and S. Weinbaum. 2008. Shear-induced reorganization of renal proximal tubule cell actin cytoskeleton and apical junctional complexes. *Proc. Natl. Acad. Sci. USA.* 105:11418–11423. http://dx.doi.org/10.1073/pnas.0804954105

Durand, E., V.S. Nguyen, A. Zoued, L. Logger, G. Péhau-Arnaudet, M.S. Aschtgen, S. Spinelli, A. Desmyter, B. Bardiaux, A. Dujeancourt, et al. 2015. Biogenesis and structure of a type VI secretion membrane core complex. *Nature.* 523:555–560. http://dx.doi.org/10.1038/nature14667

du Roure, O., A. Saez, A. Buguin, R.H. Austin, P. Chavrier, P. Silberzan, and B. Ladoux. 2005. Force mapping in epithelial cell migration. *Proc. Natl. Acad. Sci. USA.* 102:2390–2395. (published erratum appears in *Proc. Natl. Acad. Sci. USA*. 200. 102:14122) http://dx.doi.org/10.1073/pnas.0408482102

Ebnet, K. 2008. Organization of multiprotein complexes at cell–cell junctions. *Histochem. Cell Biol.* 130:1–20. http://dx.doi.org/10.1007/s00418-008-0418-7

Ebnet, K., C.U. Schulz, M.K. Meyer Zu Brickwedde, G.G. Pendl, and D. Vestweber. 2000. Junctional adhesion molecule interacts with the PDZ domain-containing proteins AF-6 and ZO-1. *J. Biol. Chem.* 275:27979–27988.

Ebrahim, S., T. Fujita, B.A. Millis, E. Kozin, X. Ma, S. Kawamoto, M.A. Baird, M. Davidson, S. Yonemura, Y. Hisa, et al. 2013. NMII forms a contractile transcellular sarcomeric network to regulate apical cell junctions and tissue geometry. *Curr. Biol.* 23:731–736. http://dx.doi.org/10.1016/j.cub.2013.03.039

Engl, W., B. Arasi, L.L. Yap, J.P. Thiery, and V. Viasnoff. 2014. Actin dynamics modulate mechanosensitive immobilization of E-cadherin at adherens junctions. *Nat. Cell Biol.* 16:587–594. http://dx.doi.org/10.1038/ncb2973

Falqui, V., F. Viazzi, G. Leoncini, E. Ratto, A. Parodi, N. Conti, C. Tomolillo, G. Deferrari, and R. Pontremoli. 2007. Blood pressure load, vascular permeability and target organ damage in primary hypertension. *J. Nephrol.* 20:S63–S67.

Farquhar, M.G., and G.E. Palade. 1963. Junctional complexes in various epithelia. *J. Cell Biol.* 17:375–412. http://dx.doi.org/10.1083/jcb.17.2.375

Fernandez-Gonzalez, R., S.M. Simoes, J.C. Röper, S. Eaton, and J.A. Zallen. 2009. Myosin II dynamics are regulated by tension in intercalating cells. *Dev. Cell.* 17:736–743. http://dx.doi.org/10.1016/j.devcel.2009.09.003

Fischer, S.C., G.B. Blanchard, J. Duque, R.J. Adams, A.M. Arias, S.D. Guest, and N. Gorfinkiel. 2014. Contractile and mechanical properties of epithelia with perturbed actomyosin dynamics. *PLoS One.* 9:e95695. http://dx.doi.org/10.1371/journal.pone.0095695

Flood, G., A.J. Rowe, D.R. Critchley, and W.B. Gratzer. 1997. Further analysis of the role of spectrin repeat motifs in alpha-actinin dimer formation. *Eur. Biophys. J.* 25:431–435. http://dx.doi.org/10.1007/s002490050057

Founounou, N., N. Loyer, and R. Le Borgne. 2013. Septins regulate the contractility of the actomyosin ring to enable adherens junction remodeling during cytokinesis of epithelial cells. *Dev. Cell.* 24:242–255. http://dx.doi.org/10.1016/j.devcel.2013.01.008

Franke, W.W. 2009. Discovering the molecular components of intercellular junctions--a historical view. *Cold Spring Harb. Perspect. Biol.* 1:a003061. http://dx.doi.org/10.1101/cshperspect.a003061

Franke, J.D., R.A. Montague, and D.P. Kiehart. 2010. Nonmuscle myosin II is required for cell proliferation, cell sheet adhesion and wing hair morphology during wing morphogenesis. *Dev. Biol.* 345:117–132. http://dx.doi.org/10.1016/j.ydbio.2010.06.028

Franzot, G., B. Sjöblom, M. Gautel, and K. Djinović Carugo. 2005. The crystal structure of the actin binding domain from α-actinin in its closed conformation: structural insight into phospholipid regulation of α-actinin. *J. Mol. Biol.* 348:151–165. http://dx.doi.org/10.1016/j.jmb.2005.01.002

Fukasawa, H., S. Bornheimer, K. Kudlicka, and M.G. Farquhar. 2009. Slit diaphragms contain tight junction proteins. *J. Am. Soc. Nephrol.* 20:1491–1503. http://dx.doi.org/10.1681/ASN.2008101117

Ganz, A., M. Lambert, A. Saez, P. Silberzan, A. Buguin, R.M. Mège, and B. Ladoux. 2006. Traction forces exerted through N-cadherin contacts. *Biol. Cell.* 98:721–730. http://dx.doi.org/10.1042/BC20060039

Garbett, D., and A. Bretscher. 2014. The surprising dynamics of scaffolding proteins. *Mol. Biol. Cell.* 25:2315–2319. http://dx.doi.org/10.1091/mbc.E14-04-0878

Gavard, J., M. Lambert, I. Grosheva, V. Marthiens, T. Irinopoulou, J.F. Riou, A. Bershadsky, and R.M. Mège. 2004. Lamellipodium extension and cadherin adhesion: two cell responses to cadherin activation relying on distinct signalling pathways. *J. Cell Sci.* 117:257–270. http://dx.doi.org/10.1242/jcs.00857

Goel, R., F. Majeed, R. Vogel, M.C. Corretti, M. Weir, C. Mangano, C. White, G.D. Plotnick, and M. Miller. 2007. Exercise-induced hypertension, endothelial dysfunction, and coronary artery disease in a marathon runner. *Am. J. Cardiol.* 99:743–744. http://dx.doi.org/10.1016/j.amjcard.2006.09.127

Gomez, G.A., R.W. McLachlan, and A.S. Yap. 2011. Productive tension: force-sensing and homeostasis of cell–cell junctions. *Trends Cell Biol.* 21:499–505. http://dx.doi.org/10.1016/j.tcb.2011.05.006

Goodenough, D.A. 1975. The structure of cell membranes involved in intercellular communication. *Am. J. Clin. Pathol.* 63:636–645.

Goodenough, D.A., and J.P. Revel. 1970. A fine structural analysis of intercellular junctions in the mouse liver. *J. Cell Biol.* 45:272–290. http://dx.doi.org/10.1083/jcb.45.2.272

Goodenough, D.A., and J.P. Revel. 1971. The permeability of isolated and in situ mouse hepatic gap junctions studied with enzymatic tracers. *J. Cell Biol.* 50:81–91. http://dx.doi.org/10.1083/jcb.50.1.81

Grikscheit, K., T. Frank, Y. Wang, and R. Grosse. 2015. Junctional actin assembly is mediated by Formin-like 2 downstream of Rac1. *J. Cell Biol.* 209:367–376. http://dx.doi.org/10.1083/jcb.201412015

Guillot, C., and T. Lecuit. 2013. Adhesion disengagement uncouples intrinsic and extrinsic forces to drive cytokinesis in epithelial tissues. *Dev. Cell.* 24:227–241. http://dx.doi.org/10.1016/j.devcel.2013.01.010

Gujral, T.S., E.S. Karp, M. Chan, B.H. Chang, and G. MacBeath. 2013. Family-wide investigation of PDZ domain-mediated protein-protein interactions implicates β-catenin in maintaining the integrity of tight junctions. *Chem. Biol.* 20:816–827. http://dx.doi.org/10.1016/j.chembiol.2013.04.021

Gumbiner, B., and K. Simons. 1986. A functional assay for proteins involved in establishing an epithelial occluding barrier: identification of a uvomorulin-like polypeptide. *J. Cell Biol.* 102:457–468. http://dx.doi.org/10.1083/jcb.102.2.457

Gumbiner, B., B. Stevenson, and A. Grimaldi. 1988. The role of the cell adhesion molecule uvomorulin in the formation and maintenance of the epithelial junctional complex. *J. Cell Biol.* 107:1575–1587. http://dx.doi.org/10.1083/jcb.107.4.1575

Guo, Z., L.J. Neilson, H. Zhong, P.S. Murray, S. Zanivan, and R. Zaidel-Bar. 2014. E-cadherin interactome complexity and robustness resolved by quantitative proteomics. *Sci. Signal.* 7:rs7. http://dx.doi.org/10.1126/scisignal.2005473

Hampton, C.M., D.W. Taylor, and K.A. Taylor. 2007. Novel structures for α-actinin:F-actin interactions and their implications for actin–membrane attachment and tension sensing in the cytoskeleton. *J. Mol. Biol.* 368:92–104. http://dx.doi.org/10.1016/j.jmb.2007.01.071

Hansen, M.D., and M.C. Beckerle. 2008. α-Actinin links LPP, but not zyxin, to cadherin-based junctions. *Biochem. Biophys. Res. Commun.* 371:144–148. http://dx.doi.org/10.1016/j.bbrc.2008.04.018

Harris, A.R., L. Peter, J. Bellis, B. Baum, A.J. Kabla, and G.T. Charras. 2012. Characterizing the mechanics of cultured cell monolayers. *Proc. Natl. Acad. Sci. USA.* 109:16449–16454. http://dx.doi.org/10.1073/pnas.1213301109

Harris, A.R., A. Daeden, and G.T. Charras. 2014. Formation of adherens junctions leads to the emergence of a tissue-level tension in epithelial monolayers. *J. Cell Sci.* 127:2507–2517. http://dx.doi.org/10.1242/jcs.142349

Harrison, O.J., J. Vendome, J. Brasch, X. Jin, S. Hong, P.S. Katsamba, G. Ahlsen, R.B. Troyanovsky, S.M. Troyanovsky, B. Honig, and L. Shapiro. 2012. Nectin ectodomain structures reveal a canonical adhesive interface. *Nat. Struct. Mol. Biol.* 19:906–915. http://dx.doi.org/10.1038/nsmb.2366

Hazan, R.B., and L. Norton. 1998. The epidermal growth factor receptor modulates the interaction of E-cadherin with the actin cytoskeleton. *J. Biol. Chem.* 273:9078–9084. http://dx.doi.org/10.1074/jbc.273.15.9078

Hazan, R.B., L. Kang, S. Roe, P.I. Borgen, and D.L. Rimm. 1997. Vinculin is associated with the E-cadherin adhesion complex. *J. Biol. Chem.* 272:32448–32453. http://dx.doi.org/10.1074/jbc.272.51.32448

Herszterg, S., A. Leibfried, F. Bosveld, C. Martin, and Y. Bellaiche. 2013. Interplay between the dividing cell and its neighbors regulates adherens junction formation during cytokinesis in epithelial tissue. *Dev. Cell.* 24:256–270. http://dx.doi.org/10.1016/j.devcel.2012.11.019

Hijikata, T., Z.X. Lin, S. Holtzer, J. Choi, H.L. Sweeney, and H. Holtzer. 1997. Unanticipated temporal and spatial effects of sarcomeric α-actinin peptides expressed in PtK2 cells. *Cell Motil. Cytoskeleton.* 38:54–74. http://dx.doi.org/10.1002/(SICI)1097-0169(1997)38:1<54::AID-CM6>3.0.CO;2-H

Hinck, L., I.S. Näthke, J. Papkoff, and W.J. Nelson. 1994. Dynamics of cadherin/catenin complex formation: novel protein interactions and pathways of complex assembly. *J. Cell Biol.* 125:1327–1340. http://dx.doi.org/10.1083/jcb.125.6.1327

Hirano, S., A. Nose, K. Hatta, A. Kawakami, and M. Takeichi. 1987. Calcium-dependent cell-cell adhesion molecules (cadherins): subclass specificities and possible involvement of actin bundles. *J. Cell Biol.* 105:2501–2510. http://dx.doi.org/10.1083/jcb.105.6.2501

Hirokawa, N. 1980. A freeze-fracture study of intercellular junctions between various kinds of epithelial cells surrounding common endolymphatic space in the hearing organ of the chick. *Anat. Rec.* 196:129–143. http://dx.doi.org/10.1002/ar.1091960203

Hirokawa, N. 1986. Cytoskeletal architecture of the chicken hair cells revealed with the quick-freeze, deep-etch technique. *Hear. Res.* 22:41–54. http://dx.doi.org/10.1016/0378-5955(86)90076-6

Hirokawa, N., and J.E. Heuser. 1981. Quick-freeze, deep-etch visualization of the cytoskeleton beneath surface differentiations of intestinal epithelial cells. *J. Cell Biol.* 91:399–409. http://dx.doi.org/10.1083/jcb.91.2.399

Hirokawa, N., and L.G. Tilney. 1982. Interactions between actin filaments and between actin filaments and membranes in quick-frozen and deeply etched hair cells of the chick ear. *J. Cell Biol.* 95:249–261. http://dx.doi.org/10.1083/jcb.95.1.249

Hirokawa, N., L.G. Tilney, K. Fujiwara, and J.E. Heuser. 1982. Organization of actin, myosin, and intermediate filaments in the brush border of intestinal epithelial cells. *J. Cell Biol.* 94:425–443. http://dx.doi.org/10.1083/jcb.94.2.425

Hirokawa, N., T.C. Keller III, R. Chasan, and M.S. Mooseker. 1983. Mechanism of brush border contractility studied by the quick-freeze, deep-etch method. *J. Cell Biol.* 96:1325–1336. http://dx.doi.org/10.1083/jcb.96.5.1325

Hoj, J.P., J.A. Davis, K.E. Fullmer, D.J. Morrell, N.E. Saguibo, J.T. Schuler, K.J. Tuttle, and M.D. Hansen. 2014. Cellular contractility changes are sufficient to drive epithelial scattering. *Exp. Cell Res.* 326:187–200. http://dx.doi.org/10.1016/j.yexcr.2014.04.011

Hong, S., R.B. Troyanovsky, and S.M. Troyanovsky. 2013. Binding to F-actin guides cadherin cluster assembly, stability, and movement. *J. Cell Biol.* 201:131–143. http://dx.doi.org/10.1083/jcb.201211054

Howarth, A.G., and B.R. Stevenson. 1995. Molecular environment of ZO-1 in epithelial and non-epithelial cells. *Cell Motil. Cytoskeleton.* 31:323–332. http://dx.doi.org/10.1002/cm.970310408

Hsueh, W.A., and P.W. Anderson. 1992. Hypertension, the endothelial cell, and the vascular complications of diabetes mellitus. *Hypertension.* 20:253–263. http://dx.doi.org/10.1161/01.HYP.20.2.253

Huang, J., B.H. Kang, M. Pancera, J.H. Lee, T. Tong, Y. Feng, H. Imamichi, I.S. Georgiev, G.Y. Chuang, A. Druz, et al. 2014. Broad and potent HIV-1 neutralization by a human antibody that binds the gp41-gp120 interface. *Nature.* 515:138–142. http://dx.doi.org/10.1038/nature13601

Huveneers, S., and J. de Rooij. 2013. Mechanosensitive systems at the cadherin–F-actin interface. *J. Cell Sci.* 126:403–413. http://dx.doi.org/10.1242/jcs.109447

Ikeda, W., H. Nakanishi, J. Miyoshi, K. Mandai, H. Ishizaki, M. Tanaka, A. Togawa, K. Takahashi, H. Nishioka, H. Yoshida, et al. 1999. Afadin: A key molecule essential for structural organization of cell-cell junctions of polarized epithelia during embryogenesis. *J. Cell Biol.* 146:1117–1132. http://dx.doi.org/10.1083/jcb.146.5.1117

Ikenouchi, J., M. Furuse, K. Furuse, H. Sasaki, S. Tsukita, and S. Tsukita. 2005. Tricellulin constitutes a novel barrier at tricellular contacts of epithelial cells. *J. Cell Biol.* 171:939–945. http://dx.doi.org/10.1083/jcb.200510043

Imamura, Y., M. Itoh, Y. Maeno, S. Tsukita, and A. Nagafuchi. 1999. Functional domains of α-catenin required for the strong state of cadherin-based cell adhesion. *J. Cell Biol.* 144:1311–1322. http://dx.doi.org/10.1083/jcb.144.6.1311

Ishiyama, N., S.H. Lee, S. Liu, G.Y. Li, M.J. Smith, L.F. Reichardt, and M. Ikura. 2010. Dynamic and static interactions between p120 catenin and E-cadherin regulate the stability of cell-cell adhesion. *Cell.* 141:117–128. http://dx.doi.org/10.1016/j.cell.2010.01.017

Ishiyama, N., N. Tanaka, K. Abe, Y.J. Yang, Y.M. Abbas, M. Umitsu, B. Nagar, S.A. Bueler, J.L. Rubinstein, M. Takeichi, and M. Ikura. 2013. An autoinhibited structure of α-catenin and its implications for vinculin recruitment to adherens junctions. *J. Biol. Chem.* 288:15913–15925. http://dx.doi.org/10.1074/jbc.M113.453928

Itoh, M., S. Yonemura, A. Nagafuchi, S. Tsukita, and S. Tsukita. 1991. A 220-kD undercoat-constitutive protein: its specific localization at cadherin-based cell-cell adhesion sites. *J. Cell Biol.* 115:1449–1462. http://dx.doi.org/10.1083/jcb.115.5.1449

Itoh, M., A. Nagafuchi, S. Moroi, and S. Tsukita. 1997. Involvement of ZO-1 in cadherin-based cell adhesion through its direct binding to α catenin and actin filaments. *J. Cell Biol.* 138:181–192. http://dx.doi.org/10.1083/jcb.138.1.181

Iwasaki, T., and Y.L. Wang. 2008. Cytoplasmic force gradient in migrating adhesive cells. *Biophys. J.* 94:L35–L37. http://dx.doi.org/10.1529/biophysj.107.124479

Jaffe, S.H., D.R. Friedlander, F. Matsuzaki, K.L. Crossin, B.A. Cunningham, and G.M. Edelman. 1990. Differential effects of the cytoplasmic domains of cell adhesion molecules on cell aggregation and sorting-out. *Proc. Natl. Acad. Sci. USA.* 87:3589–3593. http://dx.doi.org/10.1073/pnas.87.9.3589

Jiang, H., and S.X. Sun. 2013. Cellular pressure and volume regulation and implications for cell mechanics. *Biophys. J.* 105:609–619. http://dx.doi.org/10.1016/j.bpj.2013.06.021

Johnson, R.P., and S.W. Craig. 1995a. The carboxy-terminal tail domain of vinculin contains a cryptic binding site for acidic phospholipids. *Biochem. Biophys. Res. Commun.* 210:159–164. http://dx.doi.org/10.1006/bbrc.1995.1641

Johnson, R.P., and S.W. Craig. 1995b. F-actin binding site masked by the intramolecular association of vinculin head and tail domains. *Nature.* 373:261–264. http://dx.doi.org/10.1038/373261a0

Kasza, K.E., D.L. Farrell, and J.A. Zallen. 2014. Spatiotemporal control of epithelial remodeling by regulated myosin phosphorylation. *Proc. Natl. Acad. Sci. USA.* 111:11732–11737. http://dx.doi.org/10.1073/pnas.1400520111

Katz, B.Z., S. Levenberg, K.M. Yamada, and B. Geiger. 1998. Modulation of cell-cell adherens junctions by surface clustering of the N-cadherin cytoplasmic tail. *Exp. Cell Res.* 243:415–424. http://dx.doi.org/10.1006/excr.1998.4194

Kelly, D.F., D.W. Taylor, C. Bakolitsa, A.A. Bobkov, L. Bankston, R.C. Liddington, and K.A. Taylor. 2006. Structure of the α-actinin–vinculin head domain complex determined by cryo-electron microscopy. *J. Mol. Biol.* 357:562–573. http://dx.doi.org/10.1016/j.jmb.2005.12.076

Kensler, R.W., and D.A. Goodenough. 1980. Isolation of mouse myocardial gap junctions. *J. Cell Biol.* 86:755–764. http://dx.doi.org/10.1083/jcb.86.3.755

Keren, K., P.T. Yam, A. Kinkhabwala, A. Mogilner, and J.A. Theriot. 2009. Intracellular fluid flow in rapidly moving cells. *Nat. Cell Biol.* 11:1219–1224. http://dx.doi.org/10.1038/ncb1965

Kim, T.J., S. Zheng, J. Sun, I. Muhamed, J. Wu, L. Lei, X. Kong, D.E. Leckband, and Y. Wang. 2015. Dynamic visualization of α-catenin reveals rapid, reversible conformation switching between tension states. *Curr. Biol.* 25:218–224. http://dx.doi.org/10.1016/j.cub.2014.11.017

Kimura, J., O. Ichii, S. Otsuka, H. Sasaki, Y. Hashimoto, and Y. Kon. 2013. Close relations between podocyte injuries and membranous proliferative glomerulonephritis in autoimmune murine models. *Am. J. Nephrol.* 38:27–38. http://dx.doi.org/10.1159/000353093

Kishikawa, M., A. Suzuki, and S. Ohno. 2008. aPKC enables development of zonula adherens by antagonizing centripetal contraction of the circumferential actomyosin cables. *J. Cell Sci.* 121:2481–2492. http://dx.doi.org/10.1242/jcs.024109

Knight, M.M., T. Toyoda, D.A. Lee, and D.L. Bader. 2006. Mechanical compression and hydrostatic pressure induce reversible changes in actin cytoskeletal organisation in chondrocytes in agarose. *J. Biomech.* 39:1547–1551. http://dx.doi.org/10.1016/j.jbiomech.2005.04.006

Knudsen, K.A., and M.J. Wheelock. 1992. Plakoglobin, or an 83-kD homologue distinct from beta-catenin, interacts with E-cadherin and N-cadherin. *J. Cell Biol.* 118:671–679. http://dx.doi.org/10.1083/jcb.118.3.671

Knudsen, K.A., A.P. Soler, K.R. Johnson, and M.J. Wheelock. 1995. Interaction of alpha-actinin with the cadherin/catenin cell-cell adhesion complex via alpha-catenin. *J. Cell Biol.* 130:67–77. http://dx.doi.org/10.1083/jcb.130.1.67

Kobielak, A., H.A. Pasolli, and E. Fuchs. 2004. Mammalian formin-1 participates in adherens junctions and polymerization of linear actin cables. *Nat. Cell Biol.* 6:21–30. http://dx.doi.org/10.1038/ncb1075

Kremerskothen, J., C. Plaas, S. Kindler, M. Frotscher, and A. Barnekow. 2005. Synaptopodin, a molecule involved in the formation of the dendritic spine apparatus, is a dual actin/α-actinin binding protein. *J. Neurochem.* 92:597–606. http://dx.doi.org/10.1111/j.1471-4159.2004.02888.x

Kuipers, D., A. Mehonic, M. Kajita, L. Peter, Y. Fujita, T. Duke, G. Charras, and J.E. Gale. 2014. Epithelial repair is a two-stage process driven first by dying cells and then by their neighbours. *J. Cell Sci.* 127:1229–1241. http://dx.doi.org/10.1242/jcs.138289

Ladoux, B., E. Anon, M. Lambert, A. Rabodzey, P. Hersen, A. Buguin, P. Silberzan, and R.M. Mège. 2010. Strength dependence of cadherin-mediated adhesions. *Biophys. J.* 98:534–542. http://dx.doi.org/10.1016/j.bpj.2009.10.044

Lambert, M., O. Thoumine, J. Brevier, D. Choquet, D. Riveline, and R.M. Mège. 2007. Nucleation and growth of cadherin adhesions. *Exp. Cell Res.* 313:4025–4040. http://dx.doi.org/10.1016/j.yexcr.2007.07.035

Laprise, P., P. Chailler, M. Houde, J.F. Beaulieu, M.J. Boucher, and N. Rivard. 2002. Phosphatidylinositol 3-kinase controls human intestinal epithelial cell differentiation by promoting adherens junction assembly and p38 MAPK activation. *J. Biol. Chem.* 277:8226–8234. http://dx.doi.org/10.1074/jbc.M110235200

Laprise, P., M.J. Langlois, M.J. Boucher, C. Jobin, and N. Rivard. 2004. Down-regulation of MEK/ERK signaling by E-cadherin-dependent PI3K/Akt pathway in differentiating intestinal epithelial cells. *J. Cell. Physiol.* 199:32–39. http://dx.doi.org/10.1002/jcp.10432

Law, R., P. Carl, S. Harper, P. Dalhaimer, D.W. Speicher, and D.E. Discher. 2003. Cooperativity in forced unfolding of tandem spectrin repeats. *Biophys. J.* 84:533–544. http://dx.doi.org/10.1016/S0006-3495(03)74872-3

Leckband, D., and S. Sivasankar. 2012. Cadherin recognition and adhesion. *Curr. Opin. Cell Biol.* 24:620–627. http://dx.doi.org/10.1016/j.ceb.2012.05.014

le Duc, Q., Q. Shi, I. Blonk, A. Sonnenberg, N. Wang, D. Leckband, and J. de Rooij. 2010. Vinculin potentiates E-cadherin mechanosensing and is recruited to actin-anchored sites within adherens junctions in a myosin II-dependent manner. *J. Cell Biol.* 189:1107–1115. http://dx.doi.org/10.1083/jcb.201001149

Leerberg, J.M., G.A. Gomez, S. Verma, E.J. Moussa, S.K. Wu, R. Priya, B.D. Hoffman, C. Grashoff, M.A. Schwartz, and A.S. Yap. 2014. Tension-sensitive actin assembly supports contractility at the epithelial zonula adherens. *Curr. Biol.* 24:1689–1699. http://dx.doi.org/10.1016/j.cub.2014.06.028

Lenne, P.F., A.J. Raae, S.M. Altmann, M. Saraste, and J.K. Hörber. 2000. States and transitions during forced unfolding of a single spectrin repeat. *FEBS Lett.* 476:124–128. http://dx.doi.org/10.1016/S0014-5793(00)01704-X

Lin, C.W., S.T. Yen, H.T. Chang, S.J. Chen, S.L. Lai, Y.C. Liu, T.H. Chan, W.L. Liao, and S.J. Lee. 2010. Loss of cofilin 1 disturbs actin dynamics, adhesion between enveloping and deep cell layers and cell movements during gastrulation in zebrafish. *PLoS One.* 5:e15331. http://dx.doi.org/10.1371/journal.pone.0015331

Litvinov, S.V., M. Balzar, M.J. Winter, H.A. Bakker, I.H. Briaire-de Bruijn, F. Prins, G.J. Fleuren, and S.O. Warnaar. 1997. Epithelial cell adhesion molecule (Ep-CAM) modulates cell-cell interactions mediated by classic cadherins. *J. Cell Biol.* 139:1337–1348. http://dx.doi.org/10.1083/jcb.139.5.1337

Liu, Z., J.L. Tan, D.M. Cohen, M.T. Yang, N.J. Sniadecki, S.A. Ruiz, C.M. Nelson, and C.S. Chen. 2010. Mechanical tugging force regulates the size of cell-cell junctions. *Proc. Natl. Acad. Sci. USA.* 107:9944–9949. http://dx.doi.org/10.1073/pnas.0914547107

Lorentz, W.B. Jr., W.E. Lassiter, and C.W. Gottschalk. 1972. Renal tubular permeability during increased intrarenal pressure. *J. Clin. Invest.* 51:484–492. http://dx.doi.org/10.1172/JCI106836

Madara, J.L. 1990. Maintenance of the macromolecular barrier at cell extrusion sites in intestinal epithelium: physiological rearrangement of tight junctions. *J. Membr. Biol.* 116:177–184. http://dx.doi.org/10.1007/BF01868675

Madara, J.L., D. Barenberg, and S. Carlson. 1986. Effects of cytochalasin D on occluding junctions of intestinal absorptive cells: further evidence that the cytoskeleton may influence paracellular permeability and junctional charge selectivity. *J. Cell Biol.* 102:2125–2136. http://dx.doi.org/10.1083/jcb.102.6.2125

Maiden, S.L., N. Harrison, J. Keegan, B. Cain, A.M. Lynch, J. Pettitt, and J. Hardin. 2013. Specific conserved C-terminal amino acids of *Caenorhabditis elegans* HMP-1/α-catenin modulate F-actin binding independently of vinculin. *J. Biol. Chem.* 288:5694–5706. http://dx.doi.org/10.1074/jbc.M112.438093

Maiers, J.L., X. Peng, A.S. Fanning, and K.A. DeMali. 2013. ZO-1 recruitment to α-catenin--a novel mechanism for coupling the assembly of tight junctions to adherens junctions. *J. Cell Sci.* 126:3904–3915. http://dx.doi.org/10.1242/jcs.126565

Maître, J.L., and C.P. Heisenberg. 2011. The role of adhesion energy in controlling cell-cell contacts. *Curr. Opin. Cell Biol.* 23:508–514. http://dx.doi.org/10.1016/j.ceb.2011.07.004

Mandato, C.A., and W.M. Bement. 2001. Contraction and polymerization cooperate to assemble and close actomyosin rings around *Xenopus* oocyte wounds. *J. Cell Biol.* 154:785–798. http://dx.doi.org/10.1083/jcb.200103105

Martin, A.C., M. Gelbart, R. Fernandez-Gonzalez, M. Kaschube, and E.F. Wieschaus. 2010. Integration of contractile forces during tissue invagination. *J. Cell Biol.* 188:735–749. http://dx.doi.org/10.1083/jcb.200910099

Martinez-Rico, C., F. Pincet, E. Perez, J.P. Thiery, K. Shimizu, Y. Takai, and S. Dufour. 2005. Separation force measurements reveal different types of modulation of E-cadherin-based adhesion by nectin-1 and -3. *J. Biol. Chem.* 280:4753–4760. http://dx.doi.org/10.1074/jbc.M412544200

Maruthamuthu, V., B. Sabass, U.S. Schwarz, and M.L. Gardel. 2011. Cell-ECM traction force modulates endogenous tension at cell-cell contacts. *Proc. Natl. Acad. Sci. USA.* 108:4708–4713. http://dx.doi.org/10.1073/pnas.1011123108

Matsuzaki, F., R.M. Mège, S.H. Jaffe, D.R. Friedlander, W.J. Gallin, J.I. Goldberg, B.A. Cunningham, and G.M. Edelman. 1990. cDNAs of cell adhesion molecules of different specificity induce changes in cell shape and border formation in cultured S180 cells. *J. Cell Biol.* 110:1239–1252. http://dx.doi.org/10.1083/jcb.110.4.1239

McGill, M.A., R.F. McKinley, and T.J. Harris. 2009. Independent cadherin-catenin and Bazooka clusters interact to assemble adherens junctions. *J. Cell Biol.* 185:787–796. http://dx.doi.org/10.1083/jcb.200812146

McGregor, A., A.D. Blanchard, A.J. Rowe, and D.R. Critchley. 1994. Identification of the vinculin-binding site in the cytoskeletal protein α-actinin. *Biochem. J.* 301:225–233. http://dx.doi.org/10.1042/bj3010225

Meng, W., and M. Takeichi. 2009. Adherens junction: molecular architecture and regulation. *Cold Spring Harb. Perspect. Biol.* 1:a002899. http://dx.doi.org/10.1101/cshperspect.a002899

Mertz, A.F., Y. Che, S. Banerjee, J.M. Goldstein, K.A. Rosowski, S.F. Revilla, C.M. Niessen, M.C. Marchetti, E.R. Dufresne, and V. Horsley. 2013. Cadherin-based intercellular adhesions organize epithelial cell-matrix traction forces. *Proc. Natl. Acad. Sci. USA.* 110:842–847. http://dx.doi.org/10.1073/pnas.1217279110

Miyaguchi, K. 2000. Ultrastructure of the zonula adherens revealed by rapid-freeze deep-etching. *J. Struct. Biol.* 132:169–178. http://dx.doi.org/10.1006/jsbi.2000.4244

Miyahara, M., H. Nakanishi, K. Takahashi, K. Satoh-Horikawa, K. Tachibana, and Y. Takai. 2000. Interaction of nectin with afadin is necessary for its clustering at cell-cell contact sites but not for its cis dimerization or trans interaction. *J. Biol. Chem.* 275:613–618. http://dx.doi.org/10.1074/jbc.275.1.613

Miyake, Y., N. Inoue, K. Nishimura, N. Kinoshita, H. Hosoya, and S. Yonemura. 2006. Actomyosin tension is required for correct recruitment of adherens junction components and zonula occludens formation. *Exp. Cell Res.* 312:1637–1650. http://dx.doi.org/10.1016/j.yexcr.2006.01.031

Müller, S.L., M. Portwich, A. Schmidt, D.I. Utepbergenov, O. Huber, I.E. Blasig, and G. Krause. 2005. The tight junction protein occludin and the adherens junction protein alpha-catenin share a common interaction mechanism with ZO-1. *J. Biol. Chem.* 280:3747–3756. http://dx.doi.org/10.1074/jbc.M411365200

Mun, G.I., S. Park, J. Kremerskothen, and Y.C. Boo. 2014. Expression of synaptopodin in endothelial cells exposed to laminar shear stress and its role in endothelial wound healing. *FEBS Lett.* 588:1024–1030. http://dx.doi.org/10.1016/j.febslet.2014.02.012

Mundel, P., H.W. Heid, T.M. Mundel, M. Krüger, J. Reiser, and W. Kriz. 1997. Synaptopodin: an actin-associated protein in telencephalic dendrites and renal podocytes. *J. Cell Biol.* 139:193–204. http://dx.doi.org/10.1083/jcb.139.1.193

Nagafuchi, A., and M. Takeichi. 1988. Cell binding function of E-cadherin is regulated by the cytoplasmic domain. *EMBO J.* 7:3679–3684.

Näthke, I.S., L. Hinck, J.R. Swedlow, J. Papkoff, and W.J. Nelson. 1994. Defining interactions and distributions of cadherin and catenin complexes in polarized epithelial cells. *J. Cell Biol.* 125:1341–1352. http://dx.doi.org/10.1083/jcb.125.6.1341

Ng, M.R., A. Besser, G. Danuser, and J.S. Brugge. 2012. Substrate stiffness regulates cadherin-dependent collective migration through myosin-II contractility. *J. Cell Biol.* 199:545–563. http://dx.doi.org/10.1083/jcb.201207148

Nieset, J.E., A.R. Redfield, F. Jin, K.A. Knudsen, K.R. Johnson, and M.J. Wheelock. 1997. Characterization of the interactions of alpha-catenin with alpha-actinin and beta-catenin/plakoglobin. *J. Cell Sci.* 110:1013–1022.

Nishimura, W., T. Iizuka, S. Hirabayashi, N. Tanaka, and Y. Hata. 2000. Localization of BAI-associated protein1/membrane-associated guanylate kinase-1 at adherens junctions in normal rat kidney cells: polarized targeting mediated by the carboxyl-terminal PDZ domains. *J. Cell. Physiol.* 185:358–365. http://dx.doi.org/10.1002/1097-4652(200012)185:3<358::AID-JCP6>3.0.CO;2-#

Noegel, A., W. Witke, and M. Schleicher. 1987. Calcium-sensitive non-muscle α-actinin contains EF-hand structures and highly conserved regions. *FEBS Lett.* 221:391–396. http://dx.doi.org/10.1016/0014-5793(87)80962-6

Oda, Y., T. Otani, J. Ikenouchi, and M. Furuse. 2014. Tricellulin regulates junctional tension of epithelial cells at tricellular contacts through Cdc42. *J. Cell Sci.* 127:4201–4212. http://dx.doi.org/10.1242/jcs.150607

Okano, M., and Y. Yoshida. 1993. Influence of shear stress on endothelial cell shapes and junction complexes at flow dividers of aortic bifurcations in cholesterol-fed rabbits. *Front. Med. Biol. Eng.* 5:95–120.

Ooshio, T., K. Irie, K. Morimoto, A. Fukuhara, T. Imai, and Y. Takai. 2004. Involvement of LMO7 in the association of two cell-cell adhesion molecules, nectin and E-cadherin, through afadin and alpha-actinin in epithelial cells. *J. Biol. Chem.* 279:31365–31373. http://dx.doi.org/10.1074/jbc.M401957200

Ooshio, T., R. Kobayashi, W. Ikeda, M. Miyata, Y. Fukumoto, N. Matsuzawa, H. Ogita, and Y. Takai. 2010. Involvement of the interaction of afadin with ZO-1 in the formation of tight junctions in Madin-Darby canine kidney cells. *J. Biol. Chem.* 285:5003–5012. http://dx.doi.org/10.1074/jbc.M109.043760

Ortiz, V., S.O. Nielsen, M.L. Klein, and D.E. Discher. 2005. Unfolding a linker between helical repeats. *J. Mol. Biol.* 349:638–647. http://dx.doi.org/10.1016/j.jmb.2005.03.086

Otey, C.A., and O. Carpen. 2004. α-actinin revisited: a fresh look at an old player. *Cell Motil. Cytoskeleton.* 58:104–111. http://dx.doi.org/10.1002/cm.20007

Ozawa, M. 1998. Identification of the region of α-catenin that plays an essential role in cadherin-mediated cell adhesion. *J. Biol. Chem.* 273:29524–29529. http://dx.doi.org/10.1074/jbc.273.45.29524

Ozawa, M., and R. Kemler. 1992. Molecular organization of the uvomorulin-catenin complex. *J. Cell Biol.* 116:989–996. http://dx.doi.org/10.1083/jcb.116.4.989

Ozawa, M., H. Baribault, and R. Kemler. 1989. The cytoplasmic domain of the cell adhesion molecule uvomorulin associates with three independent proteins structurally related in different species. *EMBO J.* 8:1711–1717.

Ozawa, M., M. Ringwald, and R. Kemler. 1990. Uvomorulin-catenin complex formation is regulated by a specific domain in the cytoplasmic region of the cell adhesion molecule. *Proc. Natl. Acad. Sci. USA.* 87:4246–4250. http://dx.doi.org/10.1073/pnas.87.11.4246

Padmanabhan, A., M.V. Rao, Y. Wu, and R. Zaidel-Bar. 2015. Jack of all trades: functional modularity in the adherens junction. *Curr. Opin. Cell Biol.* 36:32–40. http://dx.doi.org/10.1016/j.ceb.2015.06.008

Papakonstanti, E.A., E.A. Vardaki, and C. Stournaras. 2000. Actin cytoskeleton: a signaling sensor in cell volume regulation. *Cell. Physiol. Biochem.* 10:257–264. http://dx.doi.org/10.1159/000016366

Patrie, K.M., A.J. Drescher, A. Welihinda, P. Mundel, and B. Margolis. 2002. Interaction of two actin-binding proteins, synaptopodin and α-actinin-4, with the tight junction protein MAGI-1. *J. Biol. Chem.* 277:30183–30190. http://dx.doi.org/10.1074/jbc.M203072200

Peisley, A., and G. Skiniotis. 2015. 2D projection analysis of GPCR complexes by negative stain electron microscopy. *Methods Mol. Biol.* 1335:29–38. http://dx.doi.org/10.1007/978-1-4939-2914-6_3

Peng, X., L.E. Cuff, C.D. Lawton, and K.A. DeMali. 2010. Vinculin regulates cell-surface E-cadherin expression by binding to α-catenin. *J. Cell Sci.* 123:567–577. http://dx.doi.org/10.1242/jcs.056432

Peng, X., J.L. Maiers, D. Choudhury, S.W. Craig, and K.A. DeMali. 2012. α-Catenin uses a novel mechanism to activate vinculin. *J. Biol. Chem.* 287:7728–7737. http://dx.doi.org/10.1074/jbc.M111.297481

Petrova, Y.I., M.M. Spano, and B.M. Gumbiner. 2012. Conformational epitopes at cadherin calcium-binding sites and p120-catenin phosphorylation regulate cell adhesion. *Mol. Biol. Cell.* 23:2092–2108. http://dx.doi.org/10.1091/mbc.E11-12-1060

Plotnikov, S.V., and C.M. Waterman. 2013. Guiding cell migration by tugging. *Curr. Opin. Cell Biol.* 25:619–626. http://dx.doi.org/10.1016/j.ceb.2013.06.003

Plotnikov, S.V., A.M. Pasapera, B. Sabass, and C.M. Waterman. 2012. Force fluctuations within focal adhesions mediate ECM-rigidity sensing to guide directed cell migration. *Cell.* 151:1513–1527. http://dx.doi.org/10.1016/j.cell.2012.11.034

Pokutta, S., H.J. Choi, G. Ahlsen, S.D. Hansen, and W.I. Weis. 2014. Structural and thermodynamic characterization of cadherin·β-catenin·α-catenin complex formation. *J. Biol. Chem.* 289:13589–13601. http://dx.doi.org/10.1074/jbc.M114.554709

Preston, R.A., M. Ledford, B.J. Materson, N.M. Baltodano, A. Memon, and A. Alonso. 2002. Effects of severe, uncontrolled hypertension on endothelial activation: soluble vascular cell adhesion molecule-1, soluble intercellular adhesion molecule-1 and von Willebrand factor. *J. Hypertens.* 20:871–877. http://dx.doi.org/10.1097/00004872-200205000-00021

Qin, Y., C. Capaldo, B.M. Gumbiner, and I.G. Macara. 2005. The mammalian Scribble polarity protein regulates epithelial cell adhesion and migration through E-cadherin. *J. Cell Biol.* 171:1061–1071. http://dx.doi.org/10.1083/jcb.200506094

Rajasekaran, A.K., M. Hojo, T. Huima, and E. Rodriguez-Boulan. 1996. Catenins and zonula occludens-1 form a complex during early stages in the assembly of tight junctions. *J. Cell Biol.* 132:451–463. http://dx.doi.org/10.1083/jcb.132.3.451

Rangarajan, E.S., and T. Izard. 2012. The cytoskeletal protein α-catenin unfurls upon binding to vinculin. *J. Biol. Chem.* 287:18492–18499. http://dx.doi.org/10.1074/jbc.M112.351023

Razzell, W., W. Wood, and P. Martin. 2014. Recapitulation of morphogenetic cell shape changes enables wound re-epithelialisation. *Development.* 141:1814–1820. http://dx.doi.org/10.1242/dev.107045

Reiser, J., W. Kriz, M. Kretzler, and P. Mundel. 2000. The glomerular slit diaphragm is a modified adherens junction. *J. Am. Soc. Nephrol.* 11:1–8.

Reyes, C.C., M. Jin, E.B. Breznau, R. Espino, R. Delgado-Gonzalo, A.B. Goryachev, and A.L. Miller. 2014. Anillin regulates cell-cell junction integrity by organizing junctional accumulation of Rho-GTP and actomyosin. *Curr. Biol.* 24:1263–1270. http://dx.doi.org/10.1016/j.cub.2014.04.021

Reynolds, A.B., J. Daniel, P.D. McCrea, M.J. Wheelock, J. Wu, and Z. Zhang. 1994. Identification of a new catenin: the tyrosine kinase substrate p120cas associates with E-cadherin complexes. *Mol. Cell. Biol.* 14:8333–8342.

Rief, M., J. Pascual, M. Saraste, and H.E. Gaub. 1999. Single molecule force spectroscopy of spectrin repeats: low unfolding forces in helix bundles. *J. Mol. Biol.* 286:553–561. http://dx.doi.org/10.1006/jmbi.1998.2466

Rikitake, Y., K. Mandai, and Y. Takai. 2012. The role of nectins in different types of cell–cell adhesion. *J. Cell Sci.* 125:3713–3722. http://dx.doi.org/10.1242/jcs.099572

Roh-Johnson, M., G. Shemer, C.D. Higgins, J.H. McClellan, A.D. Werts, U.S. Tulu, L. Gao, E. Betzig, D.P. Kiehart, and B. Goldstein. 2012. Triggering a cell shape change by exploiting preexisting actomyosin contractions. *Science.* 335:1232–1235. http://dx.doi.org/10.1126/science.1217869

Rosenberg, S., A. Stracher, and K. Burridge. 1981. Isolation and characterization of a calcium-sensitive alpha-actinin-like protein from human platelet cytoskeletons. *J. Biol. Chem.* 256:12986–12991.

Rüffer, C., A. Strey, A. Janning, K.S. Kim, and V. Gerke. 2004. Cell-cell junctions of dermal microvascular endothelial cells contain tight and adherens junction proteins in spatial proximity. *Biochemistry.* 43:5360–5369. http://dx.doi.org/10.1021/bi035517c

Ryu, J.R., A. Echarri, R. Li, and A.M. Pendergast. 2009. Regulation of cell-cell adhesion by Abi/Diaphanous complexes. *Mol. Cell. Biol.* 29:1735–1748. http://dx.doi.org/10.1128/MCB.01483-08

Saez, A., E. Anon, M. Ghibaudo, O. du Roure, J.M. Di Meglio, P. Hersen, P. Silberzan, A. Buguin, and B. Ladoux. 2010. Traction forces exerted by epithelial cell sheets. *J. Phys. Condens. Matter.* 22:194119. http://dx.doi.org/10.1088/0953-8984/22/19/194119

Samanta, D., U.A. Ramagopal, R. Rubinstein, V. Vigdorovich, S.G. Nathenson, and S.C. Almo. 2012. Structure of Nectin-2 reveals determinants of homophilic and heterophilic interactions that control cell-cell adhesion. *Proc. Natl. Acad. Sci. USA.* 109:14836–14840. http://dx.doi.org/10.1073/pnas.1212912109

Saravanan, S., C. Meghana, and M. Narasimha. 2013. Local, cell-nonautonomous feedback regulation of myosin dynamics patterns transitions in cell behavior: a role for tension and geometry? *Mol. Biol. Cell.* 24:2350–2361. http://dx.doi.org/10.1091/mbc.E12-12-0868

Sato, T., N. Fujita, A. Yamada, T. Ooshio, R. Okamoto, K. Irie, and Y. Takai. 2006. Regulation of the assembly and adhesion activity of E-cadherin by nectin and afadin for the formation of adherens junctions in Madin-Darby canine kidney cells. *J. Biol. Chem.* 281:5288–5299. http://dx.doi.org/10.1074/jbc.M510070200

Schiwek, D., N. Endlich, L. Holzman, H. Holthöfer, W. Kriz, and K. Endlich. 2004. Stable expression of nephrin and localization to cell-cell contacts in novel murine podocyte cell lines. *Kidney Int.* 66:91–101. http://dx.doi.org/10.1111/j.1523-1755.2004.00711.x

Schlager, M.A., H.T. Hoang, L. Urnavicius, S.L. Bullock, and A.P. Carter. 2014. In vitro reconstitution of a highly processive recombinant human dynein complex. *EMBO J.* 33:1855–1868. http://dx.doi.org/10.15252/embj.201488792

Schnabel, E., J.M. Anderson, and M.G. Farquhar. 1990. The tight junction protein ZO-1 is concentrated along slit diaphragms of the glomerular epithelium. *J. Cell Biol.* 111:1255–1263. http://dx.doi.org/10.1083/jcb.111.3.1255

Sedar, A.W., and J.G. Forte. 1964. Effects of calcium depletion on the junctional complex between oxyntic cells of gastric glands. *J. Cell Biol.* 22:173–188. http://dx.doi.org/10.1083/jcb.22.1.173

Shams, H., J. Golji, and M.R. Mofrad. 2012. A molecular trajectory of α-actinin activation. *Biophys. J.* 103:2050–2059. http://dx.doi.org/10.1016/j.bpj.2012.08.044

Shashikanth, N., Y.I. Petrova, S. Park, J. Chekan, S. Maiden, M. Spano, T. Ha, B.M. Gumbiner, and D.E. Leckband. 2015. Allosteric regulation of E-cadherin adhesion. *J. Biol. Chem.* 290:21749–21761. http://dx.doi.org/10.1074/jbc.M115.657098

Shewan, A.M., M. Maddugoda, A. Kraemer, S.J. Stehbens, S. Verma, E.M. Kovacs, and A.S. Yap. 2005. Myosin 2 is a key Rho kinase target necessary for the local concentration of E-cadherin at cell-cell contacts. *Mol. Biol. Cell.* 16:4531–4542. http://dx.doi.org/10.1091/mbc.E05-04-0330

Shibamoto, S., M. Hayakawa, K. Takeuchi, T. Hori, K. Miyazawa, N. Kitamura, K.R. Johnson, M.J. Wheelock, N. Matsuyoshi, M. Takeichi, et al. 1995. Association of p120, a tyrosine kinase substrate, with E-cadherin/catenin

complexes. *J. Cell Biol.* 128:949–957. http://dx.doi.org/10.1083/jcb.128.5.949

Shindo, A., and J.B. Wallingford. 2014. PCP and septins compartmentalize cortical actomyosin to direct collective cell movement. *Science.* 343:649–652. http://dx.doi.org/10.1126/science.1243126

Shukla, A.K., G.H. Westfield, K. Xiao, R.I. Reis, L.Y. Huang, P. Tripathi-Shukla, J. Qian, S. Li, A. Blanc, A.N. Oleskie, et al. 2014. Visualization of arrestin recruitment by a G-protein-coupled receptor. *Nature.* 512:218–222. http://dx.doi.org/10.1038/nature13430

Siliciano, J.D., and D.A. Goodenough. 1988. Localization of the tight junction protein, ZO-1, is modulated by extracellular calcium and cell-cell contact in Madin-Darby canine kidney epithelial cells. *J. Cell Biol.* 107:2389–2399. http://dx.doi.org/10.1083/jcb.107.6.2389

Sivasankar, S. 2013. Tuning the kinetics of cadherin adhesion. *J. Invest. Dermatol.* 133:2318–2323. http://dx.doi.org/10.1038/jid.2013.229

Sjöblom, B., A. Salmazo, and K. Djinović-Carugo. 2008. α-Actinin structure and regulation. *Cell. Mol. Life Sci.* 65:2688–2701. http://dx.doi.org/10.1007/s00018-008-8080-8

Slee, J.B., and L.J. Lowe-Krentz. 2013. Actin realignment and cofilin regulation are essential for barrier integrity during shear stress. *J. Cell. Biochem.* 114:782–795. http://dx.doi.org/10.1002/jcb.24416

Smutny, M., H.L. Cox, J.M. Leerberg, E.M. Kovacs, M.A. Conti, C. Ferguson, N.A. Hamilton, R.G. Parton, R.S. Adelstein, and A.S. Yap. 2010. Myosin II isoforms identify distinct functional modules that support integrity of the epithelial zonula adherens. *Nat. Cell Biol.* 12:696–702. http://dx.doi.org/10.1038/ncb2072

Staals, R.H., Y. Zhu, D.W. Taylor, J.E. Kornfeld, K. Sharma, A. Barendregt, J.J. Koehorst, M. Vlot, N. Neupane, K. Varossieau, et al. 2014. RNA targeting by the type III-A CRISPR-Cas Csm complex of *Thermus thermophilus*. *Mol. Cell.* 56:518–530. http://dx.doi.org/10.1016/j.molcel.2014.10.005

Stauffer, K.A., N.M. Kumar, N.B. Gilula, and N. Unwin. 1991. Isolation and purification of gap junction channels. *J. Cell Biol.* 115:141–150. http://dx.doi.org/10.1083/jcb.115.1.141

Stetak, A., and A. Hajnal. 2011. The *C. elegans* MAGI-1 protein is a novel component of cell junctions that is required for junctional compartmentalization. *Dev. Biol.* 350:24–31. http://dx.doi.org/10.1016/j.ydbio.2010.10.026

Stevenson, B.R., and D.A. Goodenough. 1984. Zonulae occludentes in junctional complex-enriched fractions from mouse liver: preliminary morphological and biochemical characterization. *J. Cell Biol.* 98:1209–1221. http://dx.doi.org/10.1083/jcb.98.4.1209

Stevenson, B.R., J.D. Siliciano, M.S. Mooseker, and D.A. Goodenough. 1986. Identification of ZO-1: a high molecular weight polypeptide associated with the tight junction (zonula occludens) in a variety of epithelia. *J. Cell Biol.* 103:755–766. http://dx.doi.org/10.1083/jcb.103.3.755

Stewart, M.P., J. Helenius, Y. Toyoda, S.P. Ramanathan, D.J. Muller, and A.A. Hyman. 2011. Hydrostatic pressure and the actomyosin cortex drive mitotic cell rounding. *Nature.* 469:226–230. http://dx.doi.org/10.1038/nature09642

Strale, P.O., L. Duchesne, G. Peyret, L. Montel, T. Nguyen, E. Png, R. Tampé, S. Troyanovsky, S. Hénon, B. Ladoux, and R.M. Mège. 2015. The formation of ordered nanoclusters controls cadherin anchoring to actin and cell-cell contact fluidity. *J. Cell Biol.* 210:333–346. http://dx.doi.org/10.1083/jcb.201410111

Tachibana, K., H. Nakanishi, K. Mandai, K. Ozaki, W. Ikeda, Y. Yamamoto, A. Nagafuchi, S. Tsukita, and Y. Takai. 2000. Two cell adhesion molecules, nectin and cadherin, interact through their cytoplasmic domain-associated proteins. *J. Cell Biol.* 150:1161–1176. http://dx.doi.org/10.1083/jcb.150.5.1161

Taguchi, K., T. Ishiuchi, and M. Takeichi. 2011. Mechanosensitive EPLIN-dependent remodeling of adherens junctions regulates epithelial reshaping. *J. Cell Biol.* 194:643–656. http://dx.doi.org/10.1083/jcb.201104124

Takahashi, K., H. Nakanishi, M. Miyahara, K. Mandai, K. Satoh, A. Satoh, H. Nishioka, J. Aoki, A. Nomoto, A. Mizoguchi, and Y. Takai. 1999. Nectin/PRR: an immunoglobulin-like cell adhesion molecule recruited to cadherin-based adherens junctions through interaction with Afadin, a PDZ domain-containing protein. *J. Cell Biol.* 145:539–549. http://dx.doi.org/10.1083/jcb.145.3.539

Tamada, M., T.D. Perez, W.J. Nelson, and M.P. Sheetz. 2007. Two distinct modes of myosin assembly and dynamics during epithelial wound closure. *J. Cell Biol.* 176:27–33. http://dx.doi.org/10.1083/jcb.200609116

Tang, V.W. 2006. Proteomic and bioinformatic analysis of epithelial tight junction reveals an unexpected cluster of synaptic molecules. *Biol. Direct.* 1:37. http://dx.doi.org/10.1186/1745-6150-1-37

Tang, V.W., and W.M. Brieher. 2012. α-Actinin-4/FSGS1 is required for Arp2/3-dependent actin assembly at the adherens junction. *J. Cell Biol.* 196:115–130. http://dx.doi.org/10.1083/jcb.201103116

Tang, V.W., and W.M. Brieher. 2013. FSGS3/CD2AP is a barbed-end capping protein that stabilizes actin and strengthens adherens junctions. *J. Cell Biol.* 203:815–833. http://dx.doi.org/10.1083/jcb.201304143

Tang, V.W., and D.A. Goodenough. 2003. Paracellular ion channel at the tight junction. *Biophys. J.* 84:1660–1673. http://dx.doi.org/10.1016/S0006-3495(03)74975-3

Tang, J., D.W. Taylor, and K.A. Taylor. 2001. The three-dimensional structure of α-actinin obtained by cryoelectron microscopy suggests a model for Ca^{2+}-dependent actin binding. *J. Mol. Biol.* 310:845–858. http://dx.doi.org/10.1006/jmbi.2001.4789

Thirone, A.C., P. Speight, M. Zulys, O.D. Rotstein, K. Szászi, S.F. Pedersen, and A. Kapus. 2009. Hyperosmotic stress induces Rho/Rho kinase/LIM kinase-mediated cofilin phosphorylation in tubular cells: key role in the osmotically triggered F-actin response. *Am. J. Physiol. Cell Physiol.* 296:C463–C475. http://dx.doi.org/10.1152/ajpcell.00467.2008

Thomas, W.A., C. Boscher, Y.S. Chu, D. Cuvelier, C. Martinez-Rico, R. Seddiki, J. Heysch, B. Ladoux, J.P. Thiery, R.M. Mege, and S. Dufour. 2013. α-Catenin and vinculin cooperate to promote high E-cadherin-based adhesion strength. *J. Biol. Chem.* 288:4957–4969. http://dx.doi.org/10.1074/jbc.M112.403774

Thoreson, M.A., P.Z. Anastasiadis, J.M. Daniel, R.C. Ireton, M.J. Wheelock, K.R. Johnson, D.K. Hummingbird, and A.B. Reynolds. 2000. Selective uncoupling of p120(ctn) from E-cadherin disrupts strong adhesion. *J. Cell Biol.* 148:189–202. http://dx.doi.org/10.1083/jcb.148.1.189

Ting, L.H., J.R. Jahn, J.I. Jung, B.R. Shuman, S. Feghhi, S.J. Han, M.L. Rodriguez, and N.J. Sniadecki. 2012. Flow mechanotransduction regulates traction forces, intercellular forces, and adherens junctions. *Am. J. Physiol. Heart Circ. Physiol.* 302:H2220–H2229. http://dx.doi.org/10.1152/ajpheart.00975.2011

Toret, C.P., M.V. D'Ambrosio, R.D. Vale, M.A. Simon, and W.J. Nelson. 2014. A genome-wide screen identifies conserved protein hubs required for cadherin-mediated cell-cell adhesion. *J. Cell Biol.* 204:265–279. http://dx.doi.org/10.1083/jcb.201306082

Tornavaca, O., M. Chia, N. Dufton, L.O. Almagro, D.E. Conway, A.M. Randi, M.A. Schwartz, K. Matter, and M.S. Balda. 2015. ZO-1 controls endothelial adherens junctions, cell–cell tension, angiogenesis, and barrier formation. *J. Cell Biol.* 208:821–838. http://dx.doi.org/10.1083/jcb.201404140

Travers, T., H. Shao, A. Wells, and C.J. Camacho. 2013. Modeling the assembly of the multiple domains of α-actinin-4 and its role in actin cross-linking. *Biophys. J.* 104:705–715. http://dx.doi.org/10.1016/j.bpj.2012.12.003

Tseng, Q., E. Duchemin-Pelletier, A. Deshiere, M. Balland, H. Guillou, O. Filhol, and M. Théry. 2012. Spatial organization of the extracellular matrix regulates cell–cell junction positioning. *Proc. Natl. Acad. Sci. USA.* 109:1506–1511. http://dx.doi.org/10.1073/pnas.1106377109

Tsukita, S., and S. Tsukita. 1989. Isolation of cell-to-cell adherens junctions from rat liver. *J. Cell Biol.* 108:31–41. http://dx.doi.org/10.1083/jcb.108.1.31

Tsukita, S., Y. Hieda, and S. Tsukita. 1989a. A new 82-kD barbed end-capping protein (radixin) localized in the cell-to-cell adherens junction: purification and characterization. *J. Cell Biol.* 108:2369–2382. http://dx.doi.org/10.1083/jcb.108.6.2369

Tsukita, S., M. Itoh, and S. Tsukita. 1989b. A new 400-kD protein from isolated adherens junctions: its localization at the undercoat of adherens junctions and at microfilament bundles such as stress fibers and circumferential bundles. *J. Cell Biol.* 109:2905–2915. http://dx.doi.org/10.1083/jcb.109.6.2905

Twiss, F., and J. de Rooij. 2013. Cadherin mechanotransduction in tissue remodeling. *Cell. Mol. Life Sci.* 70:4101–4116. http://dx.doi.org/10.1007/s00018-013-1329-x

Twiss, F., Q. Le Duc, S. Van Der Horst, H. Tabdili, G. Van Der Krogt, N. Wang, H. Rehmann, S. Huveneers, D.E. Leckband, and J. De Rooij. 2012. Vinculin-dependent Cadherin mechanosensing regulates efficient epithelial barrier formation. *Biol. Open.* 1:1128–1140. http://dx.doi.org/10.1242/bio.20122428

Tzima, E., M. Irani-Tehrani, W.B. Kiosses, E. Dejana, D.A. Schultz, B. Engelhardt, G. Cao, H. DeLisser, and M.A. Schwartz. 2005. A mechanosensory complex that mediates the endothelial cell response to fluid shear stress. *Nature.* 437:426–431. http://dx.doi.org/10.1038/nature03952

Underwood, J.L., C.G. Murphy, J. Chen, L. Franse-Carman, I. Wood, D.L. Epstein, and J.A. Alvarado. 1999. Glucocorticoids regulate transendothelial fluid flow resistance and formation of intercellular junctions. *Am. J. Physiol.* 277:C330–C342.

Van Itallie, C.M., A.J. Tietgens, A. Aponte, K. Fredriksson, A.S. Fanning, M. Gucek, and J.M. Anderson. 2014. Biotin ligase tagging identifies proteins proximal to E-cadherin, including lipoma preferred partner, a regulator of epithelial cell–cell and cell–substrate adhesion. *J. Cell Sci.* 127:885–895. http://dx.doi.org/10.1242/jcs.140475

Vasioukhin, V., C. Bauer, M. Yin, and E. Fuchs. 2000. Directed actin polymerization is the driving force for epithelial cell–cell adhesion. *Cell.* 100:209–219. http://dx.doi.org/10.1016/S0092-8674(00)81559-7

Vasquez, C.G., M. Tworoger, and A.C. Martin. 2014. Dynamic myosin phosphorylation regulates contractile pulses and tissue integrity during epithelial morphogenesis. *J. Cell Biol.* 206:435–450. http://dx.doi.org/10.1083/jcb.201402004

Verma, S., S.P. Han, M. Michael, G.A. Gomez, Z. Yang, R.D. Teasdale, A. Ratheesh, E.M. Kovacs, R.G. Ali, and A.S. Yap. 2012. A WAVE2-Arp2/3 actin nucleator apparatus supports junctional tension at the epithelial zonula adherens. *Mol. Biol. Cell.* 23:4601–4610. http://dx.doi.org/10.1091/mbc.E12-08-0574

Vestweber, D., and R. Kemler. 1985. Identification of a putative cell adhesion domain of uvomorulin. *EMBO J.* 4:3393–3398.

Viswanatha, R., A. Bretscher, and D. Garbett. 2014. Dynamics of ezrin and EBP50 in regulating microvilli on the apical aspect of epithelial cells. *Biochem. Soc. Trans.* 42:189–194. http://dx.doi.org/10.1042/BST20130263

Volk, T., and B. Geiger. 1986a. A-CAM: a 135-kD receptor of intercellular adherens junctions. I. Immunoelectron microscopic localization and biochemical studies. *J. Cell Biol.* 103:1441–1450. http://dx.doi.org/10.1083/jcb.103.4.1441

Volk, T., and B. Geiger. 1986b. A-CAM: a 135-kD receptor of intercellular adherens junctions. II. Antibody-mediated modulation of junction formation. *J. Cell Biol.* 103:1451–1464. http://dx.doi.org/10.1083/jcb.103.4.1451

Wachsstock, D.H., J.A. Wilkins, and S. Lin. 1987. Specific interaction of vinculin with α-actinin. *Biochem. Biophys. Res. Commun.* 146:554–560. http://dx.doi.org/10.1016/0006-291X(87)90564-X

Wachsstock, D.H., W.H. Schwartz, and T.D. Pollard. 1993. Affinity of alpha-actinin for actin determines the structure and mechanical properties of actin filament gels. *Biophys. J.* 65:205–214. http://dx.doi.org/10.1016/S0006-3495(93)81059-2

Walker, D.C., A. MacKenzie, W.C. Hulbert, and J.C. Hogg. 1985. A re-assessment of the tricellular region of epithelial cell tight junctions in trachea of guinea pig. *Acta Anat. (Basel).* 122:35–38. http://dx.doi.org/10.1159/000145982

Watabe-Uchida, M., N. Uchida, Y. Imamura, A. Nagafuchi, K. Fujimoto, T. Uemura, S. Vermeulen, F. van Roy, E.D. Adamson, and M. Takeichi. 1998. alpha-Catenin-vinculin interaction functions to organize the apical junctional complex in epithelial cells. *J. Cell Biol.* 142:847–857. http://dx.doi.org/10.1083/jcb.142.3.847

Weber, K.L., R.S. Fischer, and V.M. Fowler. 2007. Tmod3 regulates polarized epithelial cell morphology. *J. Cell Sci.* 120:3625–3632. http://dx.doi.org/10.1242/jcs.011445

Weiss, E.E., M. Kroemker, A.H. Rüdiger, B.M. Jockusch, and M. Rüdiger. 1998. Vinculin is part of the cadherin–catenin junctional complex: complex formation between α-catenin and vinculin. *J. Cell Biol.* 141:755–764. http://dx.doi.org/10.1083/jcb.141.3.755

Winter, M.J., B. Nagelkerken, A.E. Mertens, H.A. Rees-Bakker, I.H. Briaire-de Bruijn, and S.V. Litvinov. 2003. Expression of Ep-CAM shifts the state of cadherin-mediated adhesions from strong to weak. *Exp. Cell Res.* 285:50–58. http://dx.doi.org/10.1016/S0014-4827(02)00045-9

Witke, W., A. Hofmann, B. Köppel, M. Schleicher, and A.A. Noegel. 1993. The Ca(2+)-binding domains in non-muscle type alpha-actinin: biochemical and genetic analysis. *J. Cell Biol.* 121:599–606. http://dx.doi.org/10.1083/jcb.121.3.599

Wolburg, H., J. Neuhaus, U. Kniesel, B. Krauss, E.M. Schmid, M. Ocalan, C. Farrell, and W. Risau. 1994. Modulation of tight junction structure in blood-brain barrier endothelial cells. Effects of tissue culture, second messengers and cocultured astrocytes. *J. Cell Sci.* 107:1347–1357.

Wu, S.K., G.A. Gomez, M. Michael, S. Verma, H.L. Cox, J.G. Lefevre, R.G. Parton, N.A. Hamilton, Z. Neufeld, and A.S. Yap. 2014. Cortical F-actin stabilization generates apical-lateral patterns of junctional contractility that integrate cells into epithelia. *Nat. Cell Biol.* 16:167–178. http://dx.doi.org/10.1038/ncb2900

Wu, Y., P. Kanchanawong, and R. Zaidel-Bar. 2015. Actin-delimited adhesion-independent clustering of E-cadherin forms the nanoscale building blocks of adherens junctions. *Dev. Cell.* 32:139–154. http://dx.doi.org/10.1016/j.devcel.2014.12.003

Yaddanapudi, S., M.M. Altintas, A.D. Kistler, I. Fernandez, C.C. Möller, C. Wei, V. Peev, J.B. Flesche, A.L. Forst, J. Li, et al. 2011. CD2AP in mouse and human podocytes controls a proteolytic program that regulates cytoskeletal structure and cellular survival. *J. Clin. Invest.* 121:3965–3980. http://dx.doi.org/10.1172/JCI58552

Yamada, A., K. Irie, A. Fukuhara, T. Ooshio, and Y. Takai. 2004. Requirement of the actin cytoskeleton for the association of nectins with other cell adhesion molecules at adherens and tight junctions in MDCK cells. *Genes Cells.* 9:843–855. http://dx.doi.org/10.1111/j.1365-2443.2004.00768.x

Yamamoto, T., N. Harada, K. Kano, S. Taya, E. Canaani, Y. Matsuura, A. Mizoguchi, C. Ide, and K. Kaibuchi. 1997. The Ras target AF-6 interacts with ZO-1 and serves as a peripheral component of tight junctions in epithelial cells. *J. Cell Biol.* 139:785–795. http://dx.doi.org/10.1083/jcb.139.3.785

Yao, M., W. Qiu, R. Liu, A.K. Efremov, P. Cong, R. Seddiki, M. Payre, C.T. Lim, B. Ladoux, R.M. Mège, and J. Yan. 2014. Force-dependent conformational switch of α-catenin controls vinculin binding. *Nat. Commun.* 5:4525. http://dx.doi.org/10.1038/ncomms5525

Yao, N.Y., D.J. Becker, C.P. Broedersz, M. Depken, F.C. Mackintosh, M.R. Pollak, and D.A. Weitz. 2011. Nonlinear viscoelasticity of actin transiently cross-linked with mutant α-actinin-4. *J. Mol. Biol.* 411:1062–1071. http://dx.doi.org/10.1016/j.jmb.2011.06.049

Yao, N.Y., C.P. Broedersz, M. Depken, D.J. Becker, M.R. Pollak, F.C. Mackintosh, and D.A. Weitz. 2013. Stress-enhanced gelation: a dynamic nonlinearity of elasticity. *Phys. Rev. Lett.* 110:018103. http://dx.doi.org/10.1103/PhysRevLett.110.018103

Yap, A.S., W.M. Brieher, M. Pruschy, and B.M. Gumbiner. 1997. Lateral clustering of the adhesive ectodomain: a fundamental determinant of cadherin function. *Curr. Biol.* 7:308–315. http://dx.doi.org/10.1016/S0960-9822(06)00154-0

Yap, A.S., C.M. Niessen, and B.M. Gumbiner. 1998. The juxtamembrane region of the cadherin cytoplasmic tail supports lateral clustering, adhesive strengthening, and interaction with p120ctn. *J. Cell Biol.* 141:779–789. http://dx.doi.org/10.1083/jcb.141.3.779

Ylänne, J., K. Scheffzek, P. Young, and M. Saraste. 2001. Crystal structure of the α-actinin rod reveals an extensive torsional twist. *Structure.* 9:597–604. http://dx.doi.org/10.1016/S0969-2126(01)00619-0

Yokoyama, S., K. Tachibana, H. Nakanishi, Y. Yamamoto, K. Irie, K. Mandai, A. Nagafuchi, M. Monden, and Y. Takai. 2001. α-Catenin-independent recruitment of ZO-1 to nectin-based cell-cell adhesion sites through afadin. *Mol. Biol. Cell.* 12:1595–1609. http://dx.doi.org/10.1091/mbc.12.6.1595

Yonemura, S. 2011. Cadherin-actin interactions at adherens junctions. *Curr. Opin. Cell Biol.* 23:515–522. http://dx.doi.org/10.1016/j.ceb.2011.07.001

Yonemura, S., M. Itoh, A. Nagafuchi, and S. Tsukita. 1995. Cell-to-cell adherens junction formation and actin filament organization: similarities and differences between non-polarized fibroblasts and polarized epithelial cells. *J. Cell Sci.* 108:127–142.

Yonemura, S., Y. Wada, T. Watanabe, A. Nagafuchi, and M. Shibata. 2010. α-Catenin as a tension transducer that induces adherens junction development. *Nat. Cell Biol.* 12:533–542. http://dx.doi.org/10.1038/ncb2055

Yoshida, Y., M. Okano, S. Wang, M. Kobayashi, M. Kawasumi, H. Hagiwara, and M. Mitsumata. 1994. Hemodynamic-force-induced difference of interendothelial junctional complexes. *Ann. N. Y. Acad. Sci.* 748:104–120. http://dx.doi.org/10.1111/j.1749-6632.1994.tb17311.x

Zhang, J., M. Betson, J. Erasmus, K. Zeikos, M. Bailly, L.P. Cramer, and V.M. Braga. 2005. Actin at cell-cell junctions is composed of two dynamic and functional populations. *J. Cell Sci.* 118:5549–5562. http://dx.doi.org/10.1242/jcs.02639